ISSN 1307-8798

Official Publication of the Turkish Society of Anatomy and Clinical Anatomy

www.anatomy.org.tr

anatomy

An International Journal of Experimental and Clinical Anatomy

Volume 11 / Issue 1 / April 2017

Published three times a year

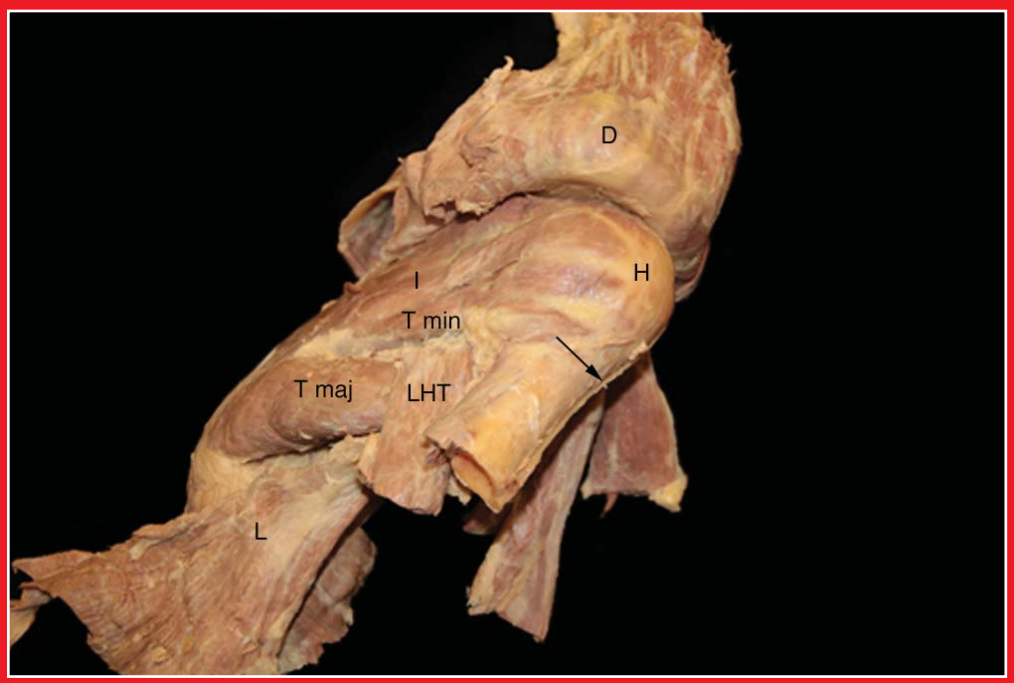

deomed®

www.anatomy.org.tr

anatomy

An International Journal of Experimental and Clinical Anatomy

Official Publication of the Turkish Society of Anatomy and Clinical Anatomy

Aim and Scope

Anatomy, an international journal of experimental and clinical anatomy, is a peer-reviewed journal published three times a year with an objective to publish manuscripts with high scientific quality from all areas of anatomy. The journal offers a forum for anatomical investigations involving gross, histologic, developmental, neurological, radiological and clinical anatomy, and anatomy teaching methods and techniques. The journal is open to original papers covering a link between gross anatomy and areas related with clinical anatomy such as experimental and functional anatomy, neuroanatomy, comparative anatomy, modern imaging techniques, molecular biology, cell biology, embryology, morphological studies of veterinary discipline, and teaching anatomy. The journal is currently indexing and abstracting in TUBITAK ULAKBIM Turkish Medical Index, Proquest, EBSCO Host, Index Copernicus and Google Scholar.

Publication Ethics

Anatomy is committed to upholding the highest standards of publication ethics and observes the principles of Journal's Publication Ethics and Malpractice Statement which is based on the recommendations and guidelines for journal editors developed by the Committee on Publication Ethics (COPE), Council of Science Editors (CSE), World Association of Medical Editors (WAME) and International Committee of Medical Journal Editors (ICMJE). Fore detailed information please visit the online version of the journal which is available at www.anatomy.org.tr

Authorship

All persons designated as authors should have participated sufficiently in the work to take public responsibility for the content of the manuscript. Authorship credit should be based on substantial contributions to (1) conception and design or analysis and interpretation of data, (2) drafting of the manuscript or revising it for important intellectual content and, (3) final approval of the version to be published. The Editor may require the authors to justify assignment of authorship. In the case of collective authorship, the key persons responsible for the article should be identified and others contributing to the work should be recognized with proper acknowledgment.

Copyright

Publication Information

Anatomy (p-ISSN 1307-8798; e-ISSN 1308-8459) is published by Deomed Publishing, Istanbul, for the Turkish Society of Anatomy and Clinical Anatomy, TSACA. Due the Press Law of Turkish Republic dated as June 26, 2004 and numbered as 5187, this publication is classified as a periodical in English language.

Ownership
On behalf of the Turkish Society of Anatomy and Clinical Anatomy,
Ahmet Kağan Karabulut, MD, PhD; Konya

Responsible Managing Editor
Nihal Apaydın, MD, PhD; Ankara

Administrative Office
Güven Mah. Güvenlik Cad. Onlar Ap. 129/2 Aşağı Ayrancı, Ankara
Phone: +90 312 447 55 52-53

Publisher
Deomed Publishing
Gür Sok. No:7/B Kadıköy, İstanbul, Turkey
Phone: +90 216 414 83 43 (Pbx) / Fax: +90 216 414 83 42
www.deomed.com / e-mail: medya@deomed.com

deomed®

Submission of Manuscripts

Contributions should be submitted for publication under the following categories to:

Gülgün Şengül, MD
Editor-in-Chief, *Anatomy*

Department of Anatomy,
Faculty of Medicine, Ege University,
35100, Bornova, Izmir, Turkey
Phone: 0090 232 390 39 84
Fax: 0090 232 342 21 42
e-mail: gulgun.sengul@gmail.com; gulgun.sengul@ege.edu.tr

Categories of Articles

- ***Original Articles*** describe substantial original research that falls within the scope of the Journal.
- ***Teaching Anatomy*** section contains regular or all formats of papers which are relevant to comparing teaching models or to introducing novel techniques, including especially the own experiences of the authors.
- ***Reviews*** section highlights current development in relevant areas of anatomy. The reviews are generally invited; other prospective authors should consult with the Editor-in-Chief.
- ***Case Reports*** include new, noteworthy or unusual cases which could be of help for basic notions and clinical practice.
- ***Technical Note*** articles cover technical innovations and developments with a specific technique or procedure or a modification of an existing technique. They should be sectioned like an original research article but not exceed 2000 words.
- ***Viewpoint*** articles give opinions on controversial topics or future projections, some of these are invited.
- ***Historical View*** category presents overview articles about historical sections from all areas of anatomy.
- ***Terminology Zone*** category is a platform for the articles which discuss some terminological controversies or opinions.

The categories above are peer-reviewed. They should include abstract and keywords. There are also categories including Letters to the Editor, Book Reviews, Abstracts, Obituary, News and Announcements which do not require a peer review process.

For detailed instructions concerning the submission of manuscripts, please refer to the Instructions to Authors.

Subscription

Please send your order to Deomed Publishing, Gür Sok. No: 7/B Kadıköy, Istanbul, Turkey. e-mail: alikoz@deomed.com

- ***Annual rates:*** Institutional 100 EUR, Individual 50 EUR (include postage and local VAT). Supplements are not included in the subscription rates.

Membership of the Turkish Society of Anatomy and Clinical Anatomy, TSACA includes a reduced subscription rate to this journal.

- ***Change of address:*** Please send to the publisher at least six weeks in advance, including both old and new addresses.
- ***Cancellations:*** Subscription cancellations will not be accepted after the first issue has been mailed.

The online version of this journal is available at www.anatomy.org.tr

Advertising and Reprint Requests

Please direct to publisher. e-mail: medya@deomed.com

Printing and Binding

Birmat Press, İstanbul, Turkey, Phone: +90 212 629 05 59-60
Printed in Turkey on acid-free paper (April 2017).

Editorial Board

www.anatomy.org.tr

anatomy
An International Journal of Experimental and Clinical Anatomy

anatomy
www.anatomy.org.tr
An International Journal of Experimental and Clinical Anatomy

Instructions to Authors

Anatomy, an international journal of experimental and clinical anatomy, is the official publication of the Turkish Society of Anatomy and Clinical Anatomy, TSACA. It is a peer-reviewed journal that publishes scientific articles in English. For a manuscript to be published in the journal, it should not be published previously in another journal or as full text in congress books and should be found relevant by the editorial board. Also, manuscripts submitted to Anatomy must not be under consideration by any other journal. Relevant manuscripts undergo conventional peer review procedure (at least three reviewers). For the publication of accepted manuscripts, author(s) should reveal to the Editor-in-Chief any conflict of interest and transfer the copyright to the Turkish Society of Anatomy and Clinical Anatomy, TSACA.

In the Materials and Methods section of the manuscripts where experimental studies on humans are presented, a statement that informed consent was obtained from each volunteer or patient after explanation of the procedures should be included. This section also should contain a statement that the investigation conforms with the principles outlined in the appropriate version of 1964 Declaration of Helsinki. For studies involving animals, all work must have been conducted according to applicable national and international guidelines. Prior approval must have been obtained for all protocols from the relevant author's institutional or other appropriate ethics committee, and the institution name and permit numbers must be provided at submission.

Anatomical terms used should comply with Terminologia Anatomica by FCAT (1998).

No publication cost is charged for the manuscripts but reprints and color printings are at authors' cost.

Preparation of manuscripts

During the preparation of the manuscripts, uniform requirements of the International Committee of Medical Journal Editors, a part of which is stated below, are valid (*see* ICMJE. Uniform requirements for manuscripts submitted to biomedical journals. Updated content is available at www.icmje.org). The manuscript should be typed double-spaced on one side of a 21x 29.7 cm (A4) blank sheet of paper. At the top, bottom and right and left sides of the pages a space of 2.5 cm should be left and all the pages should be numbered except for the title page.

Manuscripts should not exceed 15 pages (except for the title page). They must be accompanied by a cover letter signed by corresponding author and the Conflicts of Interest Disclosure Statement and Copyright Transfer Form signed by all authors. The contents of the manuscript (original articles and articles for Teaching Anatomy category) should include: 1- Title Page, 2- Abstract and Keywords, 3- Introduction, 4- Materials and Methods, 5- Results, 6- Discussion (Conclusion and/or Acknowledgement if necessary), 7- References

Title page

In all manuscripts the title of the manuscript should be written at the top and the full names and surnames and titles of the authors beneath. These should be followed with the affiliation of the author. Manuscripts with long titles are better accompanied underneath by a short version (maximum 80 characters) to be published as running head. In the title page the correspondence address and telephone, fax and e-mail should be written. At the bottom of this page, if present, funding sources supporting the work should be written with full names of all funding organizations and grant numbers. It should also be indicated in a separate line if the study has already been presented in a congress or likewise scientific meeting. Other information such as name and affiliation are not to be indicated in pages other than the title page.

Abstract

Abstract should be written after the title in 100–250 words. In original articles and articles prepared in IMRAD format for Teaching Anatomy category the abstract should be structured under sections Objectives, Methods, Results and Conclusion. Following the abstract at least 3 keywords should be added in alphabetical order separated by semicolumns.

References

Authors should provide direct references to original research sources. References should be numbered consecutively in square brackets, according to the order in which they are first mentioned in the manuscript. They should follow the standards detailed in the NLM's Citing Medicine, 2nd edition (Citing medicine: the NLM style guide for authors, editors, and publishers [Internet]. 2nd edition. Updated content is available at www.ncbi.nlm .nih.gov/books/NBK7256). The names of all contributing authors should be listed, and should be in the order they appear in the original reference. The author is responsible for the accuracy and completeness of references. When necessary, a copy of a referred article can be requested from the author. Journal names should be abbreviated as in *Index Medicus*. Examples of main reference types are shown below:

• **Journal articles:** Author's name(s), article title, journal title (abbreviated), year of publication, volume number, inclusive pages

– *Standard journal article:* Sargon MF, Celik HH, Aksit MD, Karaagaoglu E. Quantitative analysis of myelinated axons of corpus callosum in the human brain. Int J Neurosci 2007;117:749–55.

– *Journal article with indication article published electronically before print:* Sengul G, Fu Y, Yu Y, Paxinos G. Spinal cord projections to the cerebellum in the mouse. Brain Struct Funct Epub 2014 Jul 10. DOI 10.1007/s00429-014-0840-7.

• **Books:** Author's name(s), book title, place of publication, publisher, year of publication, total pages (entire book) or inclusive pages (contribution to a book or chapter in a book)

– *Entire book:*

- *Standard entire book:* Sengul G, Watson C, Tanaka I, Paxinos G. Atlas of the spinal cord of the rat, mouse, marmoset, rhesus and human. San Diego (CA): Academic Press Elsevier; 2013. 360 p.

- *Book with organization as author:* Federative Committee of Anatomical Terminology (FCAT). Terminologia anatomica. Stuttgart: Thieme; 1998. 292 p.

- *Citation to a book on the Internet:* Bergman RA, Afifi AK, Miyauchi R. Illustrated encyclopedia of human anatomic variation. Opus I: muscular system [Internet]. [Revised on March 24, 2015] Available from: http://www.anatomyatlases.org/AnatomicVariants/AnatomyHP.shtml

– *Contribution to a book:*

- *Standard reference to a contributed chapter:* Potten CS, Wilson JW. Development of epithelial stem cell concepts. In: Lanza R, Gearhart J, Blau H, Melton D, Moore M, Pedersen R, Thomson J, West M, editors. Handbook of stem cell. Vol. 2, Adult and fetal. Amsterdam: Elsevier; 2004. p. 1–11.

- *Contributed section with editors:* Johnson D, Ellis H, Collins P, editors. Pectoral girdle and upper limb. In: Standring S, editor. Gray's anatomy: the anatomical basis of clinical practice. 29th ed. Edinburgh (Scotland): Elsevier Churchill Livingstone; 2005. p. 799–942.

– *Chapter in a book:*

- *Standard chapter in a book:* Doyle JR, Botte MJ. Surgical anatomy of the hand and upper extremity. Philadelphia (PA): Lippincott Williams and Wilkins; 2003. Chapter 10, Hand, Part 1, Palmar hand; p. 532–641.

Illustrations and tables

Illustrations and tables should be numbered in different categories in the manuscript and Roman numbers should not to be used in numbering. Legends of the illustrations and tables should be added to the end of the manuscript as a separate page. Attention should be paid to the dimensions of the photographs to be proportional with 10x15 cm. Some abbreviations out of standards can be used in related illustrations and tables. In this case, abbreviation used should be explained in the legend. Figures and tables published previously can only be used when necessary for a comparison and only by giving reference after obtaining permission from the author(s) or the publisher (copyright holder).

Control list

- Length of the manuscript (max. 15 pages)
- Manuscript format (double space; one space before punctuation marks except for apostrophes)
- Title page (author names and affiliations; running head; correspondence)
- Abstract (100–250 words)
- Keywords (at least three)
- References (relevant to *Index Medicus)*
- Illustrations and tables (numbering; legends)
- Conflicts of Interest Disclosure Statement and Copyright Transfer Form
- Cover letter

Original Article

www.anatomy.org.tr
Received: July 21, 2016; Accepted: January 16, 2017
doi:10.2399/ana.16.021

anatomy
www.anatomy.org.tr
An International Journal of Experimental and Clinical Anatomy

Histomorphometric evaluation of adult male rabbit testicular tissue exposed to giant milk weed (*Calotropis procera*) treatment

Emmanuel Olusola Yawson[1], Lawal Ismail Temitayo[2], Kosisochukwu Kingsley Obasi[2], Abdulrahman Abdulfatai[1], Wasiu Olalekan Akintunde[1]

[1]*Department of Anatomy, Faculty of Basic Medical Sciences, College of Health Sciences, Ladoke Akintola University of Technology, Ogbomoso, Nigeria*
[2]*Department of Anatomy, Faculty of Basic Medical Sciences, College of Health Sciences, University of Ilorin, Ilorin, Nigeria*

Abstract

Objectives: This study was designed to investigate the effects of liquid extract of *Calotropis procera* (CP) on the testicular structure and functions of adult male rabbits. CP, commonly known as *'ewe bomubomu'* in Nigeria, contains a toxic milky sap that is extremely bitter; the milky sap contains a complex mix of chemicals. This plant is most popular and commonly used among the Fulanis in Nigeria to process cheese.

Methods: Twelve adult male rabbits weighing between 1–2 kg were used for this study. The rabbits were divided randomly into four Groups A–D; (n=3, in each group). Animals in Group A–C received CP as 750, 500 and 250 mg/kg body weight, respectively by oral intubation daily for 28 days, while Group D served as the control group. All animals were euthanized by cervical dislocation; the testes were excised and fixed in Bouin's fluid for routine histological studies using haematoxylin and eosin stain. Cauda epididymidis was also excised for semen quality evaluation.

Results: These results showed hormonal and testicular histomorphological alterations in CP treated animals such as abnormal shape and arrangement of seminiferous tubules, degeneration of spermatogenic and interstitial. CP also affected the testosterone concentration, cross-sectional area, germinal epithelium diameter and lumen diameter of the seminiferous tubules.

Conclusion: These findings show that CP caused histomorphological and hormonal alterations and thereby hampered spermatogenesis. It is therefore recommended that continuous use of CP as part of food ingredient should be discouraged and discontinued.

Keywords: *Calotropis procera*; rabbit; testes

Anatomy 2017;11(1):1–5

Introduction

Calotropis procera (CP; giant milk weed) is a species of flowering plant in the family Apocynaceae, native to North Africa, Tropical Africa, Western Asia, South Asia, and Indochina.[1] The flesh CP contains a toxic milky sap that is extremely bitter and turns into a gluey coating resistant to soap.[1] The milky sap contains a complex mix of chemicals, some of which are steroidal heart poisons known as 'cardiac aglycones'.[2,3] These belong to the same chemical family as similar chemicals found in foxgloves (*digitalis purpurea*). Alkaloids, flavonoids, sterols and uscharin have also been reported to be present in the entire part of the plant.[3] CP is referred to as *'ewe bomubomu'* among the Yoruba populace in Nigeria where it is used as a constituent of concortions to cure certain ailments. The Fulani population in Nigeria use CP as the major component in processing cheese.

The testes are double glandular organs performing both exocrine and endocrine functions in the body. Spermatogenesis occurs in the seminiferous tubule of the testes surrounded by nutrient rich basement membrane which serves as support and source of nutrients to the pro-

liferating spermatogenic cells to give rise to matured spermatozoa under the influence of testosterone hormone produced by cells located in the interstitial space of the testes.[4] Spermatogenesis and testosterone production are regulated by the secretory actions of the hypothalamus where gonadotropin releasing hormone (GnRH) is released and pituitary gland that secretes follicle stimulating hormone (FSH) and luteinizing hormone (LH) upon the action of GnRH.[4]

CP has been used in traditional medicine as purgative, anthelmintic, anticancer, as well as to treat leucoderma, ulcers, piles and disease of the spleen.[5] CP has been implicated to have an abortifacient,[6] antifertility,[7] uterine stimulating effect[8] and teratogenic effects on the developing embryo.[9]

Fresh leaf extract of CP has growth suppressing effects on the body leading to a significant reduction in body, testicular and epididymal weights in exposed animals. Significant decrease in relative weights of accessory sex glands was reported in rat treated with CP.[10,11] CP administration led to deleterious effects on the testicular microstructures and accessory sex organs, resulting in desquamation of seminiferous epithelial cells, degeneration of seminiferous tubules and presence of large-sized multinucleated cells. Significant reduction in the seminiferous tubular diameter, seminal vesicle and epididymal structures were also reported.[10]

The aim of this study was to highlight the effects of CP on testicular morphology and morphometry, and also evaluate the consequent effects on semen parameters in adult male rabbits. This became a research of interest after observation of the use of CP by local fish farmers in Nigeria in the harvesting processes of fish from various local ponds, and also from the use of CP by Fulanis (a tribe in Nigeria ethnic groups) as a major constituent of their locally produced cheese popularly known as “wara fulani”.

Materials and Methods

Twelve adult sexually active male rabbits weighing between 1–2 kg were used in this study. The rabbits were bred and maintained at the experimental animal unit in the Department of Human Anatomy, Ladoke Akintola University of Technology, Ogbomoso, Nigeria. The animals were divided into four groups (of three rabbits each), designated as Groups A–D. Groups A–C served as experimental animals, and Group D served as control.

The leaves of CP were obtained from Aroje community, Ogbomoso, and identified at the Department of Pure and Applied Biology, Ladoke Akintola University of Technology, Ogbomoso, Oyo State, Nigeria. The leaf extract of CP was prepared by macerating 50 g of fresh leaves with 250 ml of distilled water and later by squeezing and filtering. The filtrate served as the stock solution. The stock solution was administered orally at a dosage of 750 mg/kg body weight (Group A), 500 mg/kg body weight (Group B), and 250 mg/kg body weight (Group C) once daily using an oral cannula for 28 days. Control animals (Group D) received only normal saline for the same number of days.

The animals were dissected, and the testes and epididymis were collected immediately after exsanguination. The testes collected were fixed in Bouin's fluid and processed using paraffin embedment, and stained with haematoxylin and eosin. The slides of testes were evaluated for pathological changes under light microscope. The testes used for hormonal assay were crushed using a pestle and mortar in a 0.25 M sucrose solution, then centrifuged for 5 min at 5000 r/min and filtered using a plastic pipette. The specimens for the testosterone assay were kept in the freezer at a temperature of about -5°C before the assay commenced.

The epididymis was placed in normal saline for evaluation of sperm quality (*i.e.* sperm count, sperm motility and sperm morphology). The concentration of spermatozoa was determined by the haemocytometer method. The spermatozoa were evaluated by haemocytometer using the improved Neubauer chamber (Deep 1/10 mm; LABART, Munich, Germany).

The histomorphometry (*i.e.* cross section area, lumen diameter and germinal epithelium diameter) was evaluated using Image J software (National Institute of Mental Health, Bethesda, Maryland, USA) from photomicrographs of the testes.

Johnsen score was used for assessing spermatogenesis in testicular biopsy:[12] 10: complete spermatogenesis and perfect tubules; 9: many spermatozoa present but disorganized spermatogenesis; 8: only a few spermatozoa present; 7: no spermatozoa but many spermatids present; 6: only a few spermatids present; 5: no spermatozoa or spermatids present but many spermatocytes present; 4: only a few spermatocytes present; 3: only spermatogonia present; 2: no germ cells present; 1: neither germ cells nor Sertoli cells present.

Testosterone concentration was estimated using Accu Bind ELISA Microwell (Monobind Inc., Lake Forest, CA, USA).

Data collected were analyzed using two-way analysis of variance (ANOVA) followed by Tukey’s (HSD) multiple comparison test with the aid of SPSS (V20; SPSS

Inc., Chicago, IL, USA). Data were presented as means ± SEM (standard error of mean). P value less than 0.05 ($p \leq 0.05$) was considered statistically significant. All graphs were drawn using the GraphPad Prism v.6 (GraphPad Software, Inc., La Jolla, CA, USA).

Results

Histological analysis

Histological findings in the control group depicted a normal cytoarchitecture of the testes in rabbits showing a normal shape and arrangement of seminiferous tubule with intact basement membrane and progressive proliferation of spermatogenic cells to produce matured spermatozoa. Interstitium was intact with Leydig cells (**Figures 1a** and **b**). Group C rabbits had swollen spermatogonia and mild disruption in the arrangement of seminiferous tubule (**Figures 1c** and **d**). Group B treated rabbits showed impaired spermatogenesis due to degeneration of spermatogenic cells, necrosis of Leydig cells in the interstitium, and traces of haemorrhage were evident (**Figures 1e** and **f**). In Group A rabbits, there were reduced spermatogenic cells and impaired spermatogenesis, and traces of spermatogenic cells were secluded in the lumen (**Figures 1g** and **h**).

Group D (control) animals showed normal shape and arrangement of seminiferous tubule with intact basement membrane and progressive proliferation of spermatogenic cells to produce matured spermatozoa. There was intact interstitium with Leydig cells. The basement membrane covering of the seminiferous tubule was normal across all groups (**Figures 1a** and **b**). Group B animals showed swollen spermatogonia and mild disruption in the arrangement of seminiferous tubule (**Figures 1c** and **d**). Group C animals showed hampered spermatogenesis due to degeneration of spermatogenic cells, necrosis of Leydig cells in the interstitium and traces of haemorrhage were evident (**Figures 1e** and **f**). Group D animals reduced spermatogenic cells and hampered spermatogenesis as traces of spermatogenic cells were present in the lumen (**Figures 1g** and **h**).

Effect of CP on sperm count, motility and morphology in the epididymis of experimental group rabbits compared to the control group are shown in **Table 1**.

Table 1

Effect of CP on sperm parameters in the epididymis of experimental group rabbits (Groups A–C) compared to the control group (Group D).

Groups	Sperm count (10^6/ml)	Sperm motility (%)	Sperm morphology (%)
A	11.33±2.59*	46.7±12.02*	56.67±2.85*
B	33.07±5.64*	55±18.93*	53.33±3.84*
C	55±3.2*	88.73±2.02	70±5.78*
D	83±11.12	90±0.58	83.33±3.84

Values are expressed as mean±SEM. *p<0.05

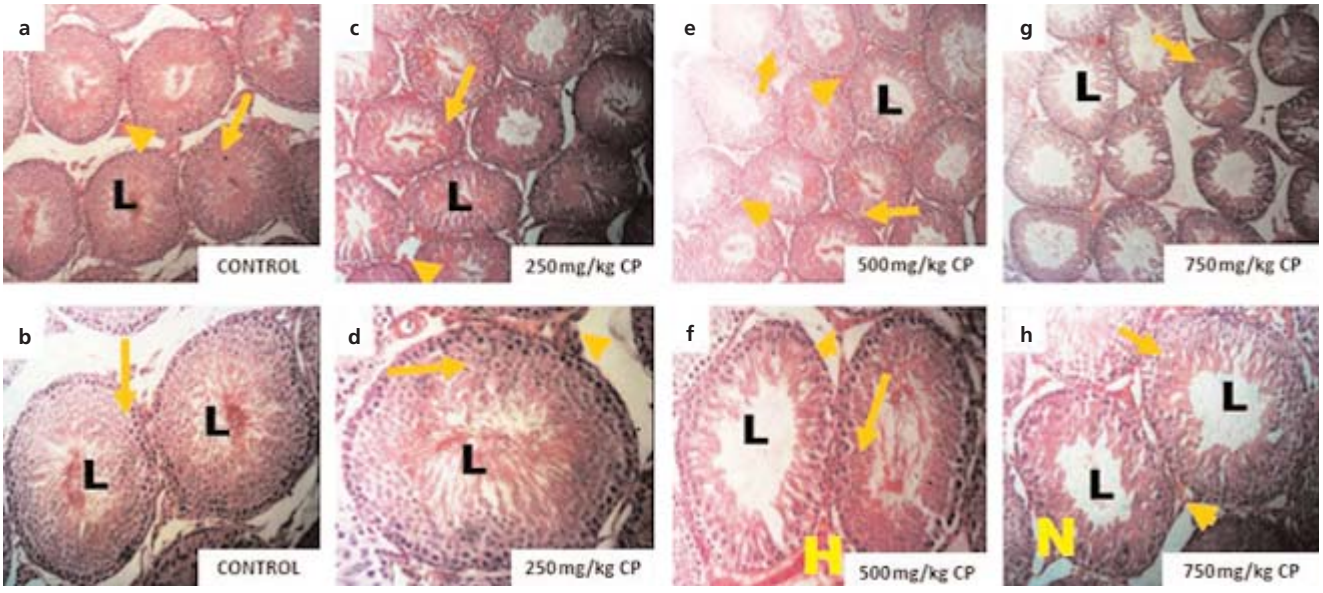

Figure 1. Photomicrographs showing rabbit testicular cytoarchitecture. Basement membrane (**arrow**), lumen (**L**), spermatogenic cells (**long arrow**), interstitial space (**arrowhead**), necrosis (**N**). H&E stain, ×100 (**a**, **c**, **e**, **g**) and ×200 (**b**, **d**, **f**, **h**). [Color figure can be viewed in the online issue, which is available at www.anatomy.org.tr]

Histomorphometric analysis and Johnsen's score

A significant decrease ($p<0.05$) in the cross sectional area (CSA) was observed in Group C treated with 250 mg/kg body weight of CP when compared with the control group. A significant increase ($p<0.05$) in the germinal epithelium diameter (GED) was observed in Group A that received 750 mg/kg body weight of CP compared to the control group (**Table 2**), while a significant decrease ($p<0.05$) in germinal epithelium diameter was also observed in Group B that received 500 mg/kg body weight of CP compared to the control group. A significant increase ($p<0.05$) in lumen diameter was observed in Group B that received 500 mg/kg body weight of CP compared to the control group (**Table 2**), while a non-significant decrease ($p>0.05$) in Johnsen's score was observed in all the treatment groups when compared to the control group (**Table 2**). These results showed a poor morphometric grading and poor Johnsen's score as a result of the effect of aqueous extract administration of CP.

Table 2

Effect of CP on histomorphometric parameters and (Jonhsen's score) in experimental group rabbits (Groups A-C), compared to the control group (Group D).

Groups	CSA (10^7 µm)	GED (10^3 µm)	LD (10^2 µm)	Johnsen's score
A	2.8±0.42	1.18±0.05*	7.7±0.66	5.7±0.33
B	2.5±0.29	0.69±0.12*	17.1±10.5*	5.7±0.33
C	1.5±0.13*	0.94±0.05	8.05±0.31	6.0±0.58
D	2.6±0.26	0.89±0.06	9.70±0.79	7.0±0.58

CSA: cross sectional area, **GED:** germinal epithelium diameter, **LD:** lumen diameter. Values are expressed as mean±SEM. *p<0.05

Hormonal assay

Testosterone concentration in the testes reduced significantly ($P\leq0.05$) in all treated groups when compared to the control group (**Figure 2**).

Discussion

CP contains toxic milky sap which is made up of complex mix of chemicals, some of which are steroidal heart poisons known as "cardiac aglycones".[2,3] CP has been reported to have numerous medicinal importance,[3,5] but was observed to be potentially injurious to the body especially male reproductive organs after prolonged or chronic use.[1,10] CP induced functional sterility, degenerating and necrotic germ cells within the seminiferous tubule and significantly reduced testicular weight.[13]

In this present study, histopathological findings revealed that CP caused mild distortions on the histomorphology of animals treated with 250 mg/kg body weight. Animals given 500 mg/kg body weight of CP and 750 mg/kg body weight of CP showed mixing of the germ cell types in stages of spermatogenesis and hypertrophy of the spermatogenic cells in animals that received 750 mg/kg body weight of CP, complemented with abnormal rise in germinal epithelium diameter, reduced spermatozoa and presence of spermatogenic cells in the lumen. The seminiferous tubules showed abnormal shape (shrinkage) and arrangement (wide interstitial space). This finding was further complimented by reduction in the cross section area of the seminiferous tubules. Wide interstitium with degenerated testosterone producing Leydig cells and traces of haemorrhage were also observed. These findings are consistent with the study of Sharma and Jacob[14] who reported that CP had anti-spermatogenic properties.

Semen quality evaluation revealed dose-dependent decrease in the semen parameters. Animals treated with CP showed significant reduction in total number of sperm cells, motility and normal morphology with increasing dosage of administered CP as most reduction in the semen parameters were observed in animals given 750 mg/kg body weight of CP for 28 days. Histomorphological alterations and reduced semen quality observed were complimented by Johnsen's spermatogenesis score. Spermatogenesis rate and population of spermatogenesis series were insignificantly reduced in CP treated animals with increasing dosage.

Testosterone concentration in the testes of CP treated animals reduced ($p<0.05$) markedly compared to control group. Testosterone drives the progression of spermatogenic series in the seminiferous tubule. Reduced testosterone implies hampered rate of sperm production. Reduction in testosterone concentration and alteration

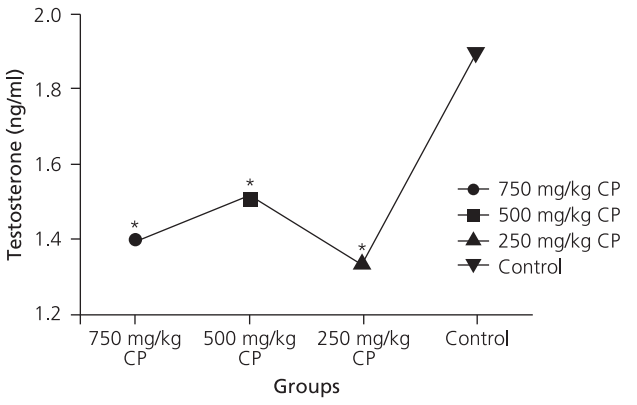

Figure 2. Testosterone concentration in control and CP-treated groups. *p≤0.05.

in spermatogenesis were observed in CP treated rabbits. This finding corroborated with studies by Aiton[1] who suggested that CP had an effect on testosterone production, thereby resulting in the histomorphological alterations observed in their work.

Conclusion

Histomorphological and hormonal alterations in CP treated animals were observed such as abnormal shapes and arrangement of seminiferous tubules, degeneration of spermatogenic and interstitial cells; thereby hampering spermatogenesis. CP also affected testosterone concentration and cross sectional area, germinal epithelium diameter and lumen diameter of the seminiferous tubules in adult male rabbits. Findings from this study conducted on male rabbits showed that CP may be one of the underlying cause of male infertility in Nigeria as a result of daily consumption of CP from the popular locally made Fulani cheese, corroborating several studies carried out on different animal species. It is therefore recommended that continuous use of CP as a food ingredient should be discouraged and discontinued as CP, causes testicular toxicity on dose dependent levels.

Acknowledgements

We would like to acknowledge KK Obasi, IA Lawal, AO Abdulrahman, and OW Akintunde for their technical assistance.

References

1. Aiton WT. *Calotropis procera*: Germplasm resources information network. United States Department of Agriculture; 2001-10-19. Retrieved 2010- 06-26.
2. Al-Robal AA, Abo-Khatwa AN, Danish EY. Toxocological studies on the latex of the usher plants *Calotropis procera* (ait). R. Br. In Saudi Arabia 111. Effects of usher latex on the fine structures, oxygen consumption and Na+/k+ transporting ATPase activity of albino rat kidneys. Arab-Gulf Journal of Scientific Research 1993;11:441–5.
3. Hussein HI, Kamel A, Abou-Zeid M, Abdel-Khalek, El-Sebae H, Saleh MA. Uscharin, the most potent molluscicidal compound tested against land snails. J Chem Ecol 1994;20:135–40.
4. Scott FG. Developmental biology online textbook. 6th ed. Sunderland (MA): Sinauer Associates Inc; 2000. p. 21.
5. Jain SC, Sharma R, Kain R, Sharma RA. Antimicrobial activity of *Calotropis procera*. Fitoterapia 1996;67275–7.
6. Saha JC, Savini EC, Kasinathan S. Ecbolic properties of Indian medicinal plants. Part 1. Indian Journal of Medical Reources 1961; 49:130–51.
7. Malhi BS, Trivedi VP. Vegetable antifertility drugs of India. Q J Crude Drug Res 1972;12:1922.
8. Hilai SH, Youngken JR. Certain poisonous plants of Egypt. A scientific manual pharmaceutical society of Egypt. National Information and Documentation; Centres Dokki, Cairo, Egypt: 1983. p. 11.
9. Prakash AO, Gupta RB, Mathur R. Effect of oral administration of forth two indigenous plant extracts on early and late pregnancy in albino rats. Probe 1978;17:315–23.
10. Akinloye AK, Abatan MO, Onwuka SK, Oke BO. Growth-suppressing effect of *Calotropis procera* (giant milkweed) on body weight and the male reproductive organs of wistar rats. Tropical Animal Health and Production 2002;20:132–8.
11. Akinloye AK, Abatan MO, Alaka OO. Histomorphometric and histopathological studies on the effect of *Calotropis procera* (giant milkweed) on the male reproductive organs of Wistar rats. International African Journal of Biomedical Research 2002;5:57–61.
12. Johnsen SG. Testicular biopsy score count – a method for registration of spermatogenesis in human testes: normal values and results in 335 hypogo- nadal males. Hormones 1970;1:2–25.
13. Meerwal P, Jain GC. Male fertility regulation with plant products: a review. International Journal of Pharmaceutical, Chemical and Biological Sciences 2015;5:146–62.
14. Sharma N, Jacob D. Inhibition of fertility and functional alteration in the genital organs of male Swiss albino mouse after administration of *Calotropis procera* flower extract. Pharmaceutical Biology 2001;39: 403–7.

Online available at:
www.anatomy.org.tr
doi:10.2399/ana.16.021
QR code:

deomed

Correspondence to: Emmanuel O. Yawson, MSc, PhD
Department of Anatomy, Faculty of Basic Medical Sciences, College of Health Sciences, Ladoke Akintola University of Technology, Ogbomoso, Nigeria
Phone: +234 813 6725089
e-mail: yawsonmmanuel@gmail.com

Conflict of interest statement: No conflicts declared.

anatomy
www.anatomy.org.tr
An International Journal of Experimental and Clinical Anatomy

Original Article

www.anatomy.org.tr
Received: December 8, 2016; Accepted: March 30, 2017
doi:10.2399/ana.16.047

Morphometric assessment of sella turcica using CT scan*

Ozan Turamanlar[1], Kenan Öztürk[2], Erdal Horata[3], Mehtap Beker Acay[4]

[1]*Department of Anatomy, Faculty of Medicine, Afyon Kocatepe University, Afyonkarahisar, Turkey*
[2]*Department of Anatomy, Isparta Süleyman Demirel University, Faculty of Medicine, Isparta, Turkey*
[3]*Atatürk Vocational School of Health Services, Afyon Kocatepe University, Afyonkarahisar, Turkey*
[4]*Department of Radiology, Afyon Kocatepe University Faculty of Medicine, Afyonkarahisar, Turkey*

Abstract

Objectives: Morphometry of sella turcica should be known to evaluate pathological sella turcica. The aim of this study was to measure the size and describe the morphology of sella turcica in a Turkish population.

Methods: This study included 101 individuals aged 17 to 70 years who went under CT scan. Sella length, sella width, sella height anterior, sella height median, sella height posterior, sella area, sella depth and sella anteroposterior (AP) diameter were measured.

Results: Sella length was measured as 9.18±1.91 mm, sella width 10.41±1.74 mm, sella height anterior 8.09±1.65 mm, sella height median 7.71±1.24 mm, sella height posterior 7.48±1.34 mm, sella area 69.15±17.45 mm^2, sella depth 7.87±1.37 mm and antero-posterior sella diameter as 11.48±1.82 mm. When these sizes were compared between males and females, only sella length and width differed significantly. When compared by decades, there was a statistically significant difference only in the sella area parameter.

Conclusion: Sella turcica dimensions of the Turkish population obtained by CT in this study can be used in estimating pituitary gland size and in determining any pathology in the sellar and parasellar regions. In addition, these results may help clinicians who encounter pathologically large sella areas in easily distinguishing it. Therefore, knowing the normal anatomy and variations of sella turcica is important for neurologists and neurosurgeons who deal with the pathologies of this area.

Keywords: computed tomography; morphometry; sella turcica

Anatomy 2017;11(1):6–11

Introduction

Sella turcica is a saddle-shaped depression located in the middle cranial fossa on the upper surface of the sphenoid bone. It is enclosed by the pituitary fossa in which the pituitary gland is lodged, tuberculum sellae on the front and dorsum sellae in the rear.[1–4]

Two anterior and two posterior clinoid processes form a protrusion on the pituitary fossa, and these are the structures that protect the pituitary gland in the sella turcica. The extensions of the sphenoid bone's ala minor to the anterior and medial form the anterior clinoid processes. The endings of the dorsum sellae form the posterior clinoid processes.[1,4,5]

Sella turcica is a bony structure that is closely related with the pituitary gland, and is of both anatomical and clinical importance. The sellar and parasellar regions are anatomically complex structures where neoplastic, infectious, inflammatory, developmental and vascular pathologies may develop.[2,6]

Research on sella turcica focuses not only on its dimensions, but also on its morphology. Sella morphology is important in both evaluating treatment outcomes

**This study has been presented as a poster at the 30th Annual Conference of Human Anatomy and Physiology Society in Atlanta, Georgia, USA in 2016.*

and late developmental changes, and in assessing the cranial morphology. The anatomy of the sella turcica and clinoid processes may vary widely among individuals.[5,7,8] Variations in sella turcica size are commonly observed and associated with the pathologies involving this region.[1] Knowledge on the anatomy of the sellar region is important for neurologists and neurosurgeons in their assessments of the pathologies in this region. Acknowledgement of sellar area variations is also important in preventing injuries of the structures that surround the sella turcica during surgery. When surgeons are familiar with the variations, they can notice them during pre-operative radiological analyses. In addition, knowledge on potential variations may alter the choice of surgical technique, operative approach and surgical devices.[1,9]

It is important to know the normal dimensions of the sella turcica in healthy individuals to be able to evaluate pathologic sella turcica. The purpose of this study was therefore to measure the size and describe the morphology of sella turcica in a Turkish population, and to compare them with earlier studies on the sella.

Materials and Methods

This study was conducted in the Research and Practice Hospital of Medical School of Afyon Kocatepe University. The subjects included were chosen amongst individuals from a Turkish population aged 17 to 70 years, admitted to the outpatient clinic of the Department of Radiology for any reason and underwent cranial computed tomography (CT) scanning. Individuals with pituitary gland pathology, e.g. tumor, cyst, hemorrhage, and those who suffered from a head trauma, high brain pressure and with cerebrovascular pathology were excluded from the study. The study included 101 (60 males, 41 females) healthy individuals. Morphometric measurements were performed using eight parameters on the sagittal section that is closest to the mid-sagittal section (**Figure 1**).

These parameters were:

- **Sella length (SL):** The distance between tuberculum sellae (TS) and dorsum sellae (DS) points.
- **Sella width (SW):** The longest antero-posterior length measured parallelly from the most anterior and posterior points of sella turcica to the Frankfort horizontal plane (FH).
- **Sella height anterior (SHA):** The vertical distance measured from TS through sella turcica base to the FH plane.
- **Sella height posterior (SHP):** The vertical distance measured from DS through sella turcica base to the FH plane.
- **Sella height median (SHM):** The vertical distance measured from the midpoint between TS and DS to the FH plane.
- **Sella area (STA):** The value, in mm^2, of the line between TS and DS included in the sella.
- **Sella turcica depth (DP):** The length of the line drawn vertically from the deepest point of the sella turcica in the direction of the sella turcica length.
- **Sella turcica antero-posterior diameter (AP):** The distance measured from the tuberculum sellae to the backmost point in the interior surface of the posterior wall of the pituitary fossa.

The subjects were grouped into seven decades: ages from 17 to 20 years as the second decade, from 21 to 30 years as the third decade, ages from 31 to 40 years as the fourth decade, ages from 41 to 50 years as the fifth decade, ages from 51 to 60 years as the sixth decade, and ages from 61 to 70 years as the seventh decade.

Data obtained from the study were evaluated using IBM SPSS (Statistical Package for the Social Sciences, version 20.0; IBM, Chicago, IL, USA) software. Descriptive data were presented as mean ± standard deviation. The independent samples t-test was used for paired groups when comparing parametric values, whereas Kruskal-Wallis test was used when comparing multiple groups for non-parametric data. Correlation analyses among the groups were performed using Pearson's correlation test. Statistical significance in inter-group comparisons was set at $p<0.05$.

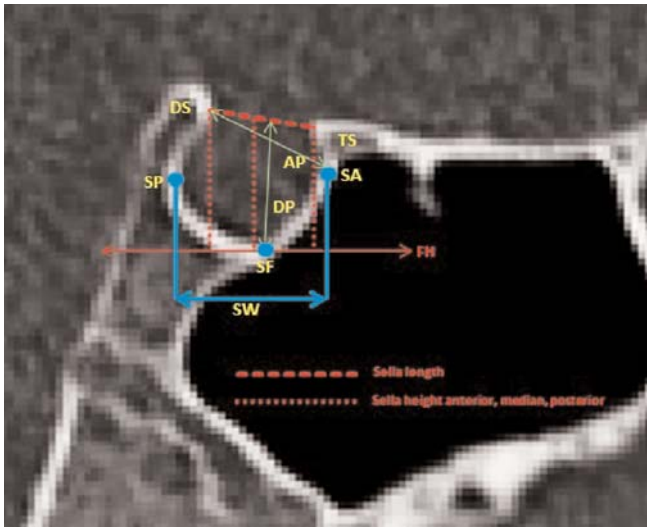

Figure 1. Linear measurements of sella turcica. **TS**: tuberculum sellae, **DS**: dorsum sellae, **DP**: sella depth, **AP**: sella anteroposterior diameter, **SW**: sella width, **FH**: Frankfort horizontal plane, **SF**: sella floor.

Table 1
Parameters of sella turcica morphometry. Values are mean ± standard deviation (SD), all in mm, except for sella area (mm²).

Parameters	All patients (n=101)		Males (n=60)		Females (n=41)		p
	Min–Max	Mean±SD	Min–Max	Mean±SD	Min–Max	Mean ± SD	
Sella length	4.03-14.4	9.18±1.91	4.03-14.05	9.64±1.97	5.07-14.4	8.5±1.63	0.003*
Sella width	6.55-15.07	10.41±1.74	7.34-15.07	10.86±1.81	6.55-12.8	9.75±1.4	0.001*
Sella height anterior	4.07-11.83	8.09±1.65	4.07-11.7	8.05±1.79	5.11-11.83	8.15±1.45	0.767
Sella height median	4.03-10.83	7.71±1.24	4.03-10.83	7.7±1.32	5.3-10.34	7.73±1.12	0.898
Sella height posterior	3.45-10.54	7.48±1.34	3.45-10.39	7.5±1.39	4.47-10.54	7.45±1.28	0.837
Sella area	27.79-121.01	69.15±17.45	35.5-121.01	70.42±18.24	27.79-104.67	67.29±16.25	0.377
Sella depth	4.03-11.43	7.87±1.37	4.03-11.43	7.79±1.45	5.3-10.75	7.98±1.26	0.508
Sella antero-posterior diameter	6.85-16.24	11.48±1.82	6.85-15.7	11.73±1.9	8.12-16.24	11.11±1.66	0.093

*p≤0.05.

Results

The subjects included in the study had an age range of 17 to 70 years, and the average age was 40. The mean sella turcica length was 9.64 mm in males and 8.5 mm in females, and 9.18 mm overall. The mean sella turcica width was 10.86 mm in males and 9.75 mm in females, and 10.41 mm in males and females. The length and width of sella turcica were different between males and females ($p<0.05$). Mean values for anterior, median and posterior heights, depth and anteroposterior diameter of the sella turcica were not found significantly different between males and females ($p>0.05$) (**Table 1**). There was an increase in all dimensions of sella turcica with age. However, this increase was statistically significant only in the length, width, median and posterior height, and area of the sella turcica ($p<0.05$) (**Figures 2–5**). When dimensions of sella turcica were assessed based on decades, only the sellar area was found to increase significantly, with maximum dimension in the seventh decade (**Table 2**, **Figure 3**).

Discussion

Sella turcica is an important component of the middle cranial fossa, and knowing its normal dimensions is important in diagnosing some pathologies.[10,11] Meschan[12] emphasized that measurements of sella turcica should be undertaken so that intrasellar lesion enlargement as well as increased intracranial pressure can be identified.

Najim and Al-Nakib,[13] in their lateral cephalometric radiography study in individuals aged 13 to 25 years from the Iraqi population, measured the sella turcica length, depth and anteroposterior diameter. Their findings were virtually close to our findings compared to

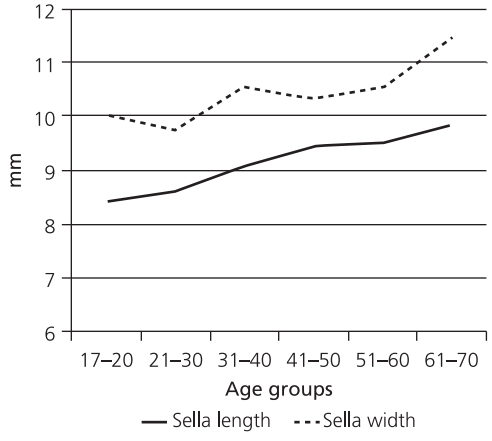

Figure 2. Graphic analysis of sella length and width according to age groups.

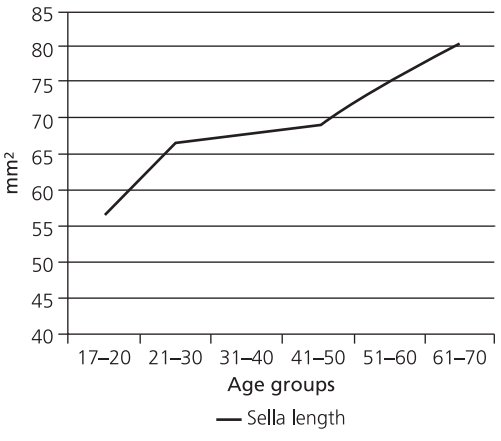

Figure 3. Graphic analysis of sella area according to age groups.

Table 2
Comparison of sella turcica morphometry according to the decades. Values are mean ± standard deviation, all in mm, except for sella area (mm²).

Parameters (n=101)	Decade 2 (17–20) (n=11)	Decade 3 (21–30) (n=15)	Decade 4 (31–40) (n=23)	Decade 5 (41–50) (n=26)	Decade 6 (51–60) (n=16)	Decade 7 (61–70) (n=10)	p
Sella length	8.43±1.65	8.61±1.19	9.06±1.53	9.43±2.28	9.51±2.25	9.84±2.13	0.352
Sella width	10.05±2.05	9.74±1.4	10.55±1.85	10.33±1.69	10.55±1.44	11.45±1.93	0.234
Sella height anterior	7.29±2.01	8.52±1.01	7.94±1.67	8.07±1.77	8.36±1.92	8.22±1.08	0.399
Sella height median	6.66±1.49	7.88±0.61	7.64±1.11	7.71±1.43	8.14±1.11	8.00±1.15	0.169
Sella height posterior	6.44±1.52	7.44±0.83	7.41±1.16	7.30±1.37	8.05±1.3	8.35±1.42	0.089
Sella area	56.40±21.21	66.52±10.05	67.71±15.93	69.12±18.42	75.30±14.43	80.61±19.61	0.038*
Sella depth	7.21±1.95	7.96±0.77	7.77±1.31	7.76±1.49	8.27±1.19	8.25±1.33	0.495
Sella anteroposterior (AP) diameter	10.89±1.94	11.04±1.36	11.74±1.81	11.50±1.92	11.61±1.91	11.86±2.07	0.696

*p≤0.05.

other earlier studies. In a study on sella anteroposterior diameter in the Saudi Arabia population, Sakran et al.[1] also found results similar to those in our study. We believe that sella depth does not decrease with age, and it can therefore be compared across studies regardless of the age groups studied. Our literature search did not yield enough studies on sella width, sella height anterior, sella height median, sella height posterior or sella area. However, of the studies performed, the study by Valizadeh et al.[14] on the median height and area of the sella in Iranian subjects aged 14 to 26 years has the closest results to our study, with respect to lateral cephalometric radiography. When these consistent findings were pooled, geographical proximity seems apparent. One may conclude that this may be due to the racial and genetic closeness. However, the number of subjects in our study and the differences in radiographic imaging, measurement methods and in individual performing the measurements etc. may influence the results, and we must underline that these differences should be taken into account during comparison (**Table 3**).

In our study, we determined that the sella turcica differed significantly between males and females only in length and width. When Hasan et al.[14] compared the dimensions of the sella turcica by gender and found no relevant differences between males and females, expect in sella height anterior. Ashraf et al.,[1] Shah et al.,[8] Najim and Al-Nakib,[13] Olubunmi et al.[15] and Nagaraj et al.[16] reported that sella morphometry did not differ between males and females. Silverman[17] found differences in the size of sella between genders in the preadulthood period, but no difference between males and

Figure 4. Graphic analysis of sella height anterior, median and posterior according to age groups.

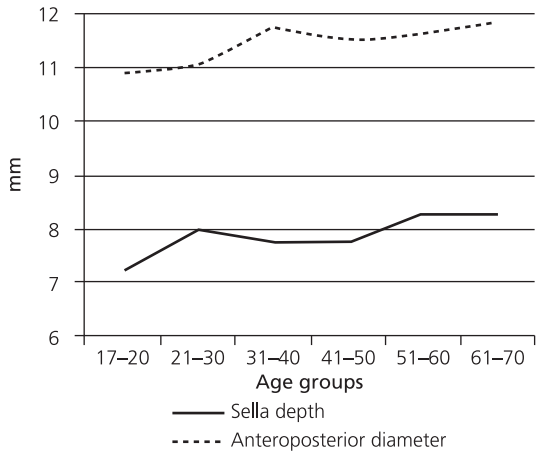

Figure 5. Graphic analysis of sella depth and anteroposterior diameter according to age groups.

Table 3
Comparison of the parameters of sella turcica in our study in a Turkish population with previous studies (data are in mm).

	Sella length	Sella width	Sella height anterior	Sella height median	Sella height posterior	Sella area	Sell depth	Sella AP diameter
Ruiz et al.[7]	10.31	-	-	6.33	-	41.21	-	-
Shah et al.[8]	11.3	-	-	-	-	-	9.9	13.9
Najim and Al-Nakib[13]	9.22	-	-	-	-	-	7.56	11.56
Olubunmi et al.[15]	9.81	-	-	-	-	-	8.49	11.37
Nagaraj et al.[16]	9.52	-	-	-	-	-	8.21	11.83
Present study	9.18	10.41	11.83	10.83	10.54	69.15	7.87	11.48

females in the adult period. In short, we could not find any studies to support these differences we observed between the genders.

In our study, there was a statistically significant increase in sella turcica length, width, median and posterior height and area with age. In the study by Najim and Al-Nakib,[13] a statistically significant difference was noted only in sella depth. Chauhan et al.[4] reported that sella dimensions were larger in the higher age group compared to the lower age group. Similarly, Preston[18] determined a close correlation between sella area and age. Nagaraj et al.[16] described increasing sella depth and AP diameter with increasing age. Hasan et al.[14] reported that sella turcica dimensions differed significantly between age groups. Conversely, Olubunmi et al.[15] determined that sella turcica dimensions showed no statistically significant difference with age. In summary, it appears from our study and the majority of earlier studies that there is an increase in sella dimensions with age.

It has been reported that radiological methods including CT and magnetic resonance imaging (MRI) provide more sensitive results compared to cephalometric radiography in conditions involving this anatomic area such as pituitary gland tumors.[4,19] We, therefore, believe that our CT study provides more accurate results than other studies that typically use cephalometric radiography.

Knowing the normal anatomy and variations of sella turcica is important for neurologists and neurosurgeons who deal with the pathologies of this area. We believe that sella turcica dimensions of the Turkish population obtained with CT in this study will provide guidance to clinicians for pituitary gland morphometry and that these measurements can be used in detecting pathologies in the sellar and parasellar area.

References

1. Sakran AMEA, Khan MA, Altaf FMN, Fragella HEH, Mustafa AYAE, Hijazi MM, Niyazi RA, Tawakul AJ, Malebari AZ, Salem AAA. A morphometric study of the sella turcica; gender effect. International Journal of Anatomy and Research 2015;3:927–34.
2. Venieratos D, Anagnostopoulou S, Garidou A. A new morphometric method for the sella turcica and the hypophyseal fossa and its clinical relevance. Folia Morphol (Warsz) 2005;64:240–7.
3. Yamashita S, Resende LA, Trindade AP, Zanini MA. A radiologic morphometric study of sellar, infrasellar and parasellar regions by magnetic resonance in adults. Springerplus 2014;3:291.
4. Chauhan P, Kalra S, Mongia SM, Ali S, Anurag A. Morphometric analysis of sella turcica in North Indian population: a radiological study. International Journal of Research in Medical Sciences 2014;2:521–6.
5. Halıcıoglu K, Yolcu G, Yavuz İ. Sella tursikanın köprülenmesi ve boyutları ile iskeletsel anomaliler arasındaki ilişki. Atatürk Üniversitesi Diş Hekimliği Fakültesi Dergisi 2009;19:177–80.
6. Rennert J, Doerfler A. Imaging of sellar and parasellar lesions. Clin Neurol Neurosurg 2007;109:111–24.
7. Ruiz CR, Wafae N, Wafae GC. Sella turcica morphometry using computed tomography. Eur J Anat 2008;12:47–50.
8. Shah AM, Bashir U, Ilyas T. The shape and size of the sella turcica in skeletal class I, II, and III in patients presenting at Islamic International Dental Hospital, Islamabad. Pakistan Oral and Dental Journal 2011;31:104–10.
9. Renn WH, Rhoton AL Jr. Microsurgical anatomy of the sellar region. J Neurosurg 1975;43:288–98.
10. Chen JK, Tang JF, Du LS, Li H. Radiologic analysis of 540 normal chinese sella turcica. Chin Med J (Engl) 1986;99:479–84.
11. Lang J. Structure and postnatal organization of heretofore uninvestigated and infrequent ossifications of the sella turcica region. Acta Anat (Basel) 1977;99:121–39.
12. Meschan I. An atlas of anatomy basic to radiology. Philadelphia (PA): WB Saunders; 1975. p. 234–348.
13. Najim AA, Al-Nakib L. A cephalometric study of sella turcica size and morphology among young Iraqi normal population in comparison to patients with maxillary malposed canine. J Bagh College Dentistry 2011;23:53–8.

14. Hasan HA, Alam MK, Yusof A, Mizushima H, Kida A, Osuga N. Size and morphology of sella turcica in Malay populations: a 3D CT study. Journal of Hard Tissue Biology 2016;25:313–20.

15. Olubunmi OP, Yinka OS, Oladele OJ, Adimchukwunaka GA, Afees OJ. An assessment of the size of sella turcica among adult Nigerians resident in Lagos. International Journal of Medical Imaging 2016;4:12–6.

16. Nagaraj T, Shruthi R, James L, Keerthi I, Balraj L, Goswami RD. The size and morphology of sella turcica: a lateral cephalometric study. Journal of Medicine, Radiology, Pathology and Surgery 2015;1:3–7.

17. Silverman FN. Roentgen standards fo-size of the pituitary fossa from infancy through adolescence. Am J Roentgenol Radium Ther Nucl Med 1957;78:451–60.

18. Preston CB. Pituitary fossa size and facial type. Am J Orthod 1979;75:259–63.

19. Kricheff II. The radiologic diagnosis of pituitary adenoma: an overview. Radiology 1979;131:263–5.

Online available at:
www.anatomy.org.tr
doi:10.2399/ana.16.047
QR code:

Correspondence to: Ozan Turamanlar, MD, PhD
Department of Anatomy, Faculty of Medicine,
Afyon Kocatepe University, Afyonkarahisar, Turkey
Phone: +90 272 246 33 04
e-mail: ozanturamanlar@hotmail.com

Conflict of interest statement: No conflicts declared.

anatomy
www.anatomy.org.tr
An International Journal of Experimental and Clinical Anatomy

Original Article

www.anatomy.org.tr
Received: July 18, 2016; Accepted: December 8, 2016
doi:10.2399/ana.16.050

Age-related morphological changes in the thymus of indigenous Large White pig cross during foetal and postnatal development

Casmir Onwuaso Igbokwe, Kelechi Ezenwaka

Department of Veterinary Anatomy, Faculty of Veterinary Medicine, University of Nigeria, Nsukka, Nigeria

Abstract

Objectives: The thymus is found in all vertebrates, the structure of the thymus differs markedly among species. This study investigated the gross anatomy, morphometric and histological changes of the thymus in the indigenous Large White pig cross at various ages of foetal and postnatal periods.

Methods: The study used slaughter house specimens obtained after adequate health inspection and slaughter. A total of fifty three samples of thymus collected from foetal, prepubertal and pubertal pigs with varied weights were used for gross and histological study.

Results: The absolute thymus weight showed significant ($p<0.05$) increase in size with advancing foetal age, but the increment was not significant in the postnatal stage. The capsule was initially thin and indistinct at 30–45 days thymus, but increased in thickness with progression of gestation. A distinct evidence of lobulation was observed in foetuses of 46–58 days of gestation. Interlobular septa matured and increased in vascularization with age, such that they were highly vascularized at 77–90 days thymus. The boundary of cortex-medulla was partially distinguishable at 46–58 days foetuses and distinctively demarcated at 60–75 days of gestation. Various sizes of lymphocytes were apparent in the cortex at 60–75 days impacting a strong basophilic colour to the cortex. Rudiments of epithelial cells were seen as eosinophilic clumps at 30–45 day thymus. Apparently well differentiated epithelial cells with dense consistency were observed at 46–58 days thymus. Macrophages were seen at the 95–113 days and were quite distinct at the prepubertal and pubertal age. Early forms of Hassal's corpuscles were present at 46–58 day thymus and increased in number with age.

Conclusion: The present study has demonstrated that the morphology of the thymus changed with age and the cellular components of the thymus attain morphological maturity during the late foetal period and may be involved in moderate prenatal immunological functions.

Keywords: foetal; indigenous pigs; morphology; thymus

Anatomy 2017;11(1):12–20

Introduction

The thymus is part of the lymphatic system that is found in all vertebrates, with the exception of the jawless fish, such as lampreys.[1] It is considered a primary organ due to its central role as being the centre for development and 'training' of T cells, which then disperse throughout the body to direct and assist with immunity. Thymus together with parathyroids is derived from single primordium in the third pharyngeal pouches of the endodermal foregut of most domestic animals. These two organs eventually migrate to their final location and separate during embryonic development.[2] For instance, in the mouse, the primordial in the third pharyngeal pouch are completely separated into thymus and parathyroid domains at embryonic day 11.5.[3] By embryonic day 12, the thymus-parathyroid primordia have completely detached from the pharynx and started their separation into two discrete organs and their migration towards the anterior of the thoracic cavity. The thymus development is a highly dynamic and complex process, involving reciprocal tissue interactions between epithelial cells derived from endoderm of the anterior foregut and neural crest-derived mesenchyme to

form rudiments of thymus. Thymocyte progenitors are attracted to this rudiment and support their differentiation and functional maturation into self-tolerant diverse groups of T cells are supported.[1]

The structure of the thymus differs markedly among species. The differences include the number per animal, anatomical position, structure of the thymic lobes, developmental origin and developmental processes.[4] The anatomical position of the thymus in the neck (cervical thymus) and or in the thorax (thoracic thymus), differ amongst vertebrates. Most domestic animals have dominant cervical thymus.[5] The mammalian thymus usually undergoes atresia and begins to involute around the period of young and adulthood pubescence). In this period, connective and adipose tissue invade the organ as the thymic parenchyma becomes reduced. There is progressive loss of mostly immature, cortical thymocytes and clear reorganization of the organ architecture, involving the loss of definition of the cortex and medulla.[6] Stressors, such as cold and pregnancy, can cause the thymus to involute more severely.[7] It also varies amongst species, strain and sex.

The local breed of pig (swine) was used for this study because swine is considered one of the major animal species of choice apart from rodents, used in translational research especially in preclinical toxicological testing of drugs.[8] In addition, most of the available literature is on development of the thymus in laboratory animals (rats, mice, rabbits and guinea pigs) and other exotic species and only a few domestic animals of the tropical climate have been investigated.[9,10–13] Even so, there was little emphasis on histological changes during foetal growth. It is expected that there would be variations in structure from exotic species in the time of histological maturation of the thymus in the indigenous cross because of differing feeding, management and climatic factors in the tropical environment.

The main objective of this investigation is to evaluate the gross anatomy, morphometric and histological changes of the thymus in the indigenous Large White pig cross at various ages of foetal and postnatal periods, with emphasis on histological changes during growth. The baseline information obtained useful in prenatal and postnatal clinical and pathological diagnosis of health conditions in the indigenous Large White pig cross.

Materials and Methods

Animals

The study samples were obtained from apparently healthy adult indigenous Large White cross slaughtered for meat at the Nsukka slaughter house. They comprised thymus from 36 foetuses (males and females), of pregnant animals slaughtered unknowingly, seven prepubertal and ten pubertal pigs (males and females). Age estimation of the foetuses was done using Crown-Rump-Length (CRL) which was measured with threads and meter rule. The age was estimated with a chart for estimation using CRL in domestic animals by McGeady et al.[14] and the pre-pubertal and pubertal age were estimated by dentition[15] and farm record information from pig sellers. The weights of all animal were obtained with mobile scale for postnatal period (Tefal Electronic kitchen scale, Rumilly, Haute-Savoie, France) and top loader Mettler weighing balance (Mettler Toledo Inc., Greifensee, Switzerland) for foetuses. The sex of the animal was not considered in this present study. The Research and Ethics committee of the University of Nigeria, Nsukka, Nigeria approved this work.

Gross dissection by parasternal incision was carried out on the foetuses, while the postnatal samples (prepubertal and pubertal) were obtained after slaughter and before singeing. The thymus in all cases was removed after thorough trimming off the adjacent fat and connective tissue. The thymic weights were measured prior to fixation and following removal of adjacent fat and connective tissue. In the older pubertal pigs, adipose and connective tissues from cranial mediastinum containing thymic tissues were collected and fixed without weighing following methods of other investigators.[16]

Fixed tissue sections were processed for study following routine histological procedure.[17] Sections were cut at 6 µm, stained with haematoxylin and eosin (H&E), and were examined under microscope. Selected tissue sections were captured into a computer with Moticam 2005 camera attachment (Moticam, Xiamen, China). For histometry, the diameters of the Hassal's corpuscles were measured with ocular micrometer calibrated with stage micrometer gauge. The average of transverse and longitudinal diameters was obtained in the spherical and round corpuscles. Several corpuscles per section were randomly measured. Polymorphic corpuscles were ignored. Using IBM SPSS (Statistical Package for the Social Sciences, version 16.0; IBM, Chicago, IL, USA) software, the means and standard error of mean (SEM) of diameter of Hassal's corpuscles were computed for each development age of thymus. Data were analyzed statistically using analysis of variance. Duncan's multiple range test was used to separate variant means, and significance was accepted at $p<0.05$.

Results

Gross anatomical observations

The thymus of the prenatal (foetal) pig in all stages of development was grayish-red in color, soft in consisten-

cy and consisted of cervical and thoracic parts which were superficially divided into lobules. The cervical part was on the ventro-lateral surface of the neck and was from the origin the digastricus muscle close to the carotid arteries on either side of the neck to the thoracic inlet, where the left and right thymus fused indistinctly. It was related superficially to the cranial portion of the omohyoideus muscle, while the thoracic part was in the precardial aspect of the thoracic cavity and related to the base of the heart (**Figures 1a** and **b**). In the pubertal pigs, a slight decrease in the size of the thymus was observed. The cervical thymus and remnants of thoracic the thymus was therefore located in the cranial mediasternal space related to the base of the heart amongst copious adipose and connective tissue. It was not clearly identifiable from these surrounding structures.

The gross morphometry and histometry of the thymus during development is shown in **Table 1**. The thymic absolute weights increased with advance of gestation and the maximum weight was obtained in the prepubertal stage, and followed by a slight decrease in weight in the old adult stage (It was not significant at $p< 0.05$). The diameter of the Hassal's corpuscles measured microscopically increased with gestational age and this was significant at foetal ages of development ($p<0.05$).

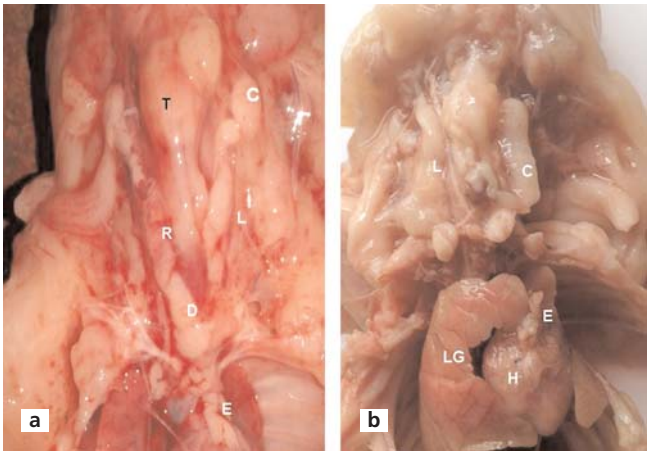

Figure 1. (**a**) Gross photograph of foetal thymus (77–79 daysl) showing left (**L**) and right (**R**) thymus with cervical part (**C**), thoracic part (**E**), caudal cervical (**D**). The heart (**H**) and trachea (**T**) are indicated. (**b**) Relationship of the thymus with other visceral structures are shown, lungs (**LG**), heart (**H**), cervical thymus (**C**) and thoracic thymus (**E**). Scale bar=15 mm. [Color figure can be viewed in the online issue, which is available at www.anatomy.org.tr]

Histological observations

In the pig fetuses of 30–45 days of gestation, the thymus showed very thin, indistinct capsule covering of the organ and there was no evidence of lobulation. Simple squamous and low cuboidal epithelial cells were seen enveloping the capsule of the organ. Primitive lymphoid cells (lymphoblast) with intermingled mesenchymal connective tissue were present in the parenchyma. The nuclei of these cells varied considerably in size but showed similar basophilic staining characteristics. The thymus was devoid of blood vessels. There was no demarcation into cortex and medulla, and the inner part of the organ which would later differentiate into the medulla contained large eosinophilic cells that resembled epithelio-reticular cells, few lymphoblast and primordial of Hassal's corpuscles (**Figures 2a** and **b**).

In 46–58 days of gestation, there was a very thin capsule covering the organ with evidence of lobulation and a very thin interlobular septae with poor vascularisation. Cells present were lymphoblast, large lymphocytes, small lymphocytes, epithelio-reticular cells and developing macrophages. The thymus partially differentiated

Table 1
Morphometry of the thymus of the Indigenous local cross pig at different ages of development.

Estimated age days (d) / months (m)	Animal weight (g)	Thymus weight absolute (g)	Relative thymus weight	Diameter of Hassal's corpuscles (μm)
30–45§	13.7±1.4 (8.3–14.1)	0.07^{a}±.01 (0.06–0.08)	.0054	4.4^{a}±0.1 (3.5–4.3)
46–58§	77.4±3.4 (66.4–78.3)	0.23^{b}±.03 (0.21–0.27)	.0029	3.2^{b}±0.9 (7.2–9.1)
60–75§	170.3±1.8 (142.4–187.6)	0.38^{c}±.12 (0.32–0.39)	.0022	10.9^{b}±0.3 (8.3–10.8)
77–90§	238.1±6.4 (232.6–318.4)	0.46^{d}±.04 (0.41–0.48)	.0019	16.5^{c}±0.3 (14.2–16.7)
95–113§	1096.5±5.1 (1023.4–10170.9)	1.72^{e}±.14 (1.65–1.74)	.0016	19.6^{d}±0.7 (18.5–19.8)
Prepubertal (3–6 m)	4003.5±16.3	1.94^{f}±.06 (1.79–1.98)	–	21.6^{d}±0.6 (20.4–22.8)
Pubertal (10–18 m)	28500.6±11.3	1.90^{f}±.03 (1.98–2.01)	–	26.2^{e}±0.8 (25.6–30.1)

Means in the same column with different superscripts (^{a,b,c,d,e,f}) differ significantly ($p<0.05$).

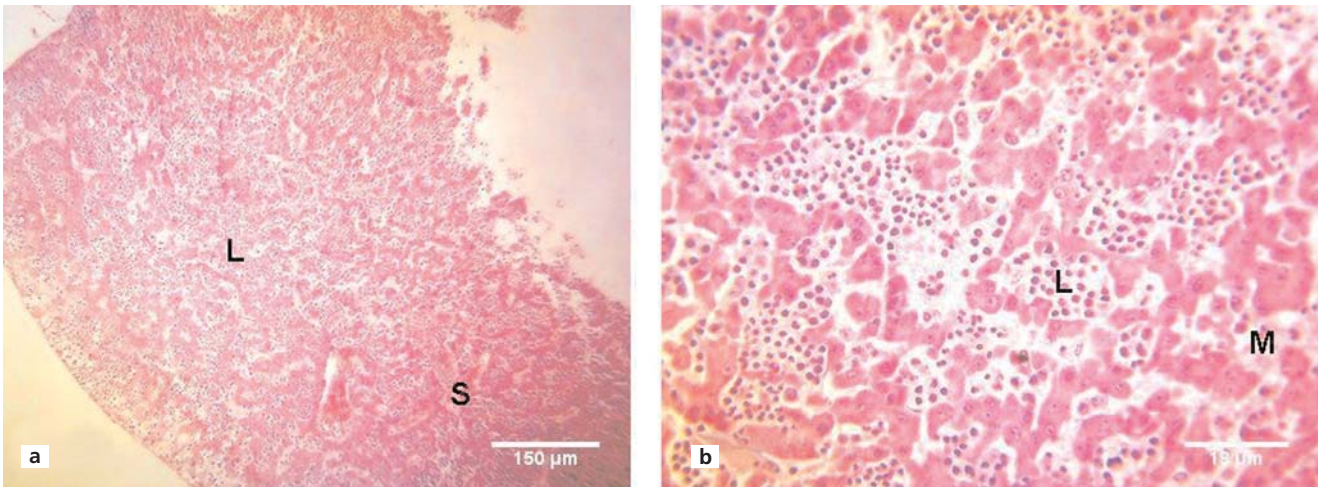

Figure 2. (**a**) Photomicrograph of thymus at 30–45 days showing rudimentary parenchyma (**L**) and septa (**S**). (**b**) Primitive lymphoid cells with mesenchymal connective tissue (**L**) and medulla (**M**). H&E stain. [Color figure can be viewed in the online issue, which is available at www.anatomy.org.tr]

into cortex and medulla with the medulla containing large cells with slightly eosinophilic cytoplasm that resembled the earlier epithelial cells and a few primitive Hassal's corpuscles (**Figures 3a** and **b**).

In thymus at gestation days 60–75, the parenchyma cellular components increased in size and differentiation compared to the previous age, and was completely divided by connective tissue septae (interlobular septa). There was an obvious demarcation into cortex and medulla; the medulla cells were less basophilic and less closely packed than the surrounding cortex. Lymphocytes and lymphoblast were much denser in the cortex. Hassal's corpuscles matured further at this age and were however few in number. Few amorphous Hassal's corpuscles were also seen. The vascularization increased (**Figures 4a** and **b**).

The thymus at 77–90 days of gestation was much larger compared to previous ages and completely lobulated with obvious demarcation into cortex and medulla. The medulla cells were less basophilic and less closely packed than the surrounding cortex. Lymphocytes were now much denser in the cortex. Well differentiated and Hassal's corpuscles were seen (**Figures 5a** and **b**) and

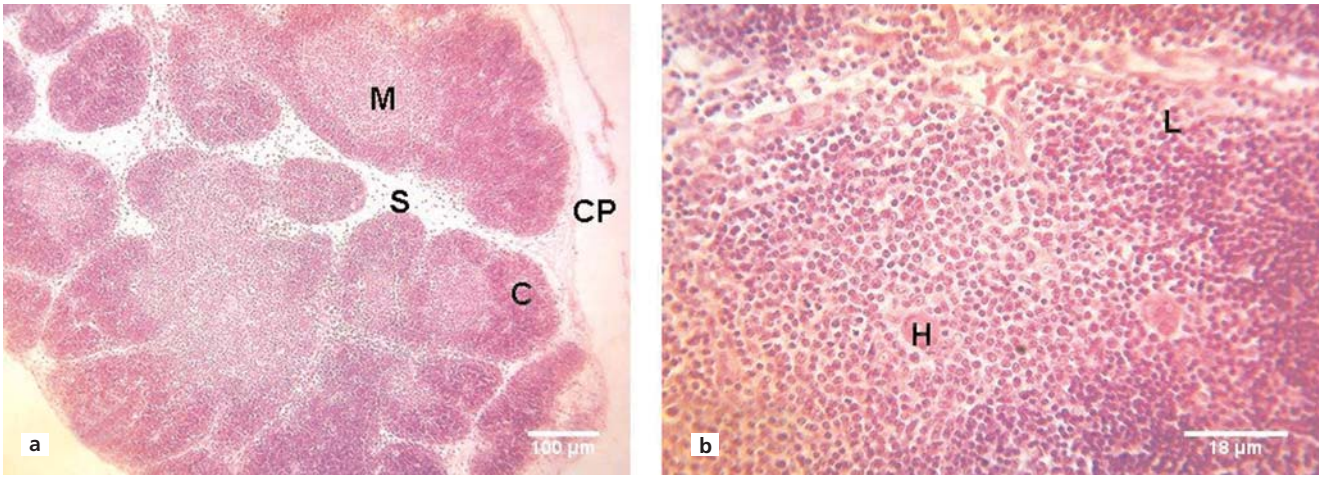

Figure 3. (**a**) Photomicrograph of thymus at 46–58 days showing lobulated organ with early divisions into cortex (**C**), medulla (**M**), interlobular tissue (**S**) and capsule (**CP**). (**b**) Early lymphocytes (**L**) and primitive Hassal's corpuscles (**H**). H&E stain. [Color figure can be viewed in the online issue, which is available at www.anatomy.org.tr]

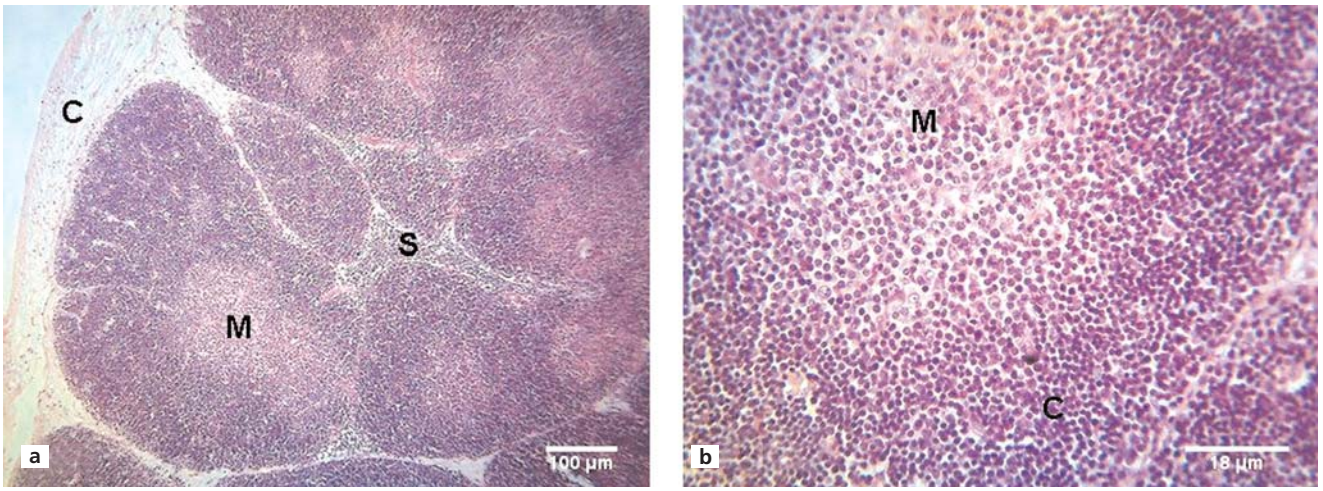

Figure 4. (**a**) Photomicrograph of thymus at 60 days showing cortex (**C**), well differentiated parenchyma with medulla (**M**) and and interlobular septa (**S**). (**b**) Medulla (**M**) with lymphocytes, cortex (**C**) and Hassal's corpuscles (**arrow**). H&E stain. [Color figure can be viewed in the online issue, which is available at www.anatomy.org.tr]

were more in number. The interlobular septae was highly vascularized.

The thymus at 95–113 gestational days showed a completely lobulated organ with fully differentiated cellular components and with a clear demarcation into cortex and medulla. The medullary cells were less basophilic and less closely packed than the surrounding cortex. Lymphocytes were packed in the cortex making the cortex deeper staining than the medulla. Mature Hassal's corpuscles were seen in the medulla and increased in number from previous age (**Figures 6a** and **b**).

In this study, there were no clear-cut histological differences between the previous late foetal thymus and the prepubertal thymus. However, in the prepubertal thymus (**Figures 7a** and **b**), most cellular components including the lymphocytes epithelio-reticular cells, trabeculae and Hassal's corpuscles increased in size and number from what was observed in the previous age. In the pubertal pig thymus of up to one year, Hassal's corpuscles displayed different sizes and shapes, being round or oval and even amorphous ones were present.

The pubertal thymus of up to 18 months (**Figures 8a** and **b**), showed evidence of morphological thymic invo-

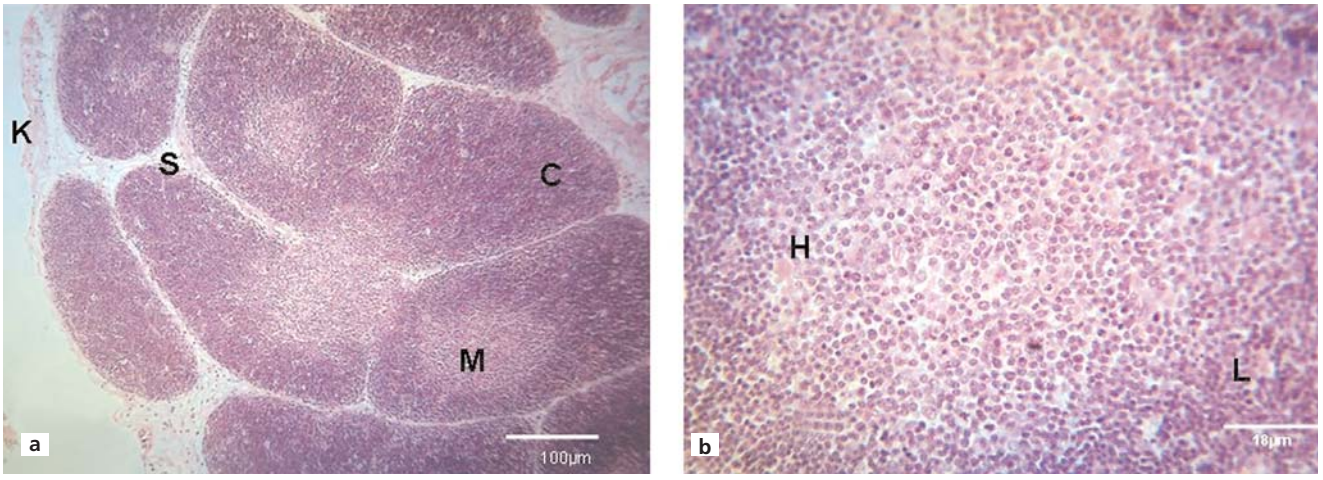

Figure 5. (**a**) Photomicrograph showing further maturation at 77–90 days with denser cortex of lymphocytes (**C**) and medulla (**M**), capsule (**K**), septa (**S**). (**b**) Hassal's corpuscles (**H**) and lymphocytes (**L**). H&E stain. [Color figure can be viewed in the online issue, which is available at www.anatomy.org.tr]

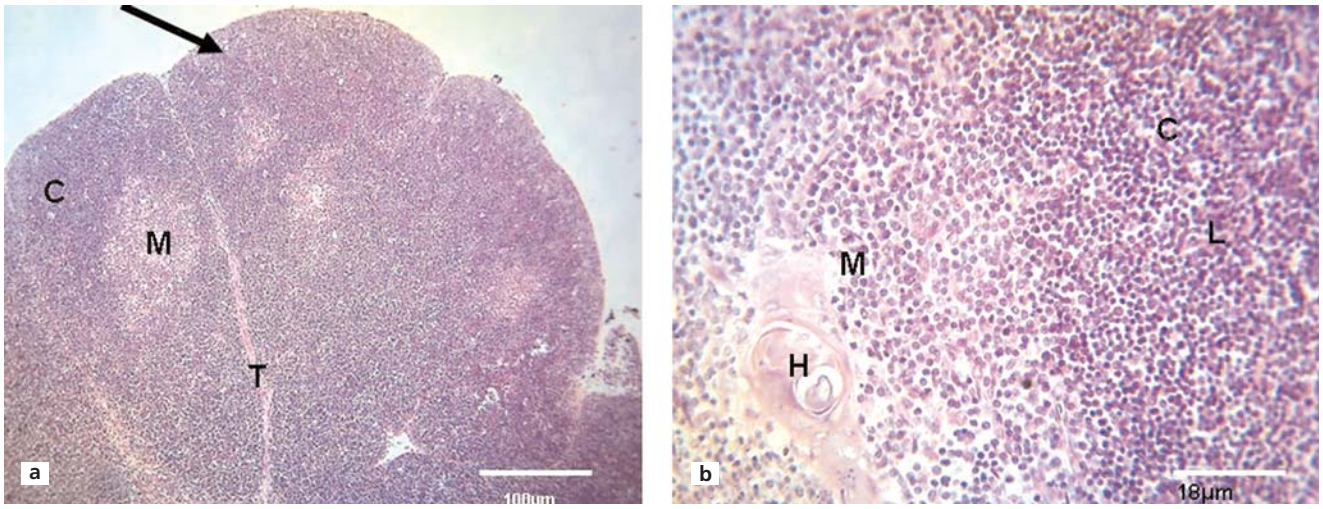

Figure 6. (**a**) Photomicrograph of thymus at 95–113 days showing copiously lobulated organ with cortex (**C**), medulla and well formed interlobular septa (**T**). (**b**) Cortex (**C**) with lymphocytes (**L**) and medulla (**M**) containing Hassal's corpuscle (**H**) with varying shape and size. H&E stain. [Color figure can be viewed in the online issue, which is available at www.anatomy.org.tr]

lution and this was reflected by fewer lymphocytes and epithelial-reticular cells in cortex and medulla. Hassal's corpuscles increased in number with several amorphous ones. Some of these corpuscles and epithelio-reticular cells indicated signs of keratinization and degeneration. There was slight loss in the loss of definition between the cortex and the medulla and increase in the perivascular spaces and the epithelial cells of the medulla became progressively more prominent. Adipose tissue occupied portions of the capsule and interlobular connective tissue.

Generally in development, the capsule was initially indistinct at 30–45 days thymus, but increased in thickness with progression of gestation, such that it was surrounded by fat tissue in the pubertal age. A distinct evidence of lobulation was observed in foetuses of 46–58 days of gestation. Interlobular septa matured and increased in vascularisation with age of development, such that they were highly vascularized at 77–90 days thymus. The boundary of cortex-medulla was partially visible at 46–58 days foetuses and was highly demarcated at 60–75 days of gestation. Various sizes of lymphocytes were apparent in the cortex at 60–75 days impacting a strong basophilic colour to the cortex. The compactness of these cells increased with age in the cortex and medul-

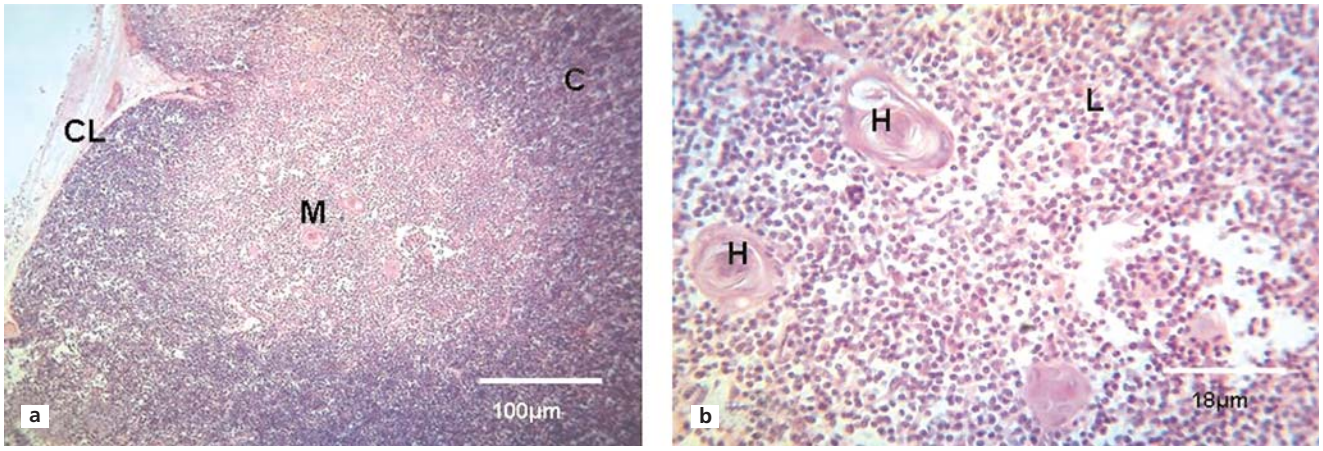

Figure 7. (**a**) Photomicrograph of prepubertal thymus showing capsule (**CL**), medulla (**M**) and cortex (**C**). (**b**) showing that medulla (**M**) contained several whorled pleomorphic corpuscles (**H**) and lymphocytes (**L**) in the cortex. H&E stain. [Color figure can be viewed in the online issue, which is available at www.anatomy.org.tr]

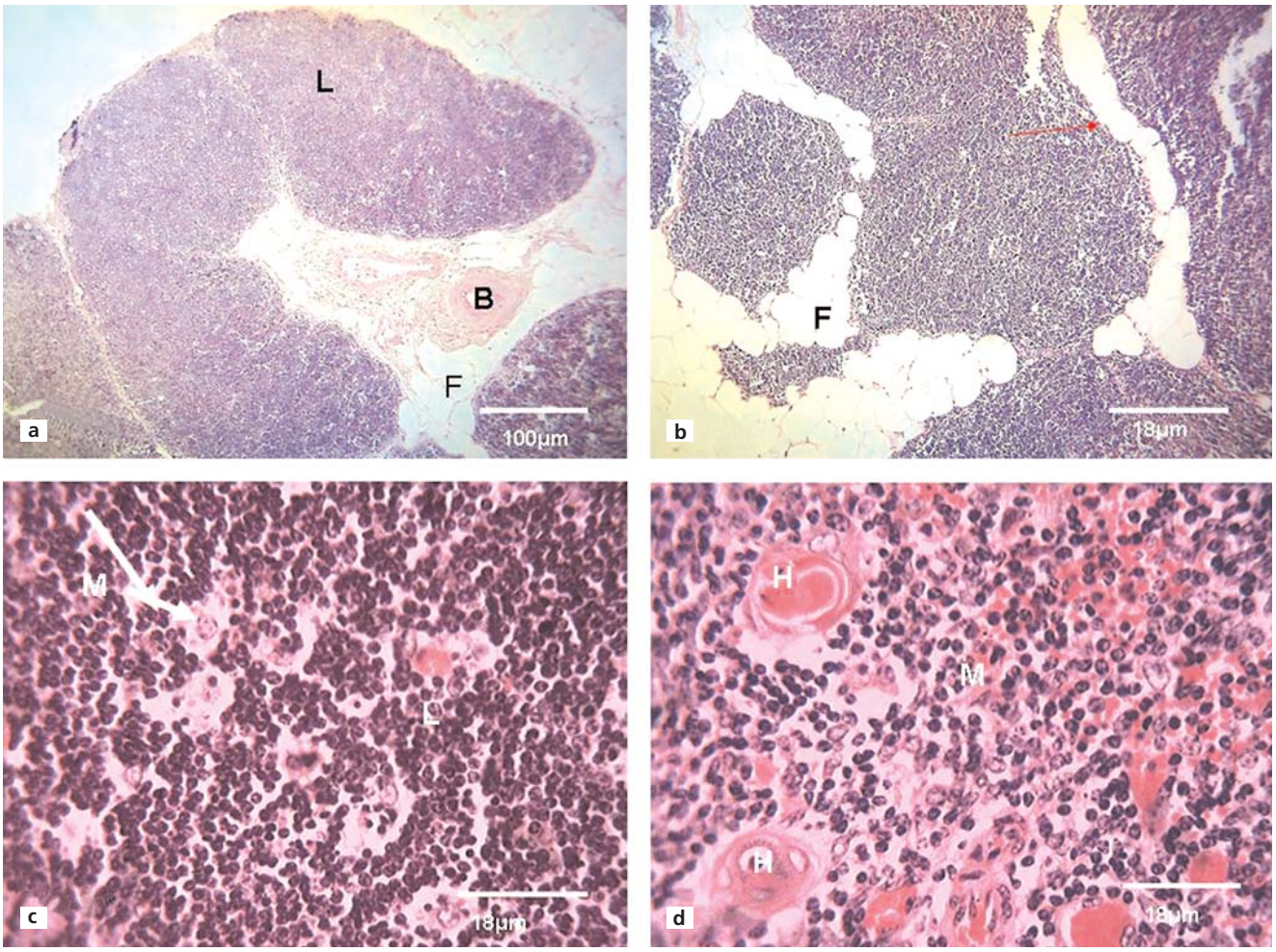

Figure 8. (**a**) Photomicrograph showing evidence of decrease in size of parenchyma; thymic lobes (**L**), septa (**T**) and fatty tissue (**F**). (**b**) Evidence of onset of involution by fatty tissue infiltration (**F**); (**c**) micrographs of older pubertal thymus showing several macrophages (**M**) and lymphocytes (**L**), and in other sections of pubertal thymus (**d**) Hassal's corpuscles (**H**) were keratinized, macrophages (**M**) were also apparent. H&E stain. [Color figure can be viewed in the online issue, which is available at www.anatomy.org.tr]

la. Rudiments of epithelial cells were seen as eosinophilic clumps at 30–45 day thymus and they increased in number with age of development. Apparently differentiated epithelial cells with dense consistency were observed at 46–58 days thymus. Macrophages were seen at the 95–113 days thymus and were quite distinct at the prepubertal and pubertal age. Early forms of Hassal's corpuscles were seen at 46–58 day thymus and they increased in content and shape with age of development. In the pubertal thymus, varied sizes and shape of Hassal's corpuscles were observed with large whorled eosinophilic appearance.

Discussion

In the present investigation, the thymus of prenatal pig consisted of cervical and thoracic parts located in located in the cervical region and cranial pericardial mediastinum. They were initially unlobulated in early fetuses of 30–45 days and gradually increased in size and lobulation with age. This observations has been reported in the ox,[14,18] goat,[11] buffalo[10] and pig.[18] Generally mammals such as sheep, cattle, goat, pigs and horse possess distinct cervical thymuses in addition to the thoracic thymus. In this present report, lobulation was noticed at 46–58 days foetal thymus, while Prasad et al.[11] reported the occurrence of lobulation in goat foetuses of 49–73 days of gestation. This shows the variability of formation of lobules of thymus in animal species. In addition the location of the thymus was more consistent in the cranial pericardial mediastinum of the thoracic cavity in the older pubertal pigs. However, in the guinea pig thymus, unlike other mammals, remains a purely cervical organ. This is due to the greater reduction

of size of thymus due to age-related physiological involution as reported in hybrid pigs by some investigators.[12] Physiological involution is associated with decrease in the cellular components of thymus including lymphocytes and epithelio-reticular cells of the organ.[19]

In this study, there was adherence of the left and right portions of the cervical thymus to form a mass and its connection beyond by a cervico-thoracic isthmus to the thoracic part of the thymus. This finding is similar to findings of in sheep foetus[9] and in buffalo foetus.[10] In addition, the left and right portions of the thymus terminated as a dense lobulated mass on either side of the larynx as also observed in the sheep foetus[9] and in some other domestic animals.[18] The relationship of the thymus to other structures and organs in the neck and thoracic cavity seen in pig foetuses in this study is similar to findings also reported by other authors.[18]

The absolute mean weights of the thymus were significantly higher in the late prenatal stages as compared to the mid prenatal and early prenatal stages in the present study. It is similar to the findings in developing pigs.[19] In addition an overall mean size and weight of thymus showed an increase with advancing of gestation was also reported by some researchers.[11,20] This may suggest onset of remarkable immunological function during the last term of prenatal foetal life. In the present report, the thymus reached it absolute maximum weight in the prepubertal age. Some investigators reported that the maximum thymic weight is reached in the late foetal period in the sheep and Japanese serows *(Capricornis crispus)*.[21] The variations may be related to species differences and climate.

The general histological structure of thymus during the gestational age showed remarkable immaturity in the early foetal age. Most of the typical structural components including capsule, cortex and medulla with lymphocytes, epithelial reticular cellular cells and Hassal's corpuscles in medulla amongst others were very sparse and may not support optimum function. In addition, blood, lymph vessels and nerves were rarely seen at this early foetal age. In late foetuses these components were fully differentiated to possibly support prenatal thymic function. There were numerous lobules and their differentiation into cortex and medulla. There were also presence of thymic corpuscles in the late foetal stage and it increased with age. Similar observations have been seen earlier in prenatal pigs.[22] Functionally active thymic lobules are characterized by the presence of the cortex, medulla and Hassal's corpuscles.[13] These functional components also increased in the prepubertal and early pubertal thymuses. But in the older pubertal thymuses, evidence of involution was noticed in sections and macrophages increased in number. At the pubertal age of about 18 months, lymphocytes and macrophages in its individual lobules were identified along with the cortex and medulla. Adipose tissues were also present in the interlobular tissue and the interlobular tissue was thickened by these fat cells. It indicated early signs of involution. Hassal's corpuscles changed in form with age. In late foetal thymus, it consisted of central degenerated hyaline mass, surrounded by concentrically arranged reticular cells. In older pubertal thymus, signs of polymorphism, keratinization and merging of corpuscles were evident and represented age-related involution. Hassal's corpuscles may have phagocytic function for those lymphocytes that could not mature while moving from cortex into the medulla and could not cross the blood-thymus barrier. It is known that those lymphocytes which had not acquired the specific markers on their membranes are phagocytosed by Hassal's corpuscles.[22] Hassal's corpuscles have also been used as indicators of the degree of age-related thymus involution in most mammals including humans.[23] These features of involution have been observed in aged cattle of 2–5 years and more.[13] Further studies will examine very old pigs of over 3 years to ascertain the progress of involution. It is known that many intrinsic and extrinsic factors may contribute to age-associated thymic involution and not much is known about the mechanisms that lead to thymic involution.[24] There are many unanswered questions as to what initiates this process and when exactly it begins. Some investigators found the involution of the thymus in pigs of about 180 days,[22] which is contrary to the present report. At the growing age, it is known that the thymus does not undergo a complete involution; part of the functions are maintained in some secretory and hematopoetical insulary cells.[22] In cattle and sheep, the thymus involutes also with increasing age with complete involution by 6 years of age in cattle and marked involution evident in 2-year-old sheep.[25] Macrophages were encountered in the late foetal and postnatal stages of development in this study. They function in phagocytosis. They characteristically contain nuclear debris in the cytoplasm, presumably coming from lymphocytes after programmed cell death (apoptosis). They increased in number with age of development of the thymus. Macrophages may also contribute to intrathymic precursor T-cell maturation.[26] The present preliminary report will enhance further studies on morphological changes of thymus in younger and older pubertal pigs using more samples and advance anatomical techniques.

Conclusion

This study has demonstrated that the gross size of the thymus changes with age of development and that the cellular components of the thymus attains morphological maturity during the late foetal period with evidence of some prenatal immunological functions. Early histological signs of age-related involution were observed in the young pubertal pigs, showing slowing down of immunological response.

References

1. Boehm T. Thymus development and function. Curr Opin Immunol 2008;20:178–84.
2. Gordon J, Manley NR. Mechanisms of thymus organogenesis and morphogenesis. Development 2011;138:3865–78.
3. Gordon J, Bennet AR, Blackburn CC, Manley NR. Gcm2 and Foxn1 mark early parathyroid- and thymus-specific domains in the developing third pharyngeal pouch. Mech Dev 2001;103:141–3.
4. Ge Q, Zhao Y. Evolution of thymus organogenesis. Dev Comp Immunol 2013;39:85–90.
5. Jordan RK. Development of sheep thymus in relation to in utero thymectomy experiments. Eur J Immunol 1976;6:693–8.
6. Bodey B, Bodey B Jr, Siegel SE, Kaiser HE. Involution of the mammalian thymus, one of the leading regulators of aging. In Vivo 1997; 11:421–40.
7. Goldbach KJ. Histological and morphometric investigation of the thymus of the Florida manatee (Trichechus manatus latirostris). MSc Thesis, University of Florida, FL, USA; 2010.
8. Swindle MM, Makin A, Herron, AJ, Clubb FJ, Frazier KS. Swine as models in biomedical research and toxicology testing. Vet Pathol 2012; 49:344–56.
9. Muthiah K, Jeeferson JJ, Lalitha PS. Morphometry of thymus in sheep foetus. Indian Journal of Veterinary Anatomy 1995;11:35–9.
10. Prakash A, Chandra G. Some gross observations on the prenatal thymus of buffalo (Bubalus bubalus). Indian Journal of Veterinary Anatomy 1999;11:178.
11. Prasad M, Prakash A, Archana M, Farooqui M, Singh, SP. Gross biometrical observations on prenatal thymus of goat (Capra hircus). The Haryana Veterinarian 2011;50: 37–9.
12. Yugesh K, Jothi SS, Ramganathan K, Jayaraman P, Chavalin V, Sujatha N. Microscopic and microscopic study of thymus of pig. IOSR Journal of Dental and Medical Sciences 2014;13:52–5.
13. Gasisova AI, Atkenova AB, Ahmetzhanova NB, Murzabekova LM, Bekenova AC. Morphostructure of immune system organs in cattle of different age. Anat Histol Embryol 2017;46:132–42.
14. McGeady TA, Quinn PJ, Fitzpatrick EA, Ryan MT. Veterinary embryology. Oxford (UK): Blackwell Publishing; 2006. p. 346–8.
15. Dyce KM, Sack, WO, Wensing CJG. Textbook of veterinary anatomy, 3rd ed. London; Saunders; 2002. p. 258.
16. Kuper F, Schuurman, HJ, Vos JG. Pathology in immunology. In: Methods in immunotoxicology. In: Burleson JD, Munson A, editors. New York (NY): Wiley-Liss; 1995. p. 397–436.
17. Bancroft JD, Gamble M. Theory and practice of histological techniques. 5th ed. Churchill Livingstone: Toronto; 2002. p. 34–78.
18. Venzke WG. Thymus. In: Sisson and Grossman's the anatomy of domestic animals. Getty R, editor. Vol. 1. Philadelphia (PA): WB Saunders Company; 1975. pp. 1359.
19. Pearse G. Normal structure, function and histology of the thymus. Toxicol Pathol 2006; 34:504–14.
20. Baishya G, Kalita A, Sarma K, Borthakur M. Ontogeny of thymus in crossbred pig-gross anatomical studies. Indian Journal of Veterinary Anatomy 2000; 12: 210.
21. Sugimura M, Suzuki Y, Atoji Y, Sugano M, Tsuchimoto N. Morphological studies on thymus of Japanese serows (Cappricornis crispus). Research Bulletin of the Faculty of Agriculture, Gifu University 1983;48:113–9.
22. Sincai M, Marcu A. Perculiary aspects about development of thymus in pigs. Ciencia Rural Santa Maria 1994;24:117–9.
23. Yurchinskij VJ. Age-related morphological changes in Hassal's corpuscles of different maturity in vertebrate animals and humans. Advances in Gerontology 2016;6:117–22.
24. Rezzani R, Nardo L, Favero G, Peroni M, Rodella LF. Thymus and aging: morphological, radiological, and functional overview. Age (Dordr) 2014;36:313–51.
25. Reynolds JD, Morris B. The evolution of Peyer's patches in fetal and postnatal sheep. Eur J Immunol 1983;13:627–35.
26. Schuurman HJ, Kuper CF, Kendall MD. Thymic microenvironment at the light microscopic level. Microsc Res Tech 1997;38:216–26.

Online available at:
www.anatomy.org.tr
doi:10.2399/ana.16.050
QR code:

Correspondence to: Casmir O. Igbokwe, PhD
Department of Veterinary Anatomy, Faculty of Veterinary Medicine,
University of Nigeria, Nsukka, Nigeria
Phone: +234 803 493 03 93
e-mail: casmir.igbokwe@unn.edu.ng

Conflict of interest statement: No conflicts declared.

Original Article

www.anatomy.org.tr
Received: February 17, 2017; Accepted: April 16, 2017
doi:10.2399/ana.16.055

anatomy
www.anatomy.org.tr
An International Journal of Experimental and Clinical Anatomy

Association between Q angle and predisposition to gonarthrosis*

Fatma Havaslı[1], Mehmet Demir[2], Mustafa Çiçek[2], Atilla Yoldaş[2]

[1]*Gaziantep Dr. Ersin Arslan State Hospital, Gaziantep, Turkey*
[2]*Department of Anatomy, Faculty of Medicine, Kahramanmaraş Sütçü İmam University, Kahramanmaraş, Turkey*

Abstract

Objectives: The aim of our study was to evaluate the relationship between quadriceps angle (Q angle), body mass index (BMI), dominant side and pain severity in gonarthrosis patients.

Methods: In order to determine the Q angle in gonarthrosis patients, 205 volunteer patients (104 men and 101 women) diagnosed with gonarthrosis and 110 control subjects (60 men and 50 women) over 40 years of age were included. In the patient group, sides with pain, pain levels, right and left leg Q angle values, and dominant sides were evaluated.

Results: Right Q angle value was found 13.21°±3.22° in patients and 13.26°±2.04° in controls, while the left Q values were 12.86°±3.35° and 12.65°±2.52° in patients and controls, respectively. No significant difference was found between the right and left Q angles both for patients (p=0.885) and controls (p=0.568). When the pain levels and right Q angles of the patients were compared, a positive correlation between the Q angle elevation and increase in pain was found (p=0.001). In addition, the pain level increase and left Q angle elevation of the patients were also found positively correlated (p=0.004).

Conclusion: The results of this study show that measuring the Q angle, despite its low sensitivity and internal consistency levels, is an effective way of diagnosing and treating the lower extremity malalignments and related pathologies.

Keywords: dominant side; gonarthrosis; pain severity; Q angle

Anatomy 2017;11(1):21–25

Introduction

Osteoarthritis (OA) is a chronic rheumatic disease with a high incidence characterized with new bone formation on the articular surface of the joints, causing symptoms due to articular cartilage degeneration. It leads to reduced mobility in daily life and various complaints such as pain. Gonarthrosis is the most common form of OA and its prevalence increases with age. Radiological and pathological changes start presenting symptoms after the third decade of life.[1] While gonarthrosis is observed in 0.1% between 25–35 years of age, this rate rises over 80% in ages 65 and above.[2] Quadriceps angle or Q angle is a parameter used for the evaluation of the biomechanical condition of the knee joint and the regularity of the lower extremities. Q angle is defined as the angle between two axes drawn in the frontal plane, from spina iliaca anterior superior to the mid-point of patella, and from the mid-point of patella to tuberositas tibiae.[3] For Q angle measurements, a goniometer is widely used in clinics due to its practicality and low cost.[4] There is no common agreement on the normal value of the Q angle in the literature.[5,6] The American Orthopedics Association considers 10º as normal and range of 15º–20º as pathological, whereas Horton and Hall[7] described the normal value as 13.5º±4.5º for the general population, 11.2º±3º for men and 15.8º±4.5º for women. Other studies described Q angle values below 8º–10º for men and 15º for women as normal.[4,8] In the study of Schulthies et al.,[9] where they statistically gathered the data from numerous studies in literature, angles ranging between 10º–14º for men and 14.5º–17º for women were reported as normal.

**This study was presented at "Anatomi Günleri 2016" in Ankara, Turkey (February 11–14, 2016).*

The aim of our study was to evaluate the relationship between Q angle, body mass index (BMI), dominant side and pain severity in gonarthrosis patients over 40 years of age.

Materials and Methods

Our study included 298 patients diagnosed with gonarthrosis according to basis of clinical and radiological examinations in the Physical Therapy Clinics of Adıyaman Training and Research Hospital and Gaziantep Dr. Ersin Arslan Training and Research Hospital. Patients who went under knee surgery, trauma, knee injection in the last six months, and who received physical therapy in the past year were excluded. In order to compare the Q angles, 110 healthy adult volunteers were used. Volunteers with lower extremity amputation, prosthesis, fracture, use of any walking assistant or walking equipment were excluded. All patients and volunteers were submitted to an assessment protocol including interview and physical examination. Of the 298 patients assessed according to the protocol, 205 patients were included; the remaining patients matched one or more of the exclusion criteria. All measurements were taken by the same physical therapist at the Physical Therapy Unit of Adıyaman Training and Research Hospital and Gaziantep Dr. Ersin Arslan Training and Research Hospital. This study was approved by the Ethics in Research Committee of Kahramanmaraş Sütçü İmam University, under protocol number 2013/15–3, and voluntary informed consent forms were obtained from the participants.

Gender, age, height, weight, occupation, complaint, medical history, background and family history information were recorded for those who met the inclusion criteria among the patients and control subjects. Manual measurements were performed with a standard goniometer compatible with the technique for Q angle assessment as shown in **Figure 1**.[10] BMI of every participant was calculated to determine obesity based on World Health Organization (WHO) obesity classification. BMI ranges were as follows - underweight: under 18.5 kg/m^2; normal weight: 18.5 kg/m^2 to 24.99 kg/m^2; overweight: 25 kg/m^2 to 30 kg/m^2; obese: over 30 kg/m^2.

For the evaluation of pain, visual analog scale (VAS) was used compatible with the technique as described in the literature.[11] The dominant sides were determined by asking the participants which hand they prefer for writing and physically demanding activities.

IBM SPSS Statistics for Windows (Version 22.0, Armonk, NY, USA) was used for statistical analyses and values of $p<0.05$ were considered statistically significant. For the control of the continuous variable's compatibility to normal distribution, Kolmogorov-Smirnov test was used. For the comparison of the variables with normal distributions between two independent groups, Student's t-test and for the two dependent measurement comparisons the paired t-test was performed. Association between the numerical variables and categorical variables were tested using Pearson's correlation coefficient and chi-square tests, respectively. For numerical variables mean ± standard deviation, and for categorical variables number and % values were calculated.

Results

In this study, 205 patients (104 men and 101 women) and 110 control subjects (60 men and 50 women) that met our inclusion criteria were included in this study. Demographic

Figure 1. Measurement of Q angle with a standard goniometer. [Color figure can be viewed in the online issue, which is available at www.anatomy.org.tr]

features of the gonarthrotic patients and control subjects are shown in **Table 1**. No significant difference was found between the two groups in terms of age, height, BMI and right and left Q values. On the other hand, patients weighed heavier than the healthy volunteers (**Table 1**; p=0.032). There was no significant difference between the Q values of the gonarthrosis patients and control subjects. In fact, the mean Q values of the individuals over 40 were observed to be approximately the same. In the patient group, no significant difference was observed between the right and left Q angle values (p=0.096). Yet, in the healthy group the right Q value was found significantly higher (**Table 2**; p=0.001). When the two groups were compared for BMI, no significant difference was observed. 136 of the patients were overweight, while 129 were Type 1 obese (**Table 3**; p=0.015). When dominant side was evaluated, no significant difference was found between the left and right sides (p=0.258). While no significant association was found for the patients that used their left side dominantly, a predisposition to gonarthrosis was observed for the patients that used their right side dominantly (**Table 4**; p=0.042). There was a positive correlation between pain severity and right Q (r=0.236, p=0.001) and left Q angle (r=0.199, p=0.004) values in gonarthrosis patients.

Discussion

This study was conducted on the hypothesis that the knowledge of the Q angle may help in the diagnosis of the commonly observed gonarthrosis disease and for being informed about the health precautions that must be taken. In recent studies, goniometers were shown to be reliable for measuring the Q angle.[12] Yet, there are also studies criticizing goniometric measurements, stating that only a 1–5 mm shift from the pivot points used for the goniometer measurements to the mid-point of the patella may result in a 1.13° to 5.53° measurement error.[13] Since errors in the pivot points may result with such outcomes, it was suggested that differences up to 4° between the right and left extremity Q angles may raise questions on its credibility.[14]

Another controversy on the Q angle is the difference between the right and left extremities. In this study, there was no significant difference found between the right and left knee Q angles of patient and healthy groups. While the mean Q angle measurements of the gonarthrosis patients was found as 13.21° for the right knee and 12.86° for the left knee, in the healthy group these values were 13.26° and 12.65°, respectively. In contrast to the study of Horton and Hall[7] where the right leg Q angle value was higher than the left leg Q angle value, Livingstone and Spaulding[4] found the left leg Q angle value higher than

Table 1
Demographic data of gonarthrosis patients and controls.

Groups	Q angle	n	Mean±SD	p
Gonarthrosis	Right	205	13.21°±3.22°	0.096
	Left	110	12.86°±3.35°	
Controls	Right	205	13.26°±2.04°	**0.001***
	Left	110	12.6°±2.52°	

*Independent samples t-test; difference is statistically significant at the level of p=0.032.

Table 2
Comparison of Q angles of gonarthrosis patients and control subjects.

Groups	Q angle	n	Mean±SD	p
Age (year)	Gonarthrosis	205	57.34±7.72	0.090
	Controls	110	55.85±6.80	
Height (cm)	Gonarthrosis	205	164.95±8.69	0.253
	Controls	110	163.83±7.42	
Weight (kg)	Gonarthrosis	205	82.55±11.21	0.032*
	Controls	110	79.99±7.33	
BMI (kg/m²)	Gonarthrosis	205	30.39±3.97	0.215
	Controls	110	29.86±2.80	
Pain severity	Gonarthrosis	205	5.95±1.53	–
	Controls	110	–	
Right Q angle	Gonarthrosis	205	13.21±3.23	0.885
	Controls	110	13.26±2.04	
Left Q angle	Gonarthrosis	205	12.86±3.35	0.568
	Controls	110	12.65±2.52	

*p=0.001

Table 3
BMI distribution in gonarthrosis patients and controls.

BMI	Gonarthrosis	Controls	Total
Normal (18.5–24.9)	16 (7.8%)	4 (3.6%)	20 (6.3%)
Overweight (25–29.9)	80 (39%)	56 (50.9%)	136 (43.2%)
Obese Type 1 (30–40)	83 (40.5%)	46 (41.8%)	129 (41%)
Obese Type 2 (40.1–50)	26 (12.7%)	4 (3.6%)	30 (9.5%)
Total	205 (100%)	110 (100%)	315 (100%)

Table 4
Comparison of the pain side and dominant side in gonarthrosis patients.

	Dominant side		
Pain side	Right	Left	Total
Right	87 (50.9%)*	10 (29.4%)	97 (47.3%)
Left	33 (19.3%)	12 (35.3%)	45 (22%)
Bilateral	51 (29.8%)	12 (35.3%)	63 (30.7%)
Total	171 (100%)	34 (100%)	205 (100%)

*Chi-square test, statistically significant at the level of p=0.042.

the right. Similarly, in the study by Denizoğlu[15] conducted on 77 healthy individuals, the left leg Q angle values were also found higher. In our study, in both patients and healthy individuals, the right leg Q angle values were found higher compared to the left side.

There is also controversy on the position of the subjects during Q angle measurement. When the Q angle is measured while standing, it is found approximately 1.4° higher in men and 2.4° higher in women compared to measurements in supine position. This variance may be due to the fact that the standing position is affected more by foot-ankle and hip joints than the supine position, and it is notified that in order to reduce this effect, the supine position should be preferred.[16] Yercan and Taskiran[17] confirmed this finding and indicated that an increase in the femoral anteversion would lead to an internal rotation of the femur. In this circumstance, the femoral cavity may turn medial and thus the patellar tendon may adhere more laterally on the tibia. Consequently, an increase in the Q angle will be observed. Likewise, in case of an external tibial torsion, characterized with extreme external physical rotation of the feet, tuberositas tibiae was reported to be located to more lateral to increase the Q angle. In this context, internal or external rotation of the feet by 15° was indicated to accompany with a 5° increase or decrease in the Q angle.[4,17] We performed our study while patients were in the standing position.

Age is also considered to have an effect on the Q angle. Bayraktar et al.[18] investigated the relationship between Q angle and age. They observed that children and adolescents had higher Q angle values compared to adults. Hsu et al.[19] found no significant relationship between age and Q angle in age groups 25–40 and 41–60. According to WHO statistics, gonarthrosis is the fourth leading cause of disabilities in women and the eighth in men.[1] The effect of obesity on gonarthrosis development has also been studied studied.[1,18,20,21] On the contrary, Kalpakçıoglu and Çakmak[20] found no difference regarding age and weight in 30 patients aged 40–60 years. In our study, no significant relation was found relating BMI between the patient and healthy groups, while a significant association was observed between the weight and the patient group.

Position of the knee joint is also counted as an additional factor affecting the Q angle. In full extension, patella does not contact the patellar surface of the femur, while at 90° flexion the lateral joint side of the patella is in touch with the outer and lower part of the patellar surface of the femur. Thus, patella can move laterally downwards. These changes of the position of the femur, tibia and patella during flexion and extension of the knee joint significantly lower the Q angle in 90° flexion compared to extension. In their study on 1340 athletes, Skalley et al.[22] suggested that the extension of the knee had no correlation with the Q angle by measuring the medial and lateral gliding limits of the patella during 0° and 35° flexion. In our study, the knee position of the patients was decided to be full extension and the measurements were taken accordingly.

Conclusion

In this study on patients diagnosed with gonarthrosis, we observed that the Q angle value increased with pain with a weak, but significant correlation. In addition, a weak yet statistically significant relation was also found between patients with right hand dominance and who had gonarthrosis on the right side. We think that being informed on the Q angle will contribute to both knee joint surgery and in diagnosis and treatment of the pathologies of lower extremities. On behalf of the accuracy of the studies, a mutual clinical agreement should be reached to for the Q angle measurement method and positioning, and further applications should be done accordingly.

References

1. Felson DT, Lawrence RC, Dieppe PA, Hirsch R, Helmick CG, Jordan JM, Kington RS, Lane NE, Nevitt MC, Zhang Y, Sowers M, McAlindon T, Spector TD, Poole AR, Yanovski SZ, Ateshian G, Sharma L, Buckwalter JA, Brandt KD, Fries JF. Osteoarthritis: new insights. Part 1: the disease and its risk factors. Ann Intern Med 2000;133:635–46.
2. Atay MB, Beyazova M, Gökçe KY. Osteoartrit. Fiziksel tıp ve rehabilitasyon. Ankara: Güneş Kitabevi; 2011. s. 2533–63.
3. Olcay E, Çetinus E , Mert M, Kara AN. Genç erkek ve bayanlarda ayakta ve yatar pozisyonlarda quadriceps açısının mukayesesi ve değerlendirilmesi. Acta Orthop Traumatol Turc 1994;28:25–7.
4. Livingston LA, Spaulding SJ. OPTOTRAK measurement of the quadriceps angle using standardized foot positions. J Athl Train 2002; 37:252–5.
5. Toraman F, Yaman H, Taşralı S. Patellofemoral açı farklılığının alt ekstremite performansı üzerine etkisi. Totbid Dergisi 2003;14:13–7.
6. Powers C. The influence of altered lower- extremity kinematics on patellofemoral joint dysfunction: a theoretical perspective. J Orthop Sports Phys Ther 2003;33:639–46.
7. Horton M, Hall T. Quadriceps femoris muscle angle: normal values and relationships with gender and selected skeletal measures. Phys Ther 1989;69:897–901.
8. Greene CC, Edwards TB, Wade MR, Carson EW. Reliability of the quadriceps angle measurement. Am J Knee Surg 2001;14:97–103.
9. Schulthies S, Francis R, Fisher A, Graaff K, Van de Graaff KM. Does the Q angle reflect the force on the patella in the frontal plane? Phys Ther 1995;75:24–30.

10. Livingston LA, Mandigo JL. Bilateral Q angle asymmetry and anterior knee pain syndrome. Clin Biomech (Bristol, Avon) 1999;14:7–13.
11. McCormack HM, Horne DJ, Sheather S. Clinical applications of visual analogue scales: a critical review. Psychol Med 1988;18:1007–19.
12. Weiss L, DeForest B, Hammond K, Schilling B, Ferreira L. Reliability of goniometry-based Q-angle. PM R 2013;5:763–8.
13. France L, Nester C. Effect of errors in the identification of anatomical landmarks on the accuracy of Q angle values. Clin Biomech (Bristol, Avon) 2001;16:710–3.
14. Livingston L, Mandigo J. Bilateral within-subject Q angle asymmetry in young adult females and males. Biomed Sci Instrum 1997;33:112–7.
15. Denizoğlu H. Sağlıklı bireylerde Q açısı ile denge arasındaki ilişki. Abant İzzet Baysal Üniversitesi Sağlık Bilimleri Enstitüsü Fizik Tedavi ve Rehabilitasyon Programı Yüksek Lisans Tezi, Bolu, 2010.
16. Byl T, Cole JA, Livingston L. What determines the magnitude of the Q angle? A preliminary study of select skeletal and muscular measures. Journal of Sport Rehabilitation 2000;9:26–34.
17. Yercan HS, Taşkıran H. Patellofemoral eklem patolojisi ile alt ekstremite torsiyonel deformitelerin ilişkisi. Eklem Hastalıkları Cerrahisi Dergisi 2004;2:71–5.
18. Bayraktar B, Yucesir I, Ozturk A, Cakmak A, Taşkara N, Kale A, Demiryurek D, Bayramoglu A, Camlica H. Change of quadriceps angle values with age and activity. Saudi Med J 2004; 25:756–60.
19. Hsu RW, Himeno S, Coventry MB, Chao EY. Normal axial alignment of the lower extremity and load-bearing distribution at the knee. Clin Orthop Relat Res 1990;(255):215–27.
20. Kalpakçıoğlu A, Çakmak B. Bahadır C. Diz osteoartritinde ultrason ve kısa dalga diatermi tedavilerinin karşılaştırması. Türk Fiziksel Tıp ve Rehabilitasyon Dergisi 2006;52:168–73.
21. Manek NJ, Hart D, Spector TD, MacGregor AJ. The association of body mass index and osteoarthritis of the knee joint: an examination of genetic and environmental influences. Arthritis Rheum 2003;48: 1024–9.
22. Skalley TC, Terry GC, Teitge RA. The quantitative measurement of normal passive medial and lateral patellar motion limits. Am J Sports Med 1993;21:728–32.

Online available at:
www.anatomy.org.tr
doi:10.2399/ana.16.055
QR code:

Correspondence to: Assist. Prof. Dr. Mehmet Demir
Department of Anatomy, Faculty of Medicine, Kahramanmaraş Sütçü İmam University, Kahramanmaraş, Turkey
Phone: +90 505 938 73 11
e-mail: mdemir2779@gmail.com

Conflict of interest statement: No conflicts declared.

anatomy
www.anatomy.org.tr
An International Journal of Experimental and Clinical Anatomy

Original Article

www.anatomy.org.tr
Received: March 19, 2017; Accepted: April 13, 2017
doi:10.2399/ana.16.056

Factors affecting foot arch development in Northern Ethiopia

Belta Asnakew Abegaz, Dereje Gizaw Awoke

Department of Human Anatomy, College of Medicine and Health Sciences, Bahir Dar University, Bahir Dar, Ethiopia

Abstract

Objectives: Bones of the foot form longitudinal and transverse arches which absorb and distribute downward forces from the body during standing and moving on different surfaces. The medial longitudinal arch is the longest, highest and most important in static position and moving. Studies classify the medial longitudinal arch as high, normal, and flat. This study was designed to determine the factors that affect the development of the medial longitudinal foot arch.

Methods: Cross-sectional study design was employed, 424 subjects were selected using quota sampling method. The footprint areas were measured using a planimeter. Descriptive statistics and multiple logistic regressions were used for data analysis and p value <0.05 was considered as statistically significant.

Results: From the total subjects, 46.2%, 42.9%, and 10.9% were high, normal and flat arched, respectively. About 6.9% of shoe-wearers and 4% of the barefooted had flat arch. From the flat arched, 8.5% were males and 2.4% were females. Among the shoe-wearers, 10.2% used closed toe shoes, and 3.3% that wore sandals were flat-arched. From 29 flat-arched, 24 (11.2%) were urban residents.

Conclusion: Sex, type of shoes, wearing shoes and being barefooted residence were significant factors affecting the development of foot arch. Shoe age did not determine arch development.

Keywords: barefooted; foot arch; planimeter; shoe-wearers; type of shoe

Anatomy 2017;11(1):26–29

Introduction

One of the important and most variable characteristics of the foot is the height of the medial longitudinal arch (MLA) above the ground plane during weight bearing activity.[1] The human foot has three arches: the medial longitudinal, lateral longitudinal, and transverse (anterior). From these the MLA is the longest, the highest, and the most important of the three during static support of the body and protect the foot from injury during movement.[2,3]

According to arch index (AI) or the height of MLA when AI<0.21 is high arch, 0.21<AI<0.26 is normal arch, and AI>0.26 is low (flat) arch.[1] There are factors that affect the development of foot arch such as improper shoe wearing, the type of shoes a child wears, residence and being overweight etc.[4,5] Children are born with flat feet, MLA slowly develops during childhood usually by about age five or six.[6,7]

There are some studies conducted about the factors affecting the development of foot arch in America, Iran, India, Saudi Arabia, and Nigeria. As far as we know, there is no similar study conducted in Ethiopia. Therefore, the current study was designed to determine the factors affecting foot arch development in Ethiopia.

Materials and Methods

Cross-sectional study design was employed for this study. The study subjects were selected by quota sampling method. A total 424 subjects from the study area were selected; their age ranged from 15 to 65 years, 207 were male and 217 were female subjects who had no foot deformity and lower limb injuries. Ethical approval was obtained from ethical review board of local authorities. Official letters were submitted to the district officials, explaining the purpose and the importance of the study and permission was obtained from each. Confidentiality was maintained at all levels of the study.

Various techniques have been proposed to evaluate foot arch types, each of them have their own limita-

tions.[8–10] Foot print parameter is better than other parameters, because it is inexpensive, easy for handling, effective for individual and population based investigations.[10] Studies show there is no difference between the right and left foot prints.[11] Therefore, we took only the right footprint. The footprints were collected using two smooth wooden plates, normal wall paint, brush, and a sheet of paper in which on its other side the questionnaire was printed. One of the wooden plates impregnated with the paint for capturing the footprints and the subjects put their footprints on the other wooden plate on which the sheet of paper was placed.

Row data were checked for clarity, consistency, accuracy and were analyzed using IBM SPSS (Statistical Package for the Social Sciences, version 16.0; IBM, Chicago, IL, USA) software. Descriptive analysis was done for basic demographic characteristics. Pearson's chi square test was used as a statistical test, and multiple logistic regressions were employed for analyzing the data. Thus, in multivariate analysis, the association between independent and outcome variables was expressed by odds ratio (OR) with 95% CI.

Arch index is the ratio of the area of the middle third of the foot print area to the footprint area excluding the toes. The area of the footprint was first measured using a planimeter and the AI was calculated with the formula: AI = B/A+B+C.[1] The three regions of the footprint areas are leveled as hind foot (A), mid foot (B), and fore foot (without the toe) (C) (**Figures 1** and **2**). High arch was defined as AI <0.21, normal arch 0.2I<AI<0.26, and low arch (flat) AI>0.26.[1,8]

Results

From the total 424 study subjects, 207 (48.8%) were males and 217 (51.2%) were females. 215 (50.7%) were shoe-wearers and 209 (49.3%) were barefooted. The mean age of the subjects was 25.86±8.7 with median 23 and ranged from 15 to 65 years. The mean arch measurement was 0.198±0.06, area ratio with median 0.21 and ranged from 0–0.35 area ratio (**Table 1**).

From 215 shoe-wearers 6.9% were flat-arched, and from 209 barefooted 4% were flat-arched. There was a significant association between wearing shoes and being barefooted (odds ratio (OR): 1.617; 95% confidence interval (CI): 1.209–1.819) (**Tables 2** and **4**). The prevalence of flat arch was more common in males, whereas high arch was more common in female subjects. From all male subjects, 36 (8.5%) had flat arch, 10 (2.4%) of female subjects had flat arch, while 79 (18.6%) males and 117 (27.6%) females were high-arched. (OR: 6.698; 95% CI: 3.123–14.351) (**Tables 2** and **4**).

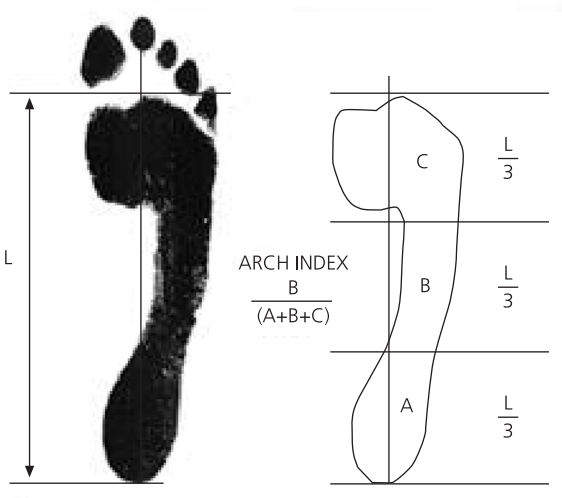

Figure 1. Measurement of arch index (AI). The three regions of the footprint areas are leveled as hind foot (**A**), mid foot (**B**), and fore foot (**C**) (excluding the toe). **L**: lenght of the footprint area excluding the toe.

From the total 215 shoe-wearers, 38 (17.7%) and 59 (27.4%) high arched were males and females, respectively. This shows that high arch is more prevalent in females than in males. Of the total 29 flat-arched individuals, 23 (10.7%) were males and only 6 (2.8%) were females. Male individuals were 7.4 times more likely to have flat arch than females (OR: 7.47; 95% CI: 2.57–21.72). There was a statistically significant association between sex and flat arch development (**Tables 2** and **4**). About 22 (10.2%) and 7 (3.3%) were flat-arched individuals who wore closed toe and sandals, respectively. There was a significant relationship between shoe type and flat arch (OR: 6.576; 95% CI: 2.391–18. 092). Closed toe shoe-wearers were 6.57 times flat arched than those who wore sandals (**Tables 3** and **4**).

A total of 54 (25.1%) urban and 43 (20%) rural residents had high foot arch. Of the flat-arched individuals, 24

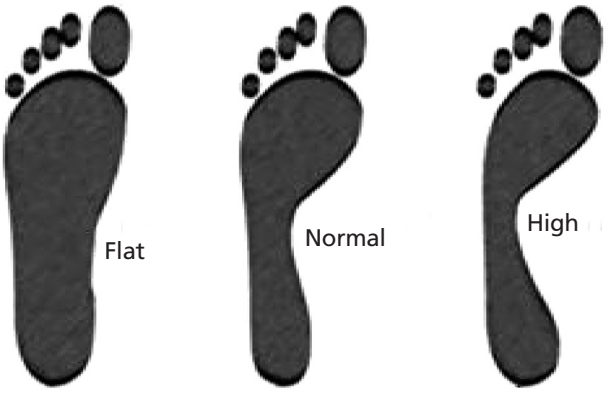

Figure 2. Sample of the three types of foot arch.

Table 1
The study subjects with their variables.

Variable		Number	Percentage (%)
Shoe condition	Shoe-wearer	215	50.7
	Barefooted	209	49.3
Age	15–24	258	60.8
	25–34	116	27.4
	35–44	28	6.6
	45–54	9	2.1
	55–65	13	3.1
Arch type	High	196	46.2
	Normal	182	42.9
	Flat	46	10.9
Barefooted	Males	100	47.8
	Females	109	52.2
Shoe-wearer	Males	107	49.8
	Females	108	50.2

Table 2
Variables (both barefooted and shoe-wearer) with their arch type.

Variable		Arch type		
		High	Normal	Flat
Sex	Males	79 (18.6%)	92 (21.7%)	36 (8.5%)
	Females	117 (27.6%)	90 (21.2%)	10 (2.4%)
Shoe condition	Shoe-wearer	97 (22.9%)	89 (21%)	29 (6.9%)
	Barefooted	99 (23.3%)	93 (21.9%)	17 (4%)
Shoe-wearer	Males	38 (17.7%)	46 (21.4%)	23 (10.7%)
	Females	59 (27.4%)	43 (20%)	6 (2.8%)
Barefooted	Males	41 (19.6%)	46 (22%)	13 (6.2%)
	Females	58 (27.8%)	47 (22.5%)	4 (1.9%)

Table 3
Shoe-wearer variables with their arch type distribution.

Variable		Arch type		
		High	Normal	Flat
Residence	Urban	54 (25.1%)	48 (22.3%)	24 (11.2%)
	Rural	43 (20%)	41 (19.1%)	5 (2.3%)
Shoe age	1–9 years	49 (22.8%)	34 (15.8%)	15 (7%)
	Age ≥10 years	48 (22.3%)	55 (25.6%)	14 (6.5%)
Shoe type	Closed toe	26 (12.1%)	32 (14.9%)	22 (10.2%)
	Sandals	71 (33%)	57 (26.5%)	7 (3.3%)

Table 4
Multiple logistic regression analysis of variables associated with adult arch type (for shoe-wearer subjects only).

Variable		Crude OR (95% CI)	Adjusted OR (95% CI)
Sex	Females*	1	1
	Males	5.952 (2.219, 15.964)	7.477 (2.573, 21.727)†
Residence	Rural*	1	1
	Urban	3.822 (1.346, 10.851)	4.350 (1.388, 13.628)†
Shoe type	Closed toe*	1	1
	Sandals	8.582 (3.280, 22.457)	6.576 (2.391, 18.092)†

*Reference category; †p<0.05. **CI:** confidence interval, **OR:** odds ratio.

(11.2%) were urban and 5 (2.3%) were rural residents. This indicated that the prevalence of flat arch was common in urban residents than the rurals. Hence, the subjects who lived in urban residences had 4.3 times flat foot than those who lived in rural areas (OR: 4.350; 95% CI: 1.388–13.629) (**Tables 3** and **4**).

There is no consistency in the relationship between shoe-wearing age and arch types. There might be other factors, such as the type of shoes the individual used to wear during childhood, and the duration of wearing shoes (**Table 3**).

Discussion

The results of this study showed there is no difference in the prevalance of flat foot in various age groups (**Table 3**). A study performed in India also showed no statistical significant difference in the prevalence of flat feet in various age groups screened, indicating significant variations in the prevalence do not occur with increasing age after skeletal maturity.[12] As a result, the age of the subjects was not considered as a determining variable of the study.

For both shoe-wearers and barefooted, male subjects had higher tendency to have flat arch than females; the reverse was true for high arch (**Tables 2** and **4**). Similar results were recorded in a study done India and Austria showing that the boys had a significant higher tendency for flat foot than the girls: the prevalence of flat foot was 52% in boys and 36% in girls (p<0.01). Boys had a significantly higher tendency for flat feet than girls, and high arch was more common in women than in men.[12–14]

In this study, wearing shoes promoted the prevalence of flat arch than being barefooted (**Tables 2** and **4**). A study conducted in India also supported the idea that the prevalence of flat arch was more significant among those who wear shoes. The incidence among children who used footwear was 8.6% compared with 2.8% in those who did not (p<0.001).[15]

The prevalence of flat feet in urban residents was found 4.3 times higher than those in rural dwellers (**Tables 3** and **4**). With similar results, another study from Saudi Arabia concluded that residents in urban areas were significantly associated with double the risk of flat feet (OR: 2.04; 95% CI: 1.1–3.48).[4]

The result of the present study showed no statistically significant difference between early shoe wearing and late shoe wearing for the prevalence of flat arch (**Table 3**), in contrast with earlier studies. However, a more recent study done in India concluded that the incidence of flat feet was 3.24% among those who started to wear shoes before the age of 6 years, 3.27% in those who started between the age of 6–15 years, and 1.75% in those who first wore shoe at the age of 16 ($p<0.001$).[12] This difference was due to type of shoe and the duration the subjects wore shoe in childhood that resulted in reducing the prevalence of flat feet in early shoe-wearers.[15]

Wearing closed toe shoe is a significant factor for the development of flat arch (**Tables 3** and **4**). This was confirmed in many studies showing that the prevalence of flat arch also varied with the type of the foot wear.[15] In more specific terms, closed toe shoes inhibited the development of the arch of the feet more than slippers and sandals did. The type of usual footwear during childhood was a significant predictor for the development of flat foot. Considering cases that went barefooted during childhood as the reference category, those who wore shoes during their early childhood were at double the risk of having flat foot (adjusted OR: 2.18; 95% CI: 1.01–5.73).[4,12,15]

Conclusion

The results showed that the person's age and shoe wearing age were not the determining factors for the arch types. Wearing closed toe shoe, being urban resident and male negatively affected the development of thr MLA. In addition, being barefooted, rural resident, female, and wearing sandals promoted the development of the MLA.

Acknowledgements

The authors would like to acknowledge Asegedech Bekele (PhD, Associate Professor) of Human Anatomy at the College of Medicine and Health Sciences, University of Gondar for her professional, technical and academic advice.

References

1. Cavanagh PR, Rodgers MM. The arch index: a useful measure from foot print. J Biomech 1987;20:47–51.
2. Chang YW, Hung W, Wu HW, Chiu YC, Hsu HC. Measurement of foot arch in standing, level of walking, vertical jump and Sprint start. International Journal of Sport and Exercise Science 2010;2: 31–8.
3. Xiong S, Goonetilleke RS, Witana CP, Weerasinghe TW, Au EY. Foot arch characterization: a review, a new metric, and a comparison. J Am Podiatr Med Assoc 2010;100:14–24.
4. Abdel-Fattah MM, Hassanin MM, Felembane FA, Nassaane MT. Flat foot among Saudi Arabian army recruits: prevalence and risk factors. East Mediterr Health J 2006;12:211–7.
5. Daneshmadi H, Rahnema N, Mehdizadeh R. Relationship between obesity and flat foot in high school boys and girls. International Journal of Sports Science and Engineering 2009;3:43–9.
6. Mortazavi SMJ, Espandar R, Baghdadi T. Flatfoot in children: how to approach? Iran J Pediatr 2007;17:163–70.
7. Eluwa MA, Omini RB, Kpela T, Ekanem TB, Akpantah AO. The incidence of pes planus amongst Akwa Ibom State Students in the University of Calabar. The Internet Journal of Forensic Sciences 2008;3:1–5.
8. Shiang TY, Lee SH, Lee SJ, Chu WC. Evaluating different footprint parameters as a predictor of arch height. IEEE Eng Med Biol Mag 1998;17:62–6.
9. Lin CH, Lee HY, Chen JJ, Lee HM, Kuo MD. Development of a quantitative assessment system for correlation analysis of footprint parameters to postural control in children. Physiol Meas 2006;27: 119–30.
10. Hernandez AJ, Kimura LK, Laraya MHF, Favaro E. Calculation of Staheli's plantar arch index and prevalence of flat feet: a study with 100 children aged 5-9 years. Acta Ortop Bras 2007;15:68– 71.
11. Chu WC, Lee SH, Chu W, Wang TJ, Lee MC. The use of arch index to characterize arch height: a digital image processing approach. IEEE Trans Biomed Eng 1995;42:1088–93.
12. Sachithanandam V, Joseph B. The influence of footwear on the prevalence of flat foot: a survey of 1846 skeletally mature persons. J Bone Joint Surg Br 1995;77:254–7.
13. Dunn JE, Link CL, Felson DT, Crincoli MG, Keysor JJ, McKinlay JB. Prevalence of foot and ankle conditions in a multiethnic community sample of older adults. Am J Epidemiol 2004;159:491–8.
14. Pfeiffer M, Kotz R, Ledl T, Hauser G, Sluga M. Prevalence of flat foot in preschool-aged children. Pediatrics 2006;118:634–9.
15. Roa UB, Joseph B. The influence of footwear on the prevalence of flat foot: a survey of 2300 children. J Bone Joint Surg Br 1992;74:525–7.

Online available at:
www.anatomy.org.tr
doi:10.2399/ana.16.056
QR code:

Correspondence to: Belta Asnakew Abegaz, MSc
Department of Human Anatomy, College of Medicine and Health Sciences, Bahir Dar University, Bahir Dar, Ethiopia
Phone: +251 918 789 549
e-mail: asbelta21@gmail.com

Conflict of interest statement: No conflicts declared.

Original Article

www.anatomy.org.tr
Received: April 3, 2017; Accepted: April 17, 2017
doi:10.2399/ana.16.060

anatomy
www.anatomy.org.tr
An International Journal of Experimental and Clinical Anatomy

Investigation of bifid mandibular canal frequency with cone beam computed tomography in a Turkish population

Gözde Serindere[1], Kaan Gündüz[2], Elif Bulut[3]

[1]*Department of Dentomaxillofacial Radiology, Faculty of Dentistry, Mustafa Kemal University, Hatay, Turkey*
[2]*Department of Dentomaxillofacial Radiology, Faculty of Dentistry, Ondokuz Mayıs University, Samsun, Turkey*
[3]*Department of Business Administration, Faculty of Economics and Administrative Sciences, Ondokuz Mayıs University, Samsun, Turkey*

Abstract

Objectives: It is important to know anatomic location and variations of the mandibular canal (MC) for surgical treatment on mandible such as implant operations, impacted molar tooth extraction and sagittal split ramus osteotomy. The purpose of our study is to determine the configuration and incidence of bifid mandibular canal (BMC) using cone beam computed tomography (CBCT).

Methods: CBCT scans of 2000 patients were retrospectively analysed. Age and gender of the patients who were included in this study were recorded. BMC was subdivided, frequency was determined. Measurements of mean lengths, superior and inferior angles were performed. The all measurements were performed by one observer in 3 times at intervals of one week to confirm intra-observer reliability. SPSS 21 (Statistical Package for Social Science 21) was used for statistical analysis. It was benefited from Chi-square test to investigate qualitative observation and from T test and one-way analysis of variance for investigation of quantative observation. Differences were considered significant at $p<0.05$.

Results: 1122 of 2000 patients (56.1%) were females and 878 of 2000 patients (43.9%) were males. BMC was observed in 61 of 2000 patients (3.05%). Because location of MC is bilateral, 122 sides in 61 patients were studied. BMC was observed in 65 of 122 sides (53.3%). In 39 of 65 sides (60%), BMC was observed in males, in 26 of 65 (40%) sides, BMC was observed in females.

Conclusion: CBCT provides important informations about MC imaging and evaluation of variations. Evaluation of MC variations frequency and informing to surgeon in surgical procedures on mandible provides advantages for successful operations.

Keywords: anatomy; bifurcation; cone beam computed tomography; mandibular canal

Anatomy 2017;11(1):30–36

Introduction

The mandibular canal (MC) or the inferior alveolar canal transmits the inferior alveolar nerve, associated vessels and a branch of the third division of the trigeminal nerve. MC is between mandibular foramen and mental foramen. The inferior alveolar nerve is subdivided to the terminal dental and incisive branches to innerve the teeth and adjacent anatomical structures.[1]

The term of 'bifid' is a Latin word that means a cleft into two parts or branches. Bifid mandibular canal (BMC) originates at the mandibular foramen. These bifid canals may include a neurovascular bundle.[2]

Panoramic radiography, CT and cone beam CT (CBCT) can be used to determine the prevalence of BMC.[3] In radiography, MC is seen as dark and linear shadow with thin radiopaque superior and inferior borders. The borders of MC are sometimes seen partially or not at all. The width of MC varies from patient to another patient. But it is usually constant anterior to the third molar area.[4]

The opposing side of mandible, the soft palate, the pharyngeal airway and the uvula cause ghost shadows. Therefore, the location of the MC is difficult in panoramic radiographs.[4] Rouas et al.[5] also reported that panoramic radiography has limitations to diagnose the BMC and

suggested CBCT that has slightly more radiation dose than panoramic radiography and far less than CT. Orhan et al.[3] found more BMC compared to earlier t studies using panoramic radiography and suggested that CBCT is very useful modality to detect the BMC. CBCT imaging technique produces submilimeter resolution images of maxillofacial region with lower doses and costs compared to CT.[4]

In addition, patients with bifid canals are at greater risk of inadequate anesthesia or difficulties with jaw surgery.[4] As a result, it is extremely important to know the anatomy and variations of MC to reduce the damage of mandibular nerve bundle in intraoral operations during lower third molar surgery, implant operations, mandibular osteotomy, and mandibular fracture. Today, implant operations have increased, and therefore BMC has become more important. For this reason, our study aimed to determine the prevalence and localisation of BMC in CBCT scans.

Materials and Methods

After the statement regarding Ethics Committee approval for the study (Approval number B.30.2.ODM.0.20.08/1088). The patients were 18 to 75 years old in age (mean age: 45.78 for males and 42.5 for females) and were referred to Ondokuz Mayıs University Dentomaxillofacial Radiology Department between the years of 2013 and 2015 with various reasons such as missing teeth, decay, orthodontic treatment etc. CBCT images performed for evaluation of 2000 patients were retrospectively analysed (878 males, 1122 females; mean age: 44.49)

Inclusion criteria for patient selection were the age of the patients (18 to 75) and sufficient quality of CBCT scans to diagnose. Patients with pathologic lesions in the posterior region of mandible were excluded from the study.

Sirona, Galileos (Sirona Dental Systems, Bensheim, Germany) (98 kV, 25 mAs) was used to obtain the images. Image analysis were done by using Sidexis (Sirona, Bensheim, Germany) program. The dedector type of device was Image Intensifier (Siemens, Munich, Germany) with 4096 brightness value. FOV size was 15× 15×15 cm^3. Voxels were isotropic and 0.25×0.25×0.25 mm^3. Half value layer was 3.9 mm Al. Cone beam angle was approximately 24°.

All CBCT images were acquired properly. After reconstruction, all images in axial, tangential and cross-section, reconstructed panoramic images and 3D images were investigated (**Figure 1**). All evaluations and measurements were performed on a 27 inch monitor with a resolution of 2560×1440 at 10 bit.

All CBCT images were evaluated by a single observer. Detected BFCs were controlled by an dentomaxillofacial radiologists who had more than 10 years of experience. Intra-class correlation was calculated for quantitative datas. Cohen's kappa values were calculated for cat-

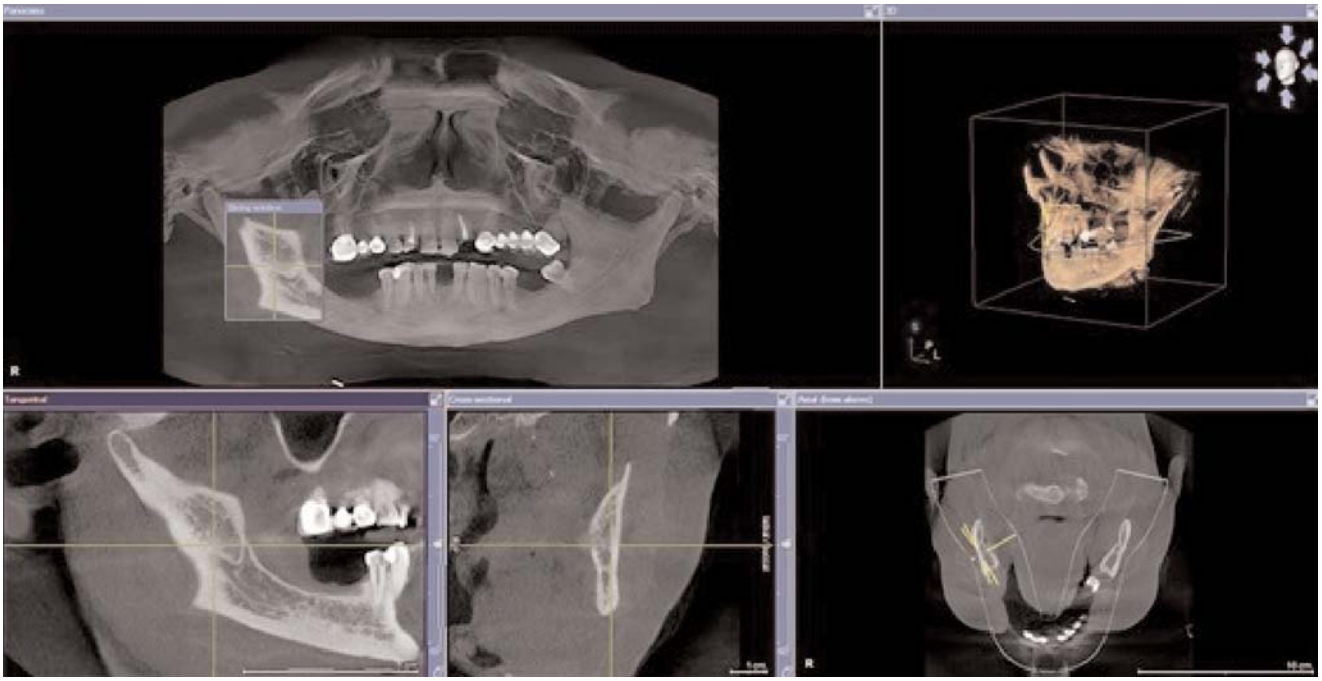

Figure 1. Reconstructed panorama, axial, tangential, cross sectional and 3D images. [Color figure can be viewed in the online issue, which is available at www.anatomy.org.tr]

egoric datas. Intra-observer reliability was found as 0.317 suggesting that the low kappa values were a result of infrequency of BMCs in the study sample because of the high numbers of evaluated patients.

The length and angle of BMCs were measured either in tangential and panoramic reconstructed CBCT images using the own software of CBCT system. The length of BMCs was measured between starting point of seperation from the main canal and the tip point. The superior and inferior angle measurements were also performed. In the superior angle measurements, the angle between the main canal and superior wall of BMCs were measured. For inferior angle measurements, the angle between the main canal and inferior wall of BMCs was measured (**Figure 2**). All measurements were performed by one observer for three times at intervals of one week to confirm intra-observer reliability. The mean values of measurements were analysed.

According to Naitoh et al.[6] classification, BMCs were divided into four groups considering location. These were forward, retromolar, dental and buccolingual canals (**Figure 3**). Forward canals were subdivided into with confluence and without confluence. Dental canals were subdivided into first, second and third molar canals according to the region of seperation from the main canal. Additionally,

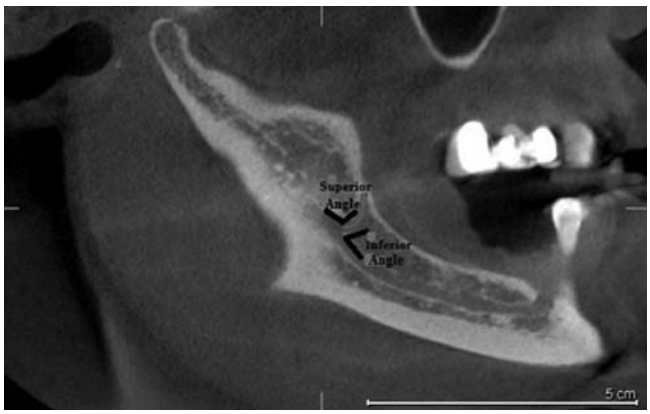

Figure 2. Sagittal scan showing superior and inferior angle measurement of BMC.

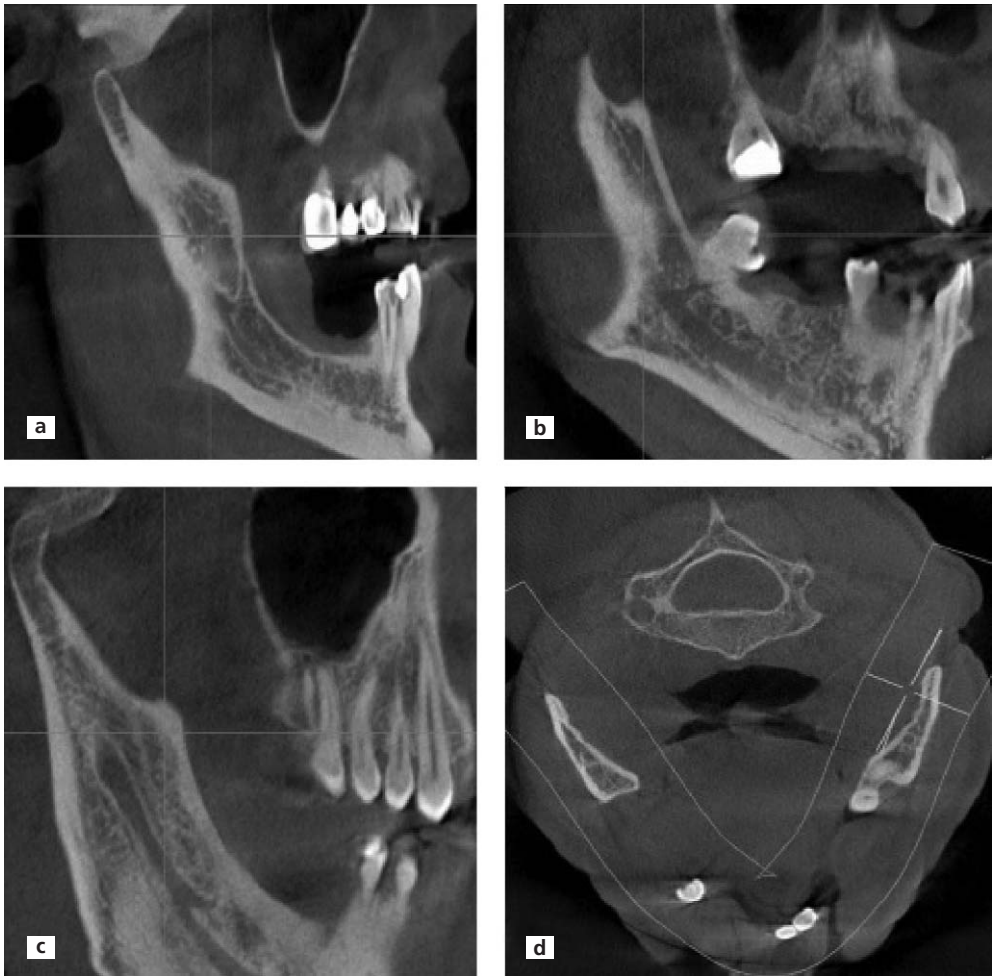

Figure 3. (**a**) Sagittal view of bifid retromolar canal. (**b**) Sagittal view of the third molar type dental canal. (**c**) Sagittal view of forward canal. (**d**) Axial view of the buccolingual canal.

the buccolingual canals were subdivided into buccal or lingual canal considering location of bifid canal.

IBM SPSS (Statistical Package for the Social Sciences, version 21; IBM, Chicago, IL, USA) software was used for statistical analysis. There were qualitative and quantitative observations in our study data, so we used Chi-square test to investigate qualitative observation and from t-test and one-way analysis of variance for investigation of quantative observation. Differences were considered significant at $p<0.05$.

Results

Bifid mandibular canals were observed in 61 of 2000 patients (3.05%). Because location of mandibular canal is bilateral, 122 sides in 61 patients (37 men and 24 women) were studied. BMC were observed in 65 of 122 sides (53.3%).The relationship between gender and canal type are showed in **Table 1**. In 39 of 65 sides (60%), BMCs were observed in males. In 26 of 65 (40%) sides, BMCs were observed in females. No statistically significant difference was found between gender and type of BMCs ($p=0.345>0.05$). BMCs were frequently found in the fourth decade. According to relationship among age groups and canal types, retromolar canals were frequently found in the fifth decade, forward canals in the fourth decade, dental canals in the third and fourth decade equally, and two buccolingual canals in the second and fifth decade. The obtained data are shown in **Table 2**. Difference between age and type of BMCs was evaluated with using chi-square test. No statistically significant differences were found between age and type of BMCs ($p>0.05$).

The number of different groups of BMCs are shown in **Table 3**. The most fequently observed type was the retromolar canal (n=39, 18 right sides, 21 left sides) followed by the dental canal (n=14, 8 right sides, 6 left sides), forward canal (n=10, 5 right sides, 5 left sides) and buccolingual canal (n=2, one right side, the other one left side). Of the 10 forward canals, 9 of them occured without confluence and one of them with confluence. Of the 14 dental canals, one of them extended to the root apex of the first molar, one of them to the second molar, and 12 to the third molar. All two buccolingual canals were positioned in buccal side. The distribution of canal types according to gender and location in detail are shown in **Table 4**. There was

Table 1
Relationship between gender and type of BMC.

Gender	Types of BMC				Total
	Retromolar canal	Forward canal	Dental canal	Buccolingual canal	
Male	25	4	8	2	39
Female	14	6	6	0	26
Total	39	10	14	2	65

Table 2
Distribution of types of BMC according to age groups.

Decade	Retromolar	Forward	Dental	Buccolingual	Total
1	-	-	1	-	1
2	5	-	3	1	9
3	7	1	4	-	12
4	8	5	4	-	17
5	12	2	1	1	16
6	4	1	1	-	6
Total	36	9	14	2	61

Table 3
The numbers of different groups of bifid canals according to gender and types.

Gender	BMC location	Types of BMCs				
		Retromolar	Forward	Dental	Buccolingual	Total
Male	Left	11	3	3	1	18
	Right	14	1	5	1	21
	Total	25	4	8	2	39
Female	Left	10	2	3		15
	Right	4	4	3		11
	Total	14	6	6		26

Table 4
The distribution of canal types according to gender and location.

Gender		Retromolar	Forward		Dental			Buccolingual	Total
			Confluence present	Absent	1st molar	2nd molar	3rd molar		
Male	Left	11 (16.92%)	3 (4.62%)	-	-	-	3 (4.62%)	1 (1.54%)	18 (27.69%)
	Right	14 (21.54%)	-	1 (1.54%)	1 (1.54%)	1 (1.54%)	3 (4.62%)	1 (1.54%)	21 (32.31%)
	Total	25 (38.46%)	3 (4.62)	1 (1.54)	1 (1.54)	1 (1.54)	6 (9.23)	2 (3.08%)	39 (60%)
Female	Left	10 (15.38%)	2 (3.08%)	-	-	-	3 (4.62%)	15 (23.07%)	
	Right	4 (6.15%)	4 (6.15)	-	-	-	3 (4.62%)	11 (16.92%)	
Total		14 (21.53%)	6 (9.23%)	-	-	-	6 (9.23%)	26 (40%)	

no statiscally significant differences between canal type and canal localisation (p>0.05).

The mean length of BMCs was 12.78 mm on the right side and 11.6 mm on the left side. According to the types BMCs, the mean length of bifid retromolar canal was 11.57 mm (right side 12.4 mm, left side 10.8 mm), the mean length of dental canal was 12.9 mm (right side 14.3 mm, left side 11.03 mm), 15.2 mm for forward canal (right side 15.08 mm, left side 15.3 mm), and 2.18 mm for buccolingual canal (right side 2.05 mm, left side 2.32 mm). Statistically significant differences were found for length between the right and left sides and location of the BMCs with using Wilcoxon signed rank test. Differences between type and length of BMCs were evaluated with using one-way analysis of variance test and statistically significant differences were found between type and length of BMCs (p<0.05).

Mean superior angle was 133.3° on the right side and 151° on the left side. Mean inferior angles was 44.9° on the right side and 44.5° on the left side. According to the canal types, mean right superior angles of retromolar, dental and forward canals were 127.4°, 141.1° and 136.5°, respectively; mean right inferior angles were 53.4°, 51.3° and 12.4°, respectively. Mean left superior angles of retromolar, dental and forward canals were 149.4°, 145.5° and 163.1°, respectively. Mean left inferior angles were 46.2°, 62.5° and 13.7° with the same order. No statistically significant differences were found between types of BMCs and superior angles with using ANOVA test, but statistically significant differences were found between types of BMC types and inferior angles (p<0.05).

Discussion

There are a large number of studies on the anatomical location and configuration of BMC using panoramic radiography. These studies reported BMC ranging from 0.08 to 0.95%.[1,2,7,8] Studies using CBCT are less than studies using panoramic radiography. CBCT studies reported the incidence of BMCs ranging from 15.6% to 66.5%.[3,6,9] Kuribayashi et al.,[9] reported the incidence as 15.6%, Naitoh et al.[6] 65%, and Orhan et al.[3] 66.5%. In our study, the incidence of BMC was 3.05% which was lower than the number reported by earlier CBCT studies. But it is possible to see that the incidence of BMC in the studies using CBCT was higher than that in the studies using panoramic radiography, indicating that panoramic radiography technique was insufficient to determine all BMCs. Due to the importance of BMC for surgical procedure, the limitations of panoramic radiography technique to diagnose BMC must be considered. However, panoramic radiography was suggested to diagnose BMC due to high cost and high radiation dose of computed tomography.[10]

In our study, we found BMC more frequently in males than in females. However, in some studies, the incidence of BMC was higher in females.[1,8] In our study, the mean age was 45.78 for males and 42.5 for females. Orhan et al.[3] reported the mean age of their subjects as 36.7 (range: 17 to 83) years

Orhan et al.[3] found the most frequently observed type of BMC as the forward canal (29.8%) and the less observed type the dental canal (8.3%). In our study, the most frequently observed type was retromolar canal and the less observed type was buccolingual canal. Naitoh et al.[9] found similar results with Orhan et al.[3] and reported that the most frequently observed type was forward canal (44.3%). But, they reported that the less observed type was buccolingual canal (1.6%), similar to our study.

Both the study of Naitoh et al.[6] and of Orhan et al.[3] reported that the most frequently observed type of dental canals as the third molar type, and of forward canals the without confluence type. 55.3% and 7% and in the study of Naitoh et al.[6] as compared to 18.4% and 3.8% in the study of Orhan et al.[3] These results are similar to the results of our study.

Orhan et al.[3] reported the mean lenght of BMC as 13.6 mm on the right side and 14.1 mm on the left side. In present study, the mean length of BMC was 12.7 mm on the right side and 11.6 mm on the left side. According to subdivided types, in the study of Orhan et al.[3] the mean length of bifid retromolar canal was 13.5 mm (13.4 mm on the right side; 13.6 mm on the left side), dental canal was 8.3 mm (8.1 mm on the right side; 8.4 mm on the left side), forward canal was 20.1 mm (19.3 mm on the right side; 21 mm on the left side) and the mean diameter of buccolingual canals was 3.8 mm (3.4 mm on the right side; 4.1 mm on the left side). In our study, the mean length of bifid retromolar and forward canals and the mean diameter of buccolingual canals were found less, but the mean length of dental canal was found more than the study of Orhan et al.[3] The mean superior angle of BMC was found 139 on the right side and 141 on the left side, while the mean inferior angle was found 38 on the right side and 32 on the left side.[3] In our study, mean right superior angle was lower, but the other values were higher than the study of Orhan et al.[3] who reported that no statistically differences were found in either lenghts or angles between the right and left sides and for gender. However, in our study, statistically significant differences were found between the mean inferior angles and canal types between the right and left sides and for gender.

Sanchis et al.[1] evaluated 2012 panoramic radiographs (736 males, 1276 females; mean age 40.4) and found seven cases (0.35%) of BMC. Four of the seven cases

were found bilaterally, the rest was found unilaterally, and the all BMCs were found in females. In our study, bilateral BMCs were found in four of 61 patients.

Kuribayashi et al.[9] evaluated 252 patients (94 males, 158 females; mean age: 33 years) and reported the incidence of BMC as 15.6% and the mean length of BMC as 1.68 mm. In our study, the incidence and mean length of BMCs and the mean age of patients were found higher.

BMCs, especially when there are two mandibular foramina, anesthesia of the inferior alveolar nerve may be inadequate. If there is only soft tissue anaesthesia around the injection site in the patient, but not of the ipsilateral lip or chin, it should be considered about a problem with local anesthesia technique that is likely to be the cause of the failure. While if there is soft tissue anaesthesia of the lips and chin but not the teeth, then anatomical variation should be considered.[11,12] Unsuccessful anesthesia is the most common problem in the patients with BMC. So, The Gow-Gates or Akinosi techniques are preferrable methods of blocking the inferior alveolar nerve in the cases of BMC.[10]

If there is a second neurovascular bundle within the BMC, complications such as traumatic neuroma, paraesthesia and bleeding may occur because of failure to diagnose this anomaly. Because of a second neurovascular bundle, other surgical procedures such as mandibular osteotomy become more complex. If alveolar bone resorbs to the proximity of the mental foramen, because of the pressure on the neurovascular bundle, patients who use mandibular prostheses may be uncomfortable.[11]

Three dimensional radiography techniques provide more exact position of the canal, especially about the buccolingual position of the canal.[13] Peker et al.[14] compared panoramic radiography, conventional (cross-sectional) tomography and CT for the location of MC before implant operation in the posterior mandible. MC couldn't be localized in 19.4% of panoramic radiographs and in 13.9% of conventional tomograms but it could be found in almost all CT images.

In another study by Angelopoulos et al.,[15] digital panoramic radiography and CBCT was compared for observation of the MC before dental implant operation. All studies found MC at higher rate in CBCT. Statistically significant differences were found between panoramic radiography and CBCT.

Tantanapornkul et al.[16] compared panoramic radiography and CBCT in detection of the relationship between the MC and impacted third molars. During the extraction of the third molar, the sensitivity and specificity were found as 93% and 77%, respectively, for CBCT in visualisation of damage of the inferior alveolar nerve. They reported that CBCT was superior to panoramic images in both sensitivity and specificity.

In the study of Kim et al.,[17] panoramic radiographs from 1000 dental patients and 40 dry mandibles were examined for the presence of BMC. According to their study, in four cases, the panoramic radiographs showed indicated double MCs, suggesting that the prevalence of BMCs in Koreans was 0.038%. Among the panoramic radiographs belonging to the dry mandibles, only one case appeared to have a BMC. Later, a CBCT scan was performed at the second molar region and the mental foramen region to determine if these canals were real BMCs. The BMC was found in the second molar area with CBCT. Two canals were detected by radio-opaque lines; one upper canal was circular in outline, whereas the other lower canal was elliptical. However, it was reported that one canal was detected in mental foramen area.

Kalender et al.[18] evaluated CBCT scans of 386 regions in 193 patients (92 males, 101 females) referred to their clinic during a 2-year period were analyzed retrospectively. Accessory mental foramina were most commonly located anteroinferior to the mental foramen, followed by locations posteroinferior to the mental foramen. Bilateral accessory mental foramina anteroinferior to the mental foramen were observed in a 24-year-old male patient. Three accessory mental foramina located anteroinferior, inferior, and posterosuperior to the mental foramen were observed in a 19-year-old female patient. In a 28-year-old male patient exhibited two accessory foramina inferior to the mental foramen on the left side were found. They reported that one MC was found on each side in all of their patients. Accessory mental foramen was important due to continuity with mandibular canal especially about injury to the neurovascular bundles and performing other invasive procedures.[18] In our study, the incidence of BMC was found at higher rates compared to studies using panoramic radiography, but less than other studies using CBCT.

As a result, the position of mental foramen and evaluation of MC variation frequency by dentomaxillofacial radiologists and informing these to the surgeon in mandibular surgical procedures is very important for successful operations and the patient's comfort, and to prevent complications. BMC is an uncommon anatomical variation, so dentists may not have adequate experience to diagnose this variations. Especially in procedures that are frequently performed such as third molar extraction and implant surgery in molar region, diagnosing this variation becomes more important. With the use of CBCT in dentistry, BMC has been found more frequently. Therefore, the right radiographic technique and development in techniques should be considered for assessment of MC

variations and for diagnosing and treatment. Further studies on MC variations will bring innovations to points to be taken into consideration in the mandibular molar region.

References

1. Sanchis JM, Peñarrocha M, Soler F. Bifid mandibular canal. J Oral Maxillofac Surg 2003;61:422–4.
2. Langlais RP, Broadus R, Glass BJ. Bifid mandibular canals in panoramic radiographs. J Am Dent Assoc 1985;110:923–6.
3. Orhan K, Aksoy S, Bilecenoglu B, Sakul BU, Paksoy CS. Evaluation of bifid mandibular canals with cone-beam computed tomography in a Turkish adult population: a retrospective study. Surg Radiol Anat 2010;33:501–7.
4. White SC, Pharoah MJ. Oral radiology: principles and ınterpretation. St. Louis (MO): Mosby Elsevier; 2009. p. 175–244.
5. Rouas P, Nancy J, Bar D. Identification of double mandibular canals: literature review and three case reports with CT scans and cone beam CT. Dentomaxillofac Radiol 2007;36:34–8.
6. Naitoh M, Hiraiwa Y, Aimiya H, Ariji E. Observation of bifid mandibular canal using cone-beam computerized tomography. Int J Oral Maxillofac Implants 2009;24:155–9
7. Grover PS, Lorton L. Bifid mandibular nerve as a possible cause of inadequate anesthesia in the mandible. J Oral Maxillofac Surg 1983;41:177–9.
8. Nortjé CJ, Farman AG, Grotepass FW. Variations in the normal anatomy of the inferior dental (mandibular) canal: a retrospective study of panoramic radiographs from 3612 routine dental patients. Br J Oral Surg 1977;15:55–63.
9. Kuribayashi A, Watanabe H, Imaizumi A, Tantanapornkul W, Katakami K, Kurabayashi T. Bifid mandibular canals: cone beam computed tomography evaluation. Dentomaxillofac Radiol 2010;39:235–9.
10. Auluck A, Pai KM, Shetty C. Pseudo bifid mandibular canal. Dentomaxillofac Radiol 2005;34:387–8.
11. Claeys V, Wackens G. Bifid mandibular canal: literature review and case report. Dentomaxillofac Radiol 2005;34:55–8.
12. Wadhwani P, Mathur RM, Kohli M, Sahu R. Mandibular canal variant: a case report. J Oral Pathol Med 2008;37:122–4.
13. Mizbah K, Gerlach N, Maal TJ, Bergé SJ, Meijer GJ. The clinical relevance of bifid and trifid mandibular canals. Oral Maxillofac Surg 2011;16:147–51.
14. Peker I, Alkurt Toraman M, Mihcioglu T. The use of 3 different imaging methods for the localization of the mandibular canal in dental implant planning. Int J Oral Maxillofac Implants 2008;23:463–70.
15. Angelopoulos C, Thomas S, Hechler S, Parissis N, Hlavacek M. Comparison between digital panoramic radiography and cone-beam computed tomography for the identification of the mandibular canal as part of presurgical dental implant assessment. J Oral Maxillofac Surg 2008;66:2130–5.
16. Tantanapornkul W, Okouchi K, Fujiwara Y, Yamashiro M, Maruoka Y, Ohbayashi N, Kurabayashi T. A comparative study of cone-beam computed tomography and conventional panoramic radiography in assessing the topographic relationship between the mandibular canal and impacted third molars. Oral Surg Oral Med Oral Pathol Oral Radiol Endod 2007;103:253–9.
17. Kim MS, Yoon SJ, Park HW, Kang JH, Yang SY, Moon YH, Jung NR, Yoo HI, Oh WM, Kim SH. A false presence of bifid mandibular canals in panoramic radiographs. Dentomaxillofac Radiol 2011;40:434–8.
18. Kalender A, Orhan K, Aksoy U. Evaluation of the mental foramen and accessory mental foramen in Turkish patients using cone-beam computed tomography images reconstructed from a volumetric rendering program. Clin Anat 2012;25:584–92.

Online available at:
www.anatomy.org.tr
doi:10.2399/ana.16.060
QR code:

Correspondence to: Gözde Serindere, PhD
Department of Dentomaxillofacial Radiology, Faculty of Dentistry,
Mustafa Kemal University, Hatay, Turkey
Phone: +90 505 865 90 63
e-mail: gozdeserindere@mku.edu.tr

Conflict of interest statement: No conflicts declared.

Teaching Anatomy

www.anatomy.org.tr
Received: March 8, 2017; Accepted: April 17, 2017
doi:10.2399/ana.16.057

anatomy
An International Journal of Experimental and Clinical Anatomy

Glenohumeral joint dissection: a new protocol

Philip A. Fabrizio, Danielle Topping, Kathleen Wolfe

The Springfield Clinic, 800 N. 1st Street, Springfield, IL 62702, USA

Abstract

Objectives: The glenohumeral joint, as a component of the shoulder girdle, is one of the most frequently injured joints of the upper extremity. Typical dissection of the glenohumeral joint does not allow an intracapsular view without sacrificing the joint capsule and surrounding structures.

Methods: A dissection method is presented which reveals the internal capsule of the glenohumeral joint, the glenoid labrum, the proximal insertion of the long head of the biceps tendon, and glenohumeral joint surfaces while preserving the posterior aspect of the capsule and surrounding supportive muscles and tendons of the joint.

Results: The novel dissection technique allowed for preservation of glenohumeral joint structures and consideration or reexamination of the relationships and structures.

Conclusion: The authors present an alternative protocol for dissection of the glenohumeral joint that minimizes destruction of the surrounding structures while allowing visualization of the internal capsule and maintains the relationships of the surrounding supporting structures of the pectoral girdle that may be used for study at a later time.

Keywords: anatomy education; applied anatomy; shoulder dissection

Anatomy 2017;11(1):37–41

Introduction

The shoulder complex, consisting of the sternoclavicular, acromioclavicular, glenohumeral and scapulothoracic joints, is one the most commonly injured regions of the upper quarter.[1-6] Glenohumeral joint injuries may involve any of the supportive structures alone or in combinations. The highest incidence of glenohumeral joint injuries involve the muscles and tendons of the rotator cuff, the glenoid labrum, glenohumeral ligaments or capsule, and glenohumeral articular surface defects.[1–3,7] Rotator cuff injuries may account for 65% of all shoulder-related patient-physician interactions, and the prevalence of rotator-cuff injury for patients aged 60–80 years has been demonstrated between 20–50%.[6,8] Vogel et al.[9] showed a population increase in superior labral anterior to posterior (SLAP) lesions and repairs of 238% during the period between 2002 and 2009 in New York state. Further, additional intra-articular injuries often accompany rotator cuff injuries and SLAP lesions.[10,11] Feeney et al.[10] showed a positive correlation between rotator cuff injuries and articular cartilage deterioration at the glenohumeral joint. Kim et al.[11] showed that as many as 85% of SLAP cases also have additional intra-articular damage.

Shoulder pathology can be seen in cadaver specimens and pathologic findings serve to illustrate clinical anatomy concepts to students performing dissections.[4,8] Reilly et al.[4] showed, in a systematic review, that full thickness rotator cuff tears were seen in 11.75% and partial thick-ness rotator cuff tears were seen in 18.49% out of 2553 shoulders from cadaver specimens. Kane et al.[8] identified rotator cuff tissue damage in 50% of cadaver shoulders examined in one study, among them 52% showed partial-thickness tears and 47%, full-thickness tears. Moreover, as the age represented by the cadaveric samples increased, the incidence and the severity of rotator-cuff damage also increased.[8] In these studies, the pathologic shoulder findings could serve to reinforce clinical anatomy to students performing dissections. Further, the positive correlation between rotator cuff pathology and articular cartilage injury indicates the need for a novel dissection protocol that would allow for the comparison of the integrity of internal joint structures to the external structures such as the rotator cuff muscles. Cadaver specimens provide an ideal medi-

um on which to explore shoulder dysfunction. However, at the present time, typical shoulder dissection protocols do not allow one to simultaneously appreciate the internal components of the glenohumeral joint, while maintaining the relationships of the surrounding musculature and other structures. Further, current traditional dissection protocols are performed in a manner that "destroys" many of the surrounding structures and does not allow one to revisit the relationships between the glenohumeral joint and supporting structures due to the removal of the superficial structures and destruction of the joint capsule.

Dissection protocols that are frequently used to examine the glenohumeral joint do not allow unobstructed visualizations of the entire glenohumeral joint, and in some techniques, the method requires release of the rotator cuff muscle attachments and completely dislocating the shoulder to view the interior capsular components, thus limiting the ability to examine and re-examine the relationships of rotator cuff to internal joint morphology. Traditional glenohumeral joint dissection protocols proceed following reflection of the muscles overlying the joint.[12–16] The deltoid, coracobrachialis, and biceps brachii muscles are typically reflected inferiorly from their proximal attachments.[12,13] The distal tendons of the infraspinatus, teres minor and supraspinatus muscles are then cut and the muscles are reflected medially from the humerus to visualize the posterior aspect of the glenohumeral joint capsule which is then incised to gain access to the interior of the glenohumeral joint.[12,13] Laurenson[16] and Cahill and Carmichael[17] describe protocols where the anterior muscles of the arm have been reflected and access into the glenohumeral joint is gained by reflecting the subscapularis muscle and incising the anterior portion of the glenohumeral joint capsule.

The purpose of the current study was to demonstrate a dissection protocol that allowed for visualizing the internal glenohumeral joint structures while maintaining superficial structures in order to maximize the utility of the cadaver. Specifically, the purpose was to develop a dissection protocol that would allow visualization of the glenoid labrum, the tendon of the long head of the biceps brachii muscle, and the articular surfaces of the glenohumeral joint while sparing surrounding supportive structures such as the distal tendons of the rotator cuff muscles and anterior and posterior aspects of the glenohumeral joint capsule, thus allowing for continued study of all of the related structures by students at a later date.

Materials and Methods

The project was reviewed and approved by the Institutional Review Board. Three embalmed cadaver shoulders were dissected in the following manner. The subcutaneous tissues of the pectoral girdle, axilla, superficial back, and arm were removed and cleaned using standard dissection techniques. After removal of these tissues, the deltoid, pectoralis major, trapezius, biceps brachii, and triceps brachii muscles were cleaned and identified. The deltoid and pectoralis major mus-cles were reflected from their distal attachments. The trapezius was reflected from its medial attachment to allow visualization of the supraspinatus muscle. With the arm in lateral rotation, the subscapularis muscle was exposed and cleaned. The deltoid muscle was reflected proximally to visualize the joint capsule and the tendons of the rotator cuff muscles which were subsequently cleaned. With the humerus positioned in lateral rotation, the tendon of the long head of the biceps brachii muscle was identified in the intertubercular groove and preserved in its place. An incision was made circumferentially at the midpoint of the arm to incise the soft tissues of the anterior and posterior compartments of the arm. The biceps brachii and coracobrachialis muscles were cut the proximal one third of the muscle bellies and reflected in a way to preserve the position of the proximal attachments. A longitudinal saw cut was made through the proximal 1/3 of the humerus, in line with the shaft of the humerus, oriented near the frontal plane (**Figure 1**). Saw cuts were made using a Dremel Multi-Maxx MM30 Oscillating Tool equipped with a 0.7 inch "wood flush cut blade" (Robert Bosch Tool Corporation, 1800 W. Central Rd., Mount Prospect, IL 60056, USA). The longitudinal saw cut was started at the greater tubercle, at a position anterior to the supraspinatus tendon, bisected the humeral head, and proceeded distally along the antero-lateral surface of the shaft of the humerus (**Figure 1**). With the biceps brachii muscle reflected superiorly, a second saw cut was made transversely through a point at the middle one third of the shaft of the humerus (**Figure 1**). The result of the two saw cuts was a bisection of the proximal half of the humerus into sections which could then be separated to expose the interior of the glenohumeral joint (**Figure 2**). To aid in the separation and improve viewing, small incisions were made to the superior and inferior portions of the glenohumeral joint capsule. The neurovascular structures were identified and dissected, but were removed for this preparation. At this point the dissection protocol was complete with the shoulder complex remaining in situ. However, the authors continued dissection with the intent of creating a prosection of the shoulder complex using the dissection protocol. Creating the prosection proceeded with cutting the serratus ante-

rior, lattissimus dorsi, levator scapula, rhomboid major and minor, and pectoralis minor muscles from their proximal attachments. The clavicle was cut at its midpoint. The result was a prosection that demonstrated the muscles and relationships associated with the scapula and glenohumeral joint (**Figures 3** and **4**).

Discussion

The current dissection protocol was modeled after a novel procedure for dissection of the knee in which the authors "split" the femur to expose the internal structures of the knee joint.[18] Similarly, the current dissection protocol is comprised of two phases that, when completed, distinguish it from previous or traditional shoulder dissection protocols. Phase one consisted of identifying, preserving, and judiciously removing soft tissue structures. In the current presentation, the muscles of the rotator cuff were emphasized. However, the neurovascular structures could also be preserved to provide additional relationships for students to consider. Once the soft tissues were removed from the pectoral girdle and superficial back region, the rotator cuff muscles were clearly identified and left intact. The current protocol is consistent with previous dissection protocols of the glenohumeral joint to the point of identifying the rotator cuff muscles. However, unlike other dissection protocols previously used, where the rotator cuff muscles were cut and/or removed and either the anterior or posterior aspect of the glenohumeral joint capsule was cut, in the current protocol, the integrity of the rotator cuff muscles and majority of the capsule were maintained throughout the dissection. Maintaining the rotator cuff muscles and the majority of the joint capsule allows the bisected humerus to be opened while visualizing the internal joint structures and then to be replaced into its original position to examine the support structures such as the muscles of the rotator cuff. Further, the more superficial muscles could be judiciously reflected to allow another layer that can remain partially intact to maintain a greater set of relationships. For example, the pectoralis major muscle could be reflected from its proximal attachments allowing students to reexamine that muscle's relationship to the glenohumeral structures.

Phase two of the current protocol, bisecting the humerus, is key to maintaining the integrity of the ante-

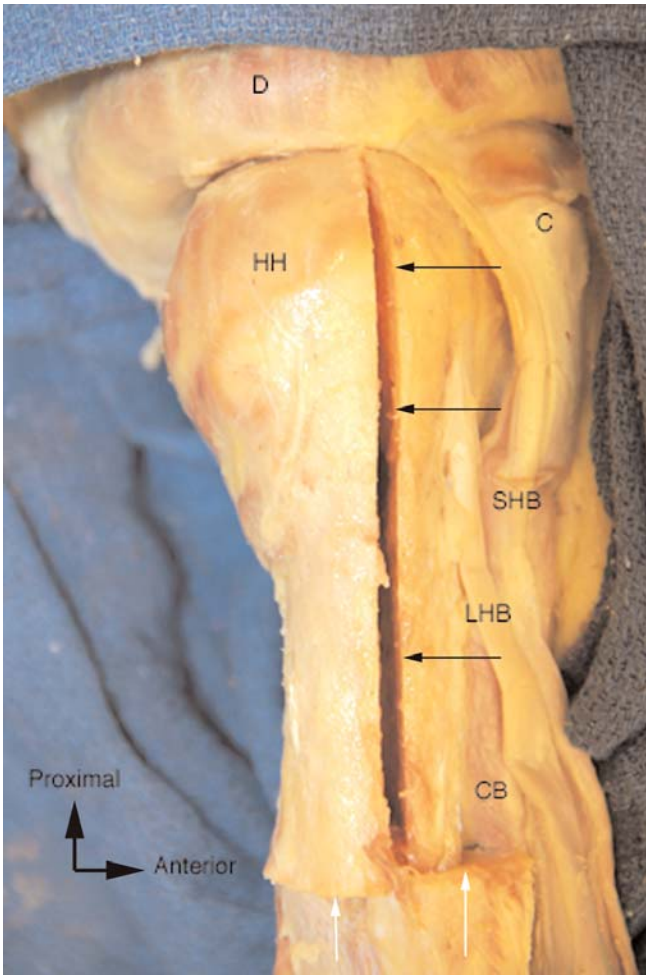

Figure 1. Photograph of the antero-lateral view of the right shoulder showing the resultant saw cuts of the novel protocol done in situ. **Black arrows:** longitudinal saw cut; **white arrows:** transverse saw cut; **C:** coracoid process; **CB:** coracobrachialis muscle; **D:** deltoid muscle; **HH:** head of the humerus; **LHB:** tendon of the long head of the biceps brachii muscle; **SHB:** tendon of the short head of the biceps brachii muscle. [Color figure can be viewed in the online issue, which is available at www.anatomy.org.tr]

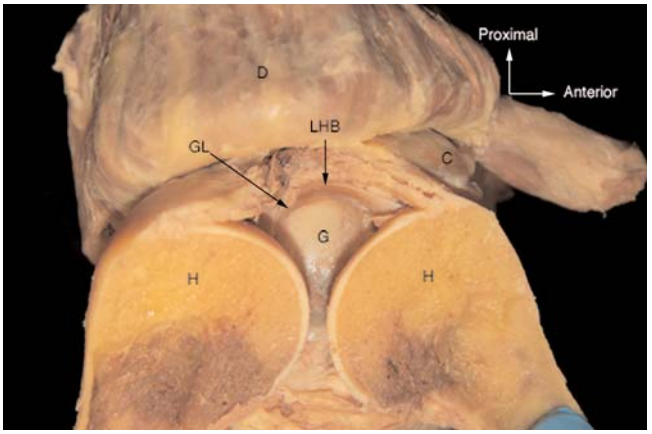

Figure 2. Photograph of the completed glenohumeral joint dissection protocol showing the interior of the glenohumeral joint taken with the completed dissection removed from the cadaver. **C:** coracoid process; **D:** deltoid muscle; **G:** glenoid cavity of the scapula; **GL:** glenoid labrum; **H:** bisected humeral head; **LHB:** tendon of the long head of the biceps brachii muscle. [Color figure can be viewed in the online issue, which is available at www.anatomy.org.tr]

rior and posterior aspects of the glenohumeral joint capsule. By cutting the humerus just anterior to the supraspinatus tendon, the humerus can be reflected within the joint capsule, thus preserving the anterior aspect of the joint capsule along with the glenohumeral ligaments. The posterior aspect of the joint capsule is also preserved, allowing students to visual the expanse of the glenohumeral joint space. When both of the critical phases of this protocol are completed, this dissection approach provides the observer with clear and full visualization of the internal joint capsule and the relationship to the outside musculature. Further, the protocol allows for greater utilization of the cadaver by creating a dissection that can be reevaluated by students for continued study at a later time without sacrificing all of the important relationships in the region.

Conclusion

The primary purpose of developing this dissection protocol was to be able to successfully examine the elements of the glenohumeral joint capsule while ensuring the preservation of the attachments of the rotator cuff muscles. Although the dissection approach presented here differs from more traditional approaches to dissecting the glenohumeral joint, it can be done by students with typical anatomy laboratory equipment. This technique could be used to improve student under-standing of structures of the internal joint capsule and their relationship to the function of the glenohumeral joint in clinical classes. This unique dissection could also be used to further a clinicians understanding of the glenohumeral joint, the structures associated with the glenohumeral joint and the joint capsule, and the attachments of the rotator cuff muscles. Finally, because this technique preserves the joint capsule and the associated structures, it improves the utilization of each specimen.

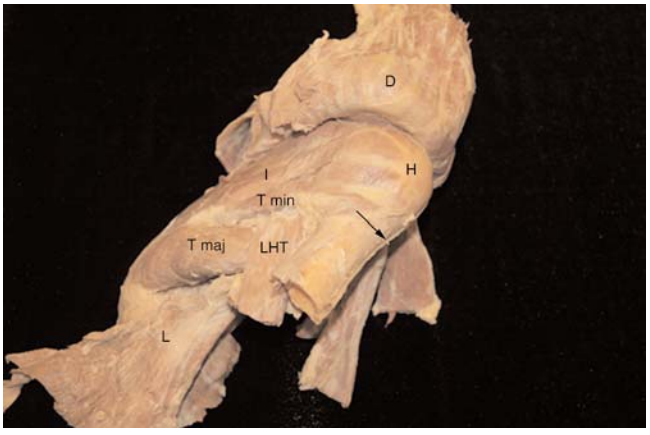

Figure 3. Photograph of completed prosection, posterolateral view, showing the bisected humerus (**black arrow**), put back together for continued study of the rotator cuff muscles. **D:** deltoid muscle; **H:** head of the humerus; **I:** infraspinatus muscle; **L:** latissimus dorsi muscle; **LHT:** long head of the triceps brachii muscle; **T maj:** teres major muscle; **T min:** teres minor muscle. [Color figure can be viewed in the online issue, which is available at www.anatomy.org.tr]

Acknowledgements

The authors wish to thank the individuals who donate their bodies and tissues for the advancement of education and research.

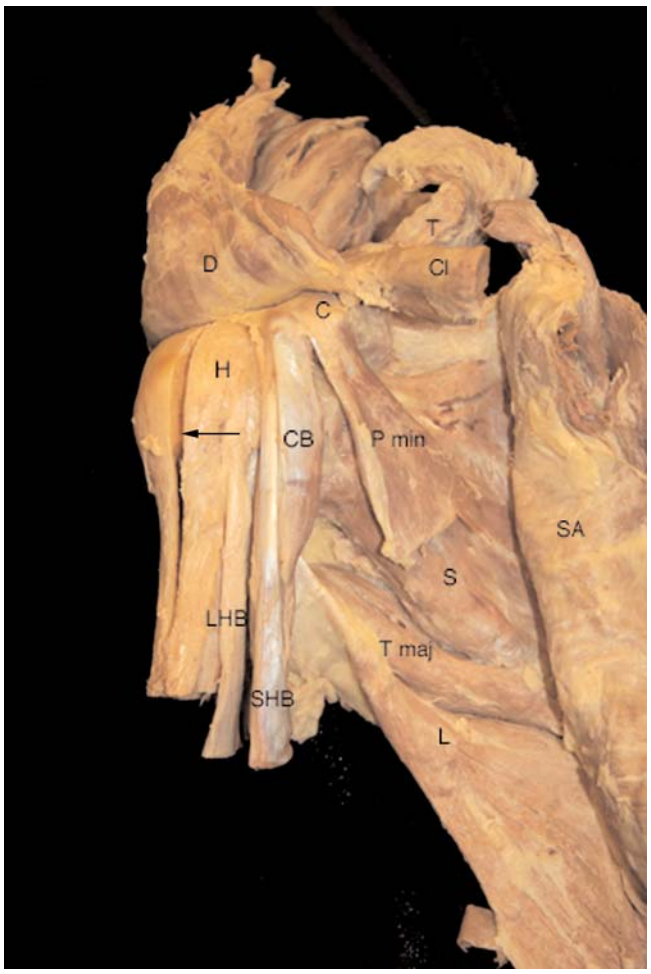

Figure 4. Photograph of the completed prosection, anterior view, showing the bisected humerus (**black arrow**), put back together for continued study of the muscles of the rotator cuff and pectoral girdle. **C:** coracoid process; **CB:** coracobrachialis muscle; **D:** deltoid muscle; **H:** head of the humerus; **L:** lattissimus dorsi muscle; **LHB:** long head of the biceps brachii muscle; **P min:** pectoralis minor muscle; **S:** subscapularis muscle; **SA**: serratus anterior muscle; **SHB:** short head of the biceps brachii muscle; **T:** trapezius muscle; **T maj:** teres major muscle. [Color figure can be viewed in the online issue, which is available at www.anatomy.org.tr]

References

1. Robinson TW, Corlette J, Collins CL, Comstock RD. Shoulder injuries among high school athletes, 2005/2006-2011/2012. Pediatrics 2007;133:272–9.
2. White JJE, Titchener AG, Fakis A, Tambe AA, Hubbard RB, Clark DI. An epidemiological study of rotator cuff pathology using The Health Improvement database. Bone Joint J 2014;96–B:350–3.
3. Bureau of Labor Statistics. 2012. US Department of Labor. Survey of occupational in-juries and illnesses in cooperation with participating state agencies. Percent distribution of nonfatal occupational injuries and illnesses involving days away from work by se-lected injury or illness characteristics and number of days away from work (Table R6). [Internet] [Cited 107 Apr 1]. Available from: http://www.bls.gov/iif/oshwc/osh/os/osh06_b2.pdf
4. Reilly P, Macleod I, Macfarlane R, Windley J, Emery RJ. Dead men and radiologists don't lie: a review of cadaveric and radiological studies of rotator cuff tear prevalence. Ann R Coll Surg Engl 2006;88:116–21.
5. Kelly BT, Williams RJ, Cordasco FA, Backus SI, Otis JC, Weiland DE, Altchek DW, Craig EV, Wickiewicz TL, Warren RF. Differential patterns of muscle activation in pa-tients with symptomatic and asymptomatic rotator cuff tears. J Shoulder Elbow Surg 2005;14:165–71.
6. Vecchio P, Kavanagh R, Hazleman BL, King RH. Shoulder pain in a community-based rheumatology clinic. Br J Rheumatol 1995; 34:440–2.
7. Leclerc A, Chastang JF, Niedhammer I, Landre MF, Roquelaure Y, Study Group on Re-petitive Work. Incidence of shoulder pain and repetitive work. Occup Environ Med 2004;61:39–44.
8. Kane SM, Dave A, Haque A, Langston K. The incidence of rotator cuff disease in smoking and non-smoking patients: a cadaveric study. Orthopedics 2006;29:363–6.
9. Vogel LA, Moen TC, Macaulay AA, Arons RR, Cadet ER, Ahmad CS, Levine WN. Superior labral anterior-to-posterior repair incidence: a longitudinal investigation of com-munity and academic databases. J Shoulder Elbow Surg 2014;23:e119-e126.
10. Feeney MS, O'Dowd J, Kay EW, Colville J. Glenohumeral articular cartilage changes in rotator cuff Disease. J Shoulder Elbow Surg 2003;12:20–3.
11. Kim TK, Queale WS, Cosgarea AJ, McFarland EG. 2003. Clinical features of different types of SLAP lesions: an analysis of one hundred and thirty-nine cases. J Bone Joint Surg 2003;85:66–71.
12. Clemente CD. Clemente's anatomy dissector. 2nd ed., Baltimore (MA): Lippincott, Williams and Wilkins; 2007. p. 65–8.
13. Tank PW. Grant's dissector. 15th ed. Baltimore (MA): Lippincott, Williams and Wilkins; 2005. p. 57–60.
14. Mizeres NJ, Jackson AJ. Methods of dissection in human anatomy. New York (NY): Elsevier; 1983. p. 34.
15. Zuckerman S. A new system of anatomy, a dissector's guide and atlas. Oxford (UK): Oxford University Press; 1981. p. 135–40.
16. Laurenson RD. An introduction to clinical anatomy by dissection of the human body. Philadelphia (PA): W.B. Saunders; 1968. p. 499–504.
17. Cahill DR, Carmichael SW. Supplemental clinical dissections for freshman gross anatomy. Anat Rec 1985;212:218–22.
18. Clemente FR, Fabrizio PA, Shumaker M. A novel approach to dissection of the knee. Anat Sci Educ 2009;2:41–6.

Online available at:
www.anatomy.org.tr
doi:10.2399/ana.16.057
QR code:

Correspondence to: Philip A. Fabrizio, PT, MS, DPT
The Springfield Clinic, 800 N. 1st Street, Springfield, IL 62702, USA
Phone: +1 404 769 8706
e-mail: pafabpt@gmail.com

Conflict of interest statement: No conflicts declared.

anatomy
www.anatomy.org.tr
An International Journal of Experimental and Clinical Anatomy

Teaching Anatomy

www.anatomy.org.tr
Received: April 9, 2017; Accepted: April 11, 2017
doi:10.2399/ana.16.061

Body donation and digital technology: the ethical issues

Jon Cornwall[1–4]

[1]*Graduate School of Nursing, Midwifery and Health, Victoria University of Wellington, Wellington, New Zealand*
[2]*Faculty of Health, Victoria University of Wellington, Wellington, New Zealand*
[3]*Department of Physiology, University of Otago, Otago, New Zealand*
[4]*Institute for Health Sciences, Zurich University of Applied Sciences, Winterthur, Switzerland*

Abstract

Digital technology influences many different areas of society, including body donation and the use of bodies donated to science. It affects the manner in which information arising from bodies donated to science can be generated, gathered and utilised. This includes information arising from medical imaging procedures, photographs, and genomic investigation. However many issues remain unclear in relation to this transaction, including the appropriate level of informed consent, family involvement in decision-making and information sharing, and how commercialisation should be addressed. Highlighting these issues shows there is a distinct lack of empirical evidence with which to guide appropriate use of digital information arising from bodies donated to science, and caution is suggested in regard to the acquisition, distribution, and possible commercialisation of such data.

Keywords: body donation; digital technology; education; commercialisation; informed consent; images

Anatomy 2017;11(1):42–45

Introduction

Digital technology has become widely embedded in society, and has revolutionised mass communication around the world. Given the widespread use of digital technology across higher education institutions, it is highly likely that such technology will eventually impact upon body donation programmes. In fact, evidence of such impact has already been seen in the uptake of 3-D printing[1] and exome analysis[2] of bodies that have been donated to science. As the use of digital technology becomes more common, it is perhaps pertinent to ask - how will digital technology impact upon body donation, and how can higher education institutions responsibly address this topic?

The Potential Benefits of Digital Technology to Body Donation

Collecting digital information from bodies donated to science has numerous benefits, with such information able to be used widely across teaching and research. Health-related imaging procedures such as magnetic resonance imaging, computer tomography, and ultrasound all use digital platforms and could be utilised to scan donated bodies; such data is useful in teaching students both how to use and interpret images arising from different diagnostic imaging modalities. Researchers can also use imaging in conjunction with dissection to explore different aspects of gross anatomy. Students can correlate digital information with physical findings and may have a patient history to guide anatomical examination, and researchers can have access to a an information source that can be easily stored and accessed.

Digital images from donated bodies can also be distributed and shared widely with little effort,[3] or stored for long (potentially infinite) periods of time. Outside of medical imaging, most photographs are now digital, and 3D printing is also based on digitally acquired information via computer scans. For 3D scanning and printing of bodies donated to science, this format provides a novel way of preserving anatomical anomalies that are identified, and for increasing anatomical teaching resources when the

supply of bodies may be compromised. Data from exome sequencing, or any genomic investigation, is also stored digitally. Storage of medical and health records are also being digitised in many countries, with some nations using their medical record database for research in order to improve healthcare outcomes.[4] It is possible that in some instances, the digitised healthcare information of a donated body may become available to the institution, and this may make up part of the information transferred to a body donation programme when they receive a body.

It is feasible that digital information from bodies donated to science may facilitate the creation of large data sets, either from newly generated digital information or from that digital healthcare information that accompanies a donated body. This information could be combined with data sets from other national or international collections, with the downstream benefit of such large data sets being the increase in power and value of the gathered information. There are obvious opportunities and benefits for the creation of such combined data sets. As an example, scans of all bodies donated to science could be acquired with a data set created and shared between researchers in order to explore variations in the morphology of various anatomical structures. Such a database could potentially be contributed to, and accessed, on a global scale. While this scenario is unlikely to occur in the immediate future for reasons of access and funding, it may be possible at some point in the future when imaging technology becomes cheaper and more widely available.

Cautions Surrounding Use of Digital Information Arising from Donated Bodies

Despite the many benefits that digital technology may offer in relation to body donation programmes, many elements of the intersection between body donation and digitisation remain unexplored. Digital information has the potential to be e-mortal (electronically immortal), and with this status comes the possibility that any acquired digital information may remain almost indefinitely accessible and usable. Because digital information can probably exist far longer than older forms of recording such as photographs and researcher notations, it is yet unclear how best to deal with many of the issues that are now more visible than in previous, pre-digital eras.

Digital information is able to be shared almost instantaneously around the world, and such widespread utilisation of information does have enormous potential. Because of this potential, the information and the databases storing it are now more likely to have a dollar value, and this attracts its own problems. For information that has a 'value', there are several questions to which there are not yet adequate answers. In the instance of digital information from bodies donated to science, who does the information 'belong' to?[5] How long are they able to keep it? How should it be used, and if it has a financial value, who should profit? How should families be involved, if at all, in the decision making process involving digital information that is derived from their loved ones? In additon, there are also medical questions and responsibilities to consider: if exome analysis of donated bodies is undertaken, how should we address incidental findings that could impact on family members?[6,7] Topics such as incidental findings, commercialisation,[8] informed consent, family consent, distribution of digital information, and intellectual property are all arguably more visible topics to consider today than in previous eras.

At present, there is little guidance on how digital information arising from bodies donated to science should be utilised or regulated. The guidelines on body donation from the International Federation of Association of Anatomists (IFAA) are silent on the specific issue of digital information,[9] however they do clearly state that there should be no commercialisation in relation to bequests of human remains. This statement has already been challenged ethically, if not legally, with 3D printed models from donated cadavers already being created[1] and made commercially available. In addition, textbook images and some educational software programmes utilise images from bodies donated to science, and it is unclear how this has been addressed in relation to informed consent and possible downstream generation of revenue. Further questions about commercialisation of donated bodies remain in regards to the capacity of body donation programmes to generate enough funding to support the cost of expensive donor programmes. It is unclear whether there exists a cost-recovery framework that outlines what is an 'ethically acceptable' profit margin, so that programmes can ethically cover the costs of their operations without exploiting the precious resource they acquire.

Guidance on the topic of body donation as it relates to informed consent and commercialisation is guided not only by ethical frameworks such as that produced by the IFAA, but also the laws of each country. However, laws in many countries may not yet provide adequate guidance on issues of informed consent or profit as they relate to digitsation of bodies donated to science. This may be for several reasons, and perhaps simply because the law may have been developed in a period where the technology did not exist or present the current range of issues. What is now clear is that digital technology has highlighted the necessity for the scientific and academic communities to engage

with the donor populations and their families, to extend our understanding of how issues such as commercialisation and informed consent should be addressed. The Guidelines of the IFAA do attempt to address good practice and ethical behaviour by body donation programmes, however when these guidelines are ignored it highlights the difficulties surrounding global adoption and enforcement of ethical practice and frameworks. Despite the non-uniform adherence to the IFAA Guidelines, transparent frameworks for the use of digital information arising from bodies donated to science should be developed by organisations like the IFAA to ensure good practice is - at the very least - visible to all involved in body donation practice. The unfortunate case of Henrietta Lacks, whose cancer cells were taken without consent and utilised for decades prior to a public backlash against such exploitation,[10] reminds us of the potential downfalls of unethical behaviour in the medical and anatomical sciences, and it remains imperative that emerging issues are considered in a timely and transparent fashion in order to guide the development of good ethical practice and standards in regards to the future use of digital information.

Where to from Here?

There are many questions surrounding how we should ethically use the various forms of digital information that can be acquired from bodies donated to science, be they images, diagnostic scans, exome analysis, or within medical records that may accompany a donation. However, it is not that the problems we now face are entirely new issues; we are revisiting these topics because the instantaneous transfer of information and consequent opportunity exploitation of data are perhaps more prevalent now because thanks to digital technology. As a consequence, with the increase in opportunities to embrace the various positive uses of digital technology comes the added potential for exploitation and unethical use of bodies donated to science; this is accompanied by the risk of compromising the relationships between established body donation programmes and the generous members of society that underpin the success of body donation programmes worldwide. In a digital age, where information transfer is worldwide and almost instantaneous, such risks are a not just a regional issue, but a global one. It is unclear how previous instances of negative press involving inappropriate conduct with donated cadavers have affected body donation programmes on a local scale,[11,12] however it is safe to suggest that adverse publicity of any kind is not beneficial to long-term sustainability of body donation programmes around the world.

The increasing use of digital technology has illuminated several ethical issues with respect to body donation, including the necessity to revisit those of informed consent and commercialisation, as well as new issues such as incidental findings that will become an important consideration with exome analysis of bodies donated to science. Mostly these are not new issues, however the rapid development of digital technology has provided the stimulus for these to be revisited in the near future. What is now required are publicly informed findings to guide how institutions implement evidence-based frameworks to guide sustainable and responsible use of digital technology within body donation programmes. This should be undertaken by exploring these issues with registered body donors and their families, in a manner similar to a recent exploration in Denmark,[13] to ask how digital technology can be most ethically utilised at its juncture with body donation. It is important that the issues surrounding digitisation of donated bodies are addressed in a timely manner, so as to inform not only ethical behaviour for donor programmes, but also to inform the shaping of new law and regulatory frameworks in an era of widespread digitisation.

References

1. McMenamin P, Quayle MR, McHenry CR, Adams JW. The production of anatomical teaching resources using three-dimensional (3D) printing technology. Anat Sci Educ 2014;7:479–86.
2. Gerhard GS, Paynton B, Popoff SN. Integrating cadaver exome sequencing into a first-year medical student curriculum. JAMA 2016;E1–2.
3. Cornwall J, Callahan D, Wee R. Ethical issues surrounding the use of images from donated cadavers in the anatomical sciences. Clin Anat 2016;29:30–6.
4. Arnar DO, Andersen K, Thorgeirsson G. Genetics of cardiovascular diseases: lessons learned from a decade of genomics research in Iceland. Scand Cardiovasc J 2016;1–6.
5. Cornwall J. The ethics of 3D-printing body parts from donated cadavers in medical education and research: what is there to worry about? Australas Med J 2016;9:8–11.
6. Cornwall J, Slatter T, Print C, Guilford P, Henaghan M, Wee R. Culture, law, ethics, and social implications: is society ready for advanced genomic medicine? Australas Med J 2014;7:200–2.
7. Cornwall J, Winkelmann A, Hildebrandt S. The ethical issues associated with exome analysis of cadavers donated to medical science. JAMA 2016;316:102–3.
8. Champney T. The business of bodies: ethical perspectives on for-profit body donation companies. Clin Anat 2016;29:25–9.
9. Federative International Committee for Ethics and Medical Humanities guidelines, Recommendations of Good Practice for the Donation and Study of Human Bodies and Tissues for Anatomical Examination (2012). [Internet] [Cited 2017 Apr 8]. Available from: http://www.ifaa.net/index.php/ficem
10. Greely HT, Cho MK. The Henrietta Lacks legacy grows. EMBO Rep 2013;14:849.

11. Anon. [Internet] [Cited 2017 Apr 8]. Available from: http://www.news.com.au/technology/online/high-school-student-sparks-anger-after-posting-selfie-with-dead-body/story-fnjwmwrh-1226820128333.
12. Bond A. 2013. 'Hello from the stiffs!' University staff disciplined for posting pictures of body parts on Instagram in Switzerland. [Internet] [Cited 2017 Apr 8]. Available from: http://www.dailymail.co.uk/ news/article-2383718/Zurich-University-staff-disciplined-posting-pictures-body-parts-Instagram Switzerland.html #ixzz3h3LtLi42
13. Olejaz M, Hoeyer K. Meet the donors: a qualitative analysis of what donation means to Danish whole body donors. Eur J Anat 2016;20:19–29.

Online available at:
www.anatomy.org.tr
doi:10.2399/ana.16.061
QR code:

Correspondence to: Jon Cornwall, PhD
Graduate School of Nursing, Midwifery and Health,
Victoria University of Wellington, Wellington, New Zealand
Phone: +64 4 4636650
e-mail: jon.cornwall@vuw.ac.nz

Conflict of interest statement: No conflicts declared.

anatomy
www.anatomy.org.tr
An International Journal of Experimental and Clinical Anatomy

Case Report

www.anatomy.org.tr
Received: March 11, 2017; Accepted: March 28, 2017
doi:10.2399/ana.16.058

A case of a hepatosplenomesenteric trunk combined with a hepatocolic trunk

Sarah E. Johnson, David D. Odineal, Amy E. Steele, Valerie M. Stone, Richard P. Tucker

Department of Cell Biology and Human Anatomy, University of California at Davis, Davis, California, USA.

Abstract

An understanding of the variations in the blood supply of the foregut and midgut are of critical importance to surgeons performing transplants, liver and biliary surgery, resection of tumors and various gastrointestinal procedures, as well as to interventional radiologists engaged in vessel embolization. During the dissection of a 95-year-old female cadaver as part of a course in medical gross anatomy at the University of California at Davis a rare series of vascular variations were observed. The left gastric artery arose independently from the abdominal aorta at the location of a typical celiac trunk. The common hepatic artery and splenic artery branched from a common vessel originating from a hepatosplenomesenteric trunk. Just inferior to the hepatosplenic trunk a hepatocolic trunk, which gave rise to an accessory right hepatic artery, dorsal pancreatic artery and a wandering mesenteric artery, branched from the superior mesenteric artery. This rare combination of clinically relevant variations was likely due to the abnormal partitioning and regression of the primitive splanchnic arteries during embryonic development.

Keywords: anatomical variation; arc of Riolan; celiac trunk; celiacomesenteric trunk; superior mesenteric artery

Anatomy 2017;11(1):46–49

Introduction

The celiac trunk is a large, unpaired vessel that arises from the abdominal aorta just inferior to the aortic hiatus. It is typically tripartite in arrangement, giving rise to the left gastric artery, splenic artery and common hepatic artery.[1] The superior mesenteric artery, which is a source of jejunal and iliac branches, arises from the anterior surface of the abdominal aorta approximately 1 cm inferior to the celiac trunk. Variations in this arrangement are common, well documented, and have clinical relevance to surgeons and radiologists. For example, Chen et al.[2] found that 875 of 974 cadavers (89.8%) dissected at the Gifu University School of Medicine between 1980 and 2007 had a typical tripartite celiac trunk arising independently from the superior mesenteric artery. According to the classification system introduced by Adachi (as cited by Chen et al.,[2]) this typical pattern is referred to as Type I. The most common variation is characterized by the left gastric artery arising independently from, and just superior to, a hepatosplenic trunk. This variation, referred to as Type II, was noted by Chen et al.[2] in 4.3% of the cadavers examined. Variant Type III is characterized by a left gastric artery arising independently from the abdominal aorta and the hepatosplenic trunk arising from a trunk common with the superior mesenteric artery, with the common vessel referred to as a hepatosplenomesenteric trunk. This rare arrangement was seen in only 7 of 974 cadavers (0.7%). The remaining variants are classified as Type IV (a single, common celiacomesenteric trunk; 0.7%), Type V (a common trunk for the left gastric artery and splenic artery and a common trunk for the common hepatic artery and superior mesenteric artery; 1.5%) and Type VI (a common trunk for the left gastric and splenic arteries and a common hepatic artery arising from the superior mesenteric artery that travels posterior to the portal vein; 1.8%). Here we report a case of a hepatosplenomesenteric trunk (variant Type III) combined with a hepatocolic trunk featuring an accessory right hepatic artery that travels posterior to the portal vein and a wandering mesenteric artery, a combination that is particularly rare. The aim of the study is to raise awareness of vascular anomalies that may have profound clinical consequences.

Case Report

As part of a dissection-based course in medical gross anatomy an example of a hepatosplenomesenteric trunk was discovered. The cadaver was a 95-year-old female-who died from urosepsis and who suffered from chronic anticoagulation, cerebrovascular disease and valvular heart disease. Due to university policies intended to protect donor anonymity, no additional information about the donor is known.

The donor's left gastric artery arises from the anterior surface of the abdominal aorta approximately 1 cm inferior to the diaphragm at the general location of a typical celiac trunk (**Figure 1a**). An inferior phrenic artery branches from the left gastric artery 1.7 cm from the abdominal aorta. The left gastric artery follows the course of the lesser curvature of the stomach where it forms an anastomosis with the right gastric artery. A hepatosplenomesenteric trunk arises from the anterior surface of the abdominal aorta 1.3 cm inferior to the left gastric artery (**Figures 1a** and **b**). Its first branch is a hepatosplenic trunk that arises 5.4 cm from the origin of the hepatosplenomesenteric trunk. This trunk for the common hepatic artery and splenic artery is 1.5 cm in length. The splenic artery is tortuous and gives rise to two branches, each 5.3 cm from the splenic artery's origin, which eventually meet and form a superior polar artery; the superior polar artery is the source of both short gastric arteries and a branch to the abdominal esophagus. Distal to the arteries that form the superior polar artery and 10.8 cm from its origin at the hepatosplenic trunk the splenic artery gives rise to the left gastroepiploic artery, which forms an anastomosis with the right gastroepiploic artery along the greater curvature of the stomach. The left and right hepatic arteries arise from the common hepatic artery 3.5 cm from its origin from the hepatosplenic trunk. The right hepatic artery is the source of a cystic artery, the right gastric artery and the gastroduodenal artery. A branch arises from the right margin of the superior mesenteric artery just 3 mm inferior to the hepatosplenic trunk (**Figure 1c**). This vessel branches 4 mm from its origin into an accessory right hepatic artery that passes posterior to the portal vein and an artery that joins with a branch of the left colic artery, i.e., a meandering mesenteric artery, also known as an arc of Riolan. This variant is referred to as a hepatocolic trunk.[3] Near the gall bladder another cystic artery arises from the accessory right hepatic artery. These variations are illustrated schematically in **Figure 1d**.

Discussion

Variations in the celiac axis are well studied, especially in regards to the origins and courses of the cystic and hepatic arteries. In addition to the system used to characterize these variations proposed by Adachi, others including Varotti et al.[4] have proposed classification systems or have proposed modifications to older systems. Using the system of Varotti et al.[4] the variant in the current study would best fall under Type 3a as the accessory right hepatic artery is derived from superior mesenteric artery. However, in Varotti's system the right hepatic artery is ultimately derived from a traditional celiac trunk and not from a hepatosplenomesenteric trunk.

Panagouli et al.[5] recently completed a comprehensive survey of studies and case reports involving variations of the celiac trunk. They found the hepatosplenomesenteric trunk to be one of the rarest variants, present in only 49 of 12,196 cases (0.4%). According to Chen et al.[2] there are only four case reports based on cadaveric dissection describing a hepatosplenomesenteric trunk: three are described by Adachi and one is in a report by Sekiya et al.[6] In the latter study, the left gastric artery is the source of both an inferior phrenic artery and the left hepatic artery. Unfortunately, details of the branches of the hepatosplenomesenteric trunk are not provided,[6] but it is interesting to note that the cadaver they studied had a number of other vascular variations including a persistent sciatic artery, a meandering mesenteric artery, accessory renal arteries and a retroesophageal right subclavian artery. Of these additional variations only a meandering mesenteric artery, which in our case was derived from the hepatocolic trunk, was observed. Thus, a hepatosplenomesenteric artery can be present in individuals with otherwise typical vasculature outside the superior aspect of the abdomen. Since the review of the literature by Chen et al.[2] hepatosplenomesenteric trunks were reported in a patient undergoing surgery to repair a splenic artery aneurysm[7] and in a patient using computerized tomography.[8] A recently published cadaveric study describes a phrenicogastric trunk arising proximal to the hepatosplenomesenteric trunk,[9] as do we.

The cadaver examined in our study shows variant vasculature throughout the field of supply of a typical celiac trunk, including a superior polar splenic artery with esophageal branches and an accessory right hepatic artery arising independently from the superior mesenteric artery that travels posterior to the portal vein. This artery is also the source of a dorsal pancreatic artery and the wandering mesenteric artery. Considered individually these additional variations are relatively common. Superior polar arteries have been reported in as many as 51% of cadavers examined,[10] but to the best of our knowledge this artery has not been reported previously to be the source of esophageal branches. Accessory right

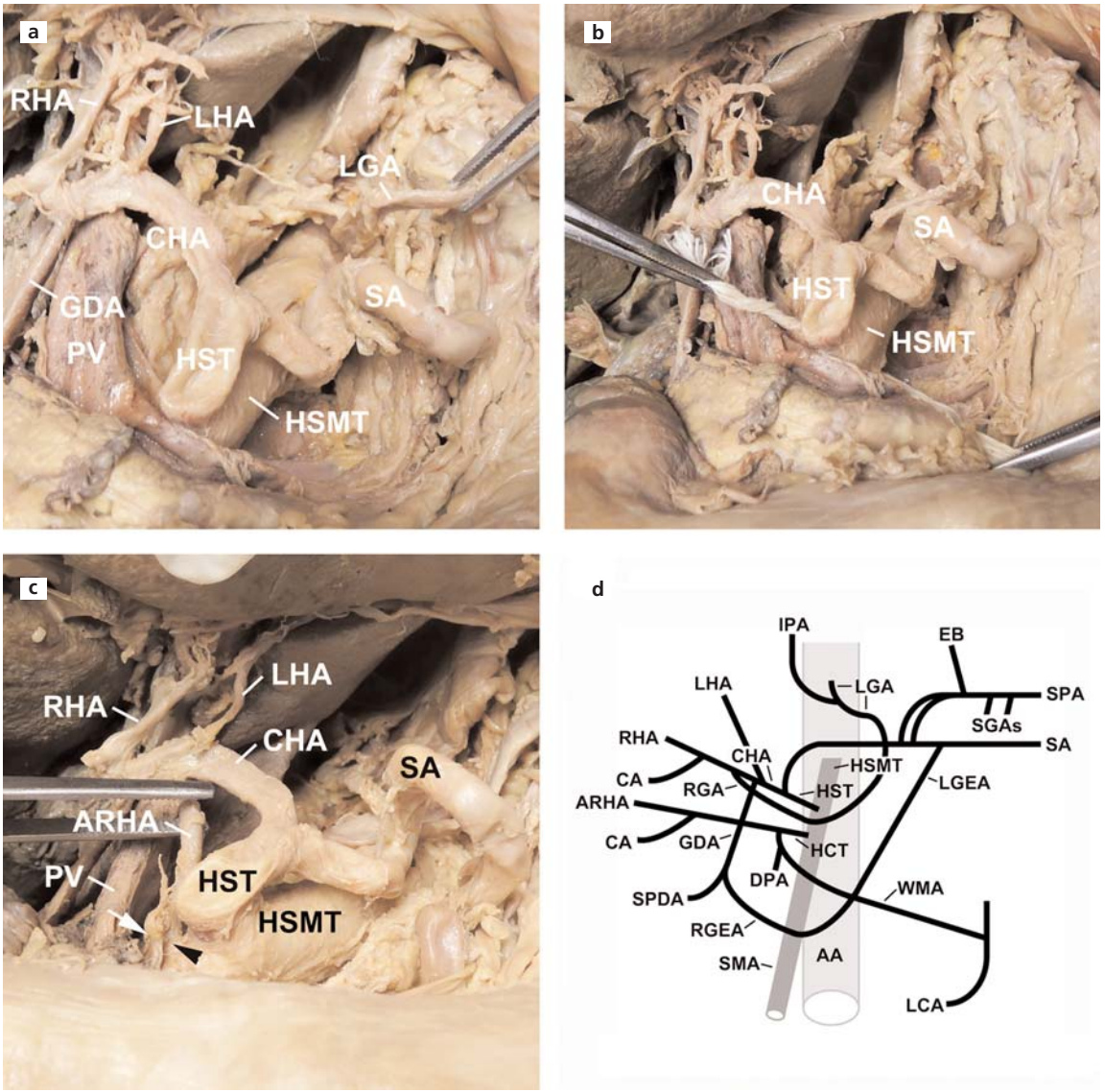

Figure 1. A hepatosplenomesenteric trunk. (**a**) The left gastric artery (**LGA**), held by forceps, arises independently from the abdominal aorta. The hepatosplenomesenteric trunk (**HSMT**) gives rise to a hepatosplenic trunk (**HST**), which is the source of the splenic artery (**SA**) and common hepatic artery (**CHA**). **GDA:** gastroduodenal artery; **LHA:** left hepatic artery; **PV:** portal vein; **RHA:** right hepatic artery. (**b**) The HSMT is demonstrated by passing a string between the trunk and the abdominal aorta. (**c**) A hepatocolic artery (**black arrowhead**) arises from the superior mesenteric artery approximately 3 mm inferior to the HST. It is the source of an accessory right hepatic artery (**ARHA**) that passes posterior to the PV, and a wandering mesenteric artery (**white arrow**). (**d**) A schematic drawing illustrating the branches of the HSMT. **AA:** abdominal aorta; **CA:** cystic artery; **DPA:** dorsal pancreatic artery; **EB:** esophageal branch; **HCT:** hepatocolic trunk; **IPA:** inferior phrenic artery; **LCA:** left colic artery; **LGEA:** left gastroepiploic artery; **RGA:** right gastric artery; **RGEA:** right gastroepiploic artery; **SGAs:** superior gastric arteries; **SMA:** superior mesenteric artery; **SPA:** superior polar artery; **SPDA:** superior pancreaticoduodenal artery; **WMA:** wandering mesenteric artery. [Color figure can be viewed in the online issue, which is available at www.anatomy. org.tr]

hepatic arteries arising directly from the superior mesenteric artery are seen in 5% of cadavers.[2] When it is the source of the dorsal pancreatic artery, as it was in the current study, this vessel typically courses posterior to the portal vein.[11] Wandering mesenteric arteries are present in 10% of the population.[3]

In the embryo, the abdominal aorta is a paired structure connected with a series of channels to ventrally and laterally located splanchnic arteries that supply the developing viscera. As the aortas fuse these channels typically regress, leaving three arteries –the celiac trunk, the superior mesenteric artery and the inferior mesenteric artery–

supplying the viscera of the foregut, midgut and hindgut, respectively. The variations in this blood supply described by others as well as the series of variations reported here are likely to be the results of the atypical regression and selective retention of the channels connecting the developing aorta with the embryonic splanchnic arteries.[12,13]

Though rare, surgeons and radiologists should be aware of the potential for their patients to have a hepatosplenomesenteric trunk, which can be present both in patients with[6] or without (the current case) significant vascular variations outside the abdomen. Failure to recognize the presence of such variations can result in complications following organ transplantation, gastrointestinal procedures and the surgical excision of tumors, as well as the inadequate embolization of unexpected vessels by interventional radiologists.

Acknowledgements

S.E.J., D.D.O, A.E.S. and V.S.M. contributed equally to this study. The authors are grateful to staff of the University of California at Davis Body Donation Program and wish to thank the individuals who donated their bodies and tissues for the advancement of education and research. The authors declare that they have no conflict of interest.

References

1. Haller AV. Icones anatomicae in quibus aliquae partes corporis humani delineatae proponuntur et arteriarum potissimum historia continetur. Göttingen: A. Vandenhoeck; 1756.
2. Chen H, Yano R, Emura S, Shoumura S. Anatomic variation of the celiac trunk with special reference to hepatic artery patterns. Ann Anat 2009;191:399–407.
3. Michels NA, Siddharth P, Kornblith PL, Parke WW. The variant blood supply to the descending colon, rectosigmoid and rectum based on 400 dissections. Its importance in regional resections: a review of medical literature. Dis Colon Rectum 1965;8:251-78.
4. Varotti G, Gondolesi GE, Goldman J, Wayne M, Florman SS, Schwartz ME, Miller CM, Sukru E. Anatomic variations in right liver living donors. J Am Coll Surg 2004;198:577–82.
5. Panagouli E, Venieratos D, Lolis E, Skandalakis P. Variations in the anatomy of the celiac trunk: a systematic review and clinical implications. Ann Anat 2013;195:501–11.
6. Sekiya S, Horiguchi M, Komatsu H, Kowada S, Yokoyama S, Yoshida K, Isogai S, Nakano M, Koizumi M. Persistent primitive sciatic artery associated with other various anomalies of vessels. Acta Anat (Basel) 1997;158:143–9.
7. Sakakibara K, Shindo S, Matsumoto M, Yoshida Y, Kimura M, Honda Y, Kamiya K, Katsu M, Kaga S, Suzuki S. Splenic artery aneurysm of the hepatosplenomesenteric trunk. Ann Vasc Dis 2013; 6:730–3.
8. Maldjian PD, Chorney MA. Celiomesenteric and hepatosplenomesenteric trunks: characterization of two rare vascular anomalies with CT. Abdom Imaging 2015;40:1800–7.
9. Prasanna LC, Alva R, Sneha GK, Bhat KM. Rare variations in the origin, branching pattern and course of the celiac trunk: report of two cases. Malays J Med Sci 2016;23:77–81.
10. Sahni DA, Jit IB, Gupta CN, Gupta DM, Harjeet E. Branches of the splenic artery and splenic arterial segments. Clin Anat 2003;16:371–7.
11. Matsumura H. The significance of the morphology of the dorsal pancreatic artery in determining the presence of the accessory right hepatic artery passing behind the portal vein. Kaibogaku Zasshi 1998;73:517–27.
12. Tandler J. Über die varietäten der Arteria coeliaca und deren Entwicklung. Anat Hefte 1904;25:473–500.
13. Cavdar S, Sehirli U, Pekin B. Celiacomesenteric trunk. Clin Anat 1997;10:231–4.

Online available at:
www.anatomy.org.tr
doi:10.2399/ana.16.058
QR code:

Correspondence to: Richard P. Tucker, PhD
Department of Cell Biology and Human Anatomy University of California, Davis, 1 Shields Avenue, Davis, CA 95616, USA
Phone: +001 530 752 0238
e-mail: rptucker@ucdavis.edu

Conflict of interest statement: No conflicts declared.

Tıp Fakültesi

TÜRK ANATOMİ VE KLİNİK ANATOMİ DERNEĞİ •1991•

18.Ulusal
Anatomi Kongresi

25-27 Eylül 2017 / Abant Palace Hotel Abant

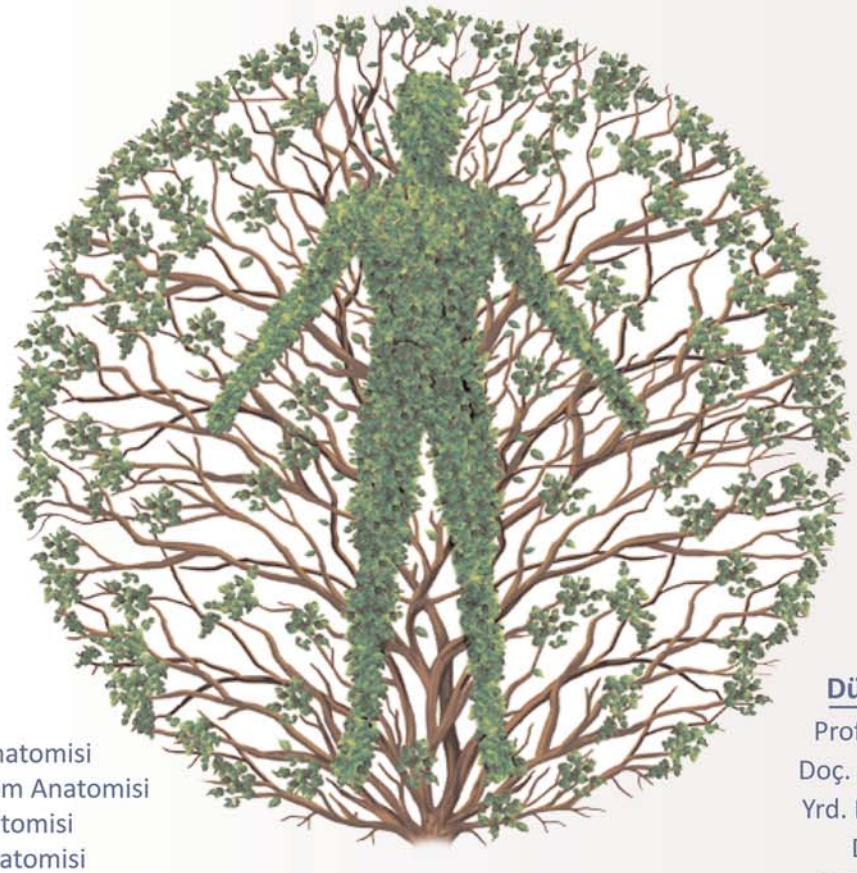

ANA KONULAR

Anatomi Eğitimi
Kas İskelet Sistemi Anatomisi
Gastrointestinal Sistem Anatomisi
Solunum Sistemi Anatomisi
Ürogenital Sistem Anatomisi
Kardiovasküler Sistem Anatomisi

Düzenleme Kurulu

Prof. Dr. Ümit S. Şehirli
Doç. Dr. Ömer Özdoğmuş
Yrd. Doç. Dr. Ural Verimli
Dr. Özlem Kirazlı
Hüsniye Hacıoğlu Bay
Mazhar Özkan
Sercan D. Yıldız
Hatice Boracı

www.anatomikongresi2017.org

www.facebook.com/groups/anatomikongresi2017
www.instagram.com/anatomikongresi_2017
www.twitter.com/anatomi_2017

Organizasyon Sekreteryası

coremice

Barbaros Mh. Deluxia Palace Kat:17 No: 461
34746 Batı Ataşehir / İstanbul
Tel: (0 216) 510 51 51
Faks: (0 216) 510 52 40
info@cormice.com - www.coremice.com

Table of Contents

Volume **11** / Issue **1** / April **2017**

(Continued from back cover)

Teaching Anatomy

Glenohumeral joint dissection: a new protocol **37**
Philip A. Fabrizio, Danielle Topping, Kathleen Wolfe

Body donation and digital technology: the ethical issues **42**
Jon Cornwall

Case Report

A case of a hepatosplenomesenteric trunk combined with a hepatocolic trunk **46**
Sarah E. Johnson, David D. Odineal, Amy E. Steele, Valerie M. Stone, Richard P. Tucker

On the Front Cover:
Photograph of completed prosection, posterolateral view, showing the bisected humerus (**black arrow**), put back together for continued study of the rotator cuff muscles. **D:** deltoid muscle; **H:** head of the humerus; **I:** infraspinatus muscle; **L:** latissimus dorsi muscle; **LHT:** long head of the triceps brachii muscle; **T maj:** teres major muscle; **T min:** teres minor muscle. From Fabrizio PA, Topping D, Wolfe K. Glenohumeral joint dissection: a new protocol. *Anatomy* 2017;11(1):37–41.

Colored images of the published articles can be found in the online version of the journal which is available at www.anatomy.org.tr

www.anatomy.org.tr

anatomy

An International Journal of Experimental and Clinical Anatomy

Table of Contents

Volume **11** / Issue **1** / April **2017**

Original Articles

Histomorphometric evaluation of adult male rabbit testicular tissue exposed to giant milk weed *(Calotropis procera)* treatment **1**

Emmanuel Olusola Yawson, Lawal Ismail Temitayo, Kosisochukwu Kingsley Obasi, Abdulrahman Abdulfatai, Wasiu Olalekan Akintunde

Morphometric assessment of sella turcica using CT scan **6**

Ozan Turamanlar, Kenan Öztürk, Erdal Horata, Mehtap Beker Acay

Age-related morphological changes in the thymus of indigenous Large White pig cross during foetal and postnatal development **12**

Casmir Onwuaso Igbokwe, Kelechi Ezenwaka

Association between Q angle and predisposition to gonarthrosis **21**

Fatma Havaslı, Mehmet Demir, Mustafa Çiçek, Atilla Yoldaş

Factors affecting foot arch development in Northern Ethiopia **26**

Belta Asnakew Abegaz, Dereje Gizaw Awoke

Investigation of bifid mandibular canal frequency with cone beam computed tomography in a Turkish population **30**

Gözde Serindere, Kaan Gündüz, Elif Bulut

(Contents continued on inside back cover)

deomed®